

**T.C.**  
**ISTANBUL AYDIN UNIVERSITY**  
**INSTITUTE OF NATURAL AND APPLIED SCIENCES**



**IMPLEMENTATION AND EVALUATION MAXIMUM POWER  
POINT TRACKING (MPPT) BASED ON ADAPTIVE NEURO  
FUZZY INFERENCE SYSTEMS FOR PHOTOVOLTAIC PV  
SYSTEM**

**M.Sc. THESIS**

**ABD EL HAKIM ALI BOBAKIR ELAGORI**

**Department of Electrical & Electronic Engineering**

**Istanbul – 2017**







**T.C.**  
**ISTANBUL AYDIN UNIVERSITY**  
**INSTITUTE OF NATURAL AND APPLIED SCIENCES**



**IMPLEMENTATION AND EVALUATION MAXIMUM POWER  
POINT TRACKING (MPPT) BASED ON ADAPTIVE NEURO  
FUZZY INFERENCE SYSTEMS FOR PHOTOVOLTAIC PV  
SYSTEM**

**M.Sc. THESIS**

**ABD HAKIM ALI BOBAKIR ELAGORI**  
**(Y1513.300001)**

**Department of Electrical & Electronic Engineering**

**Thesis Advisor: Prof. Dr. Mehmet Emin Tace**

**Istanbul – 2017**





T.C.  
ISTANBUL AYDIN UNIVERSITY  
COLLEGE OF ENGINEERING AND TECHNOLOGY

**Yüksek Lisans Tez Onay Belgesi**

Enstitümüz Elektrik- Elektronik Mühendisliği Ana Bilim Dalı Elektrik- Elektronik Mühendisliği (İngilizce) Tezli Yüksek Lisans Programı Y1513.300001 numaralı öğrencisi ABDEL HAKIM .A.BOBAKIR EL AGOREI' nın "IMPLEMENTATION AND EVALUATION MAXIMUM POWER POINT TRACKING (MPPT) BASED ON ADAPTIVE NEURO-FUZZY INFERENCE SYSTEMS FOR PHOTOVOLTAIC PV SYSTEM" adlı tez çalışması Enstitümüz Yönetim Kurulunun 25.07.2017 tarih ve 2017/16 sayılı kararıyla oluşturulan jüri tarafından *oybirliği* ile Tezli Yüksek Lisans tezi olarak *kabul*... edilmiştir.

Öğretim Üyesi Adı Soyadı

İmzası

Tez Savunma Tarihi : 09/08/2017

1) Tez Danışmanı: Prof. Dr. Mehmet Emin TACER

2) Jüri Üyesi : Yrd. Doç. Dr. Evrim TETİK

3) Jüri Üyesi : Yrd. Doç. Dr. Gürkan SOYKAN

Not: Öğrencinin Tez savunmasında **Başarılı** olması halinde bu form **imzalanacaktır**. Aksi halde geçersizdir.





To my Family ....



## **FOREWORD**

I thank Allah for grant me to complete this thesis. I would like to thank my advisor prof. Dr. Mehmet Emin Tacer, head of the Electrical & Electronic Engineering Department, for his provided guidance and support to wrote and complete this thesis. And, thanks and appreciation to prof. Dr. Necip Gökhan Kasapoğlu for his help understand programming some MATLAB codes.

I hereby declare that this thesis entitled "**IMPLEMENTATION AND EVALUATION MAXIMUM POWER POINT TRACKING (MPPT) BASED ON ADAPTIVE NEURO FUZZY INFERENCE SYSTEMS FOR PHOTOVOLTAIC PV SYSTEM**" is entirely the result of my own work; it contains no material previously published or written by another person nor material which has been accepted for the award of any other degree except where due acknowledgment has been made in the text. the research was carried out and the dissertation was prepared under my direct supervision.

---

June 2017

Abd El Hakim A Bobakir Elagori



## TABLE OF CONTENTS

	<u>Page</u>
<b>TABLE OF CONTENTS</b> .....	III
<b>ABBREVIATIONS</b> .....	V
<b>LIST OF TABLES</b> .....	VII
<b>LIST OF FIGURES</b> .....	IX
<b>ÖZET</b> .....	XIII
<b>ABSTRACT</b> .....	XV
<b>1. INTRODUCTION</b> .....	17
1.1 Background .....	17
1.2 Problem Statement .....	19
1.3 Organization of The Thesis .....	20
<b>2. PHOTOVOLTAIC CELL</b> .....	21
2.1 Introduction .....	21
2.2 Photovoltaic Cell's Equivalent Circuit .....	23
2.3 Characteristic of the PV Cell Output.....	24
2.4 Cell Efficiency .....	26
2.5 Temperature and Solar Radiation Affection on PV Output .....	26
2.6 Formats of PV system .....	27
<b>3. MAXIMUM POWER POINT TRACKING</b> .....	29
3.1 Introduction .....	29
3.2 Boost DC-DC Converter .....	29
3.3 MPPT Algorithms .....	34
3.3.1 Perturb and Observe Method .....	34
3.3.2 Fuzzy Logic Control based MPPT.....	37
3.3.2.1 Fuzzy Logic Control Cine Steps .....	38
3.3.2.2 Fuzzy Controller Based MPPT .....	40
3.3.3 Neural Networks Based MPPT .....	42
3.3.3.1 Backpropagation Learning Algorithm .....	44
3.3.4 Adaptive Neuro-Fuzzy Inference System Based MPPT.....	48
3.3.4.1 Structure of ANFIS .....	49
3.3.4.2 Basic ANFIS Learning Algorithm .....	50
3.4 MPP Tracking efficiency .....	52
<b>4. PV MODEL AND CASE STUDIES SIMULATIONS</b> .....	53
4.1 Introduction .....	53
4.2 PV Model Simulation.....	53
4.2.1 Temperature and Solar Irradiation Affection on I-V curve .....	55
4.2.2 Simulation Testing .....	55
4.2.3 Simulation Results of PV model Testing and Conclusion.....	57

4.3	Boost Convertor Model .....	59
4.4	Perturb and Observe MPPT Controller.....	59
4.5	Fuzzy Logic Controller Model .....	60
4.6	Neural Network Controller Model.....	62
4.7	Neuro-Fuzzy Controller Model .....	63
4.8	Simulation Circuit of all Proposed PV Systems .....	65
<b>5.</b>	<b>SIMULATION RESULTS AND CONCLUSION.....</b>	<b>69</b>
5.1	Simulation Results .....	69
5.1.1	CASE 1: System without MPPT .....	69
5.1.2	CASE 2: PV System with P&O MPPT algorithm .....	73
5.1.3	CASE 3: PV System with MPPT using the proposed FLC method.....	76
5.1.4	CASE 4: PV System with MPPT using the proposed ANN method ...	79
5.1.5	CASE 5: System with MPPT using the proposed AFNIS method.....	82
5.2	Conclusion .....	85
5.3	Summary of the study .....	86
	<b>References .....</b>	<b>89</b>
	<b>APPENDIX A .....</b>	<b>93</b>
	<b>APPENDIX B.....</b>	<b>97</b>
	<b>APPENDIX C .....</b>	<b>104</b>
	<b>RESUME .....</b>	<b>111</b>

## ABBREVIATIONS

<b>PV</b>	: Photovoltaic Cells
<b>MPP</b>	: Maximum Power Point
<b>P-V Curve</b>	: Plotting the relation of power (P) with voltage (V)
<b>I-V Curve</b>	: Plotting the relation of current (I) with voltage (V)
<b>MPPT</b>	: Maximum Power Point Tracking
<b>P&amp;O</b>	: Perturb and Observe
<b><math>V_{MPP}</math></b>	: Voltage at the MPP (V)
<b><math>I_{MPP}</math></b>	: Current at the MPP (A)
<b><math>P_{MPP}</math></b>	: Power at the MPP (W)
<b>ANN</b>	: Artificial neural networks
<b>PWM</b>	: Pulse Width Modulation
<b>FLC</b>	: Fuzzy Logic Control
<b>MFs</b>	: Membership Functions
<b>ANFIS</b>	: Adaptive Neural Fuzzy Interference System
<b>MFs</b>	: Membership Functions
<b><math>\eta</math>-MPPT</b>	: Efficiency of MPPT
<b>DC-DC</b>	: Direct current level to other direct current level





## LIST OF TABLES

	<u>Page</u>
<b>Table 1.1:</b> Advantage and disadvantage of photovoltaic.....	18
<b>Table 3.1:</b> Truth table of the P&O MPPT algorithm.....	37
<b>Table 3.2:</b> Rule base of fuzzy logic controller based MPPT .....	41
<b>Table 4.1:</b> Electrical Data of <b>PPS130W AS8118</b> PV Module .....	56
<b>Table 4.2:</b> Boos DC-DC convertor simulation parameters.....	59
<b>Table 5.1:</b> Comparing results of purposed MPPT algorithms.....	86
<b>Table B.2.1:</b> PV Power at MPP as function of varing G AND T.....	101
<b>Table B.2.2:</b> PV Voltage at MPP as function of varying G AND T.....	101
<b>Table C.1:</b> ANN & ANFIS Training Data.....	104
<b>Table C.4:</b> Testing result of ANN and FLC based ANFIS duye cycle decition.....	110



## LIST OF FIGURES

	<u>Page</u>
<b>Figure 1.1:</b> A large array of PV modules on a rooftop in Switzerland. ....	16
<b>Figure 2.1:</b> Principle work of photovoltaic cell. ....	21
<b>Figure 2.3:</b> Effect of adding cells on I-V PV curve. (a) Series. (b) Parallel [40]. ....	22
<b>Figure 2.4:</b> Forms of the photovoltaic panels. ....	23
<b>Figure 2.5:</b> Electrical equivalent circuit of a Single PV cell. ....	23
<b>Figure 2.6:</b> Power curves and maximum power point (MPP) ....	24
<b>Figure 2.7:</b> Influences of radiation and temperature on the cell I–V characteristics. (a) Influence of the irradiation. (b) Influence of temperature [1]. ....	27
<b>Figure 3.1:</b> The Proposed PV system with MPPT. ....	29
<b>Figure 3.2:</b> The boost converter circuit. ....	30
<b>Figure 3.3:</b> The Equivalent circuit of the boost converter. (a) closed switch mode. (b) open switch mode. ....	32
<b>Figure 3.4:</b> P&O MPPT Algorithm flowchart. ....	35
<b>Figure 3.5:</b> Understanding P&O running on I-V curve of the PV. ....	36
<b>Figure 3.6:</b> Perturbation of operation point around actual MPP. ....	36
<b>Figure 3.7:</b> Block diagram of P&O MPPT algorithm. ....	37
<b>Figure 3.8:</b> Situations of the operation point on the P-V curve. ....	38
<b>Figure 3.9:</b> (a) Classical sets. (b) Fuzzy sets. ....	38
<b>Figure 3.10:</b> Triangle fuzzy sets. ....	39
<b>Figure 3.11:</b> DE fuzzification converts fuzzy output to crisp output. ....	39
<b>Figure 3.12:</b> Membership function for inputs and outputs of MPPT based FLC [1]. ....	41
<b>Figure 3.13:</b> MPPT based fuzzy logic control Block diagram. ....	41
<b>Figure 3.14:</b> Three layer of multi-layer feed forward network. ....	43
<b>Figure 3.15:</b> Block diagram of ANN based MPPT algorithm. ....	47
<b>Figure 3.16:</b> Architecture of ANFIS with four rules and two membership function. ....	48
<b>Figure 3.17:</b> Block diagram of ANFIS based MPPT ....	52
<b>Figure 4.1:</b> Block diagram for all system connections. ....	53
<b>Figure 4.2:</b> Internal subsystems of the PV model. ....	54
<b>Figure 4.3:</b> The main model of the PV. (a) PV model block. (b) Subsystem mask parameters of the PV model. ....	55
<b>Figure 4.4:</b> Block diagram testing of the PV mode. ....	56
<b>Figure 4.5:</b> MATLAB simulation circuit for testing PV simulation model. ....	56
<b>Figure 4.6:</b> Influence of the temperature on V-I and P-V curves. ....	57
<b>Figure 4.7:</b> Influence of the solar radiation on V-I and P-V curves. ....	57
<b>Figure 4.8:</b> Influence of solar radiation and temperature on $P_{mpp}$ . ....	58
<b>Figure 4.9:</b> Influence of solar radiation and temperature on $V_{mpp}$ . ....	58
<b>Figure 4.10:</b> Boost converter simulation circuit. ....	59
<b>Figure 4.11:</b> Simulation circuit of P&O MPPT controller. ....	60
<b>Figure 4.12:</b> Properties of FLC based MPPT. ....	60
<b>Figure 4.13:</b> Membership functions of FLC based MPPT. (a) MFs of input error E(k). (b) MFs of input delta E(k). (c) MFs of output decision delta D. ....	61

<b>Figure 4.14:</b> Inference rule base surface of FLC based MPPT.....	61
<b>Figure 4.15:</b> Simulation circuit of FLC controller based MPPT .....	62
<b>Figure 4.16:</b> Neural network structure based MPPT. ....	62
<b>Figure 4.17:</b> Simulation circuit of ANN controller based MPPT. ....	63
<b>Figure 4.18:</b> Structure of generated Sugeno FLC system after training by ANFIS. ....	63
<b>Figure 4.19:</b> Generated membership functions (a)MFs of temperature. (b)MFs of solar irradiation. (c) Output samples of the Sugeno FLC system. ....	64
<b>Figure 4.20:</b> Generated rules base from ANFIS training. ....	64
<b>Figure 4.21:</b> Inference rule surface of FLC generated by ANFIS.....	65
<b>Figure 4.22:</b> Purposed FLC controller based MPPT whose parameters generated by ANFIS training. ....	65
<b>Figure 4.23:</b> Simulation circuit of all PV systems for evaluating the performance of each MPPT .....	66
<b>Figure 4.24:</b> Variation value of slow and sudden changing on the operation Solar radiation. ....	67
<b>Figure 4.25:</b> Variation value of slow and sudden changing on the operation temperature. ..	67
<b>Figure 5.1:</b> Connection simulation circuit of PV system without MPPT control.....	70
<b>Figure 5.2:</b> Case 1 simulation results with variation in G. (a) Output load power. (b) Output load voltage. (c) Operation Solar Radiation Power. (c) Operation temperature. ....	71
<b>Figure 5.3:</b> Case 1 simulation results with variation in T. (a) Output load power (b) Output load voltage (c) Operation Solar Radiation Power (c) Operation temperature. ....	72
<b>Figure 5.4:</b> Connection simulation circuit of PV system with P&O MPPT controller.....	73
<b>Figure 5.5:</b> Case2 simulation results with variation in G. (a) Output load power (b) Output load voltage (c) Operation Solar Radiation Power (c) Operation temperature. ....	74
<b>Figure 5.6:</b> Case 2 simulation results with variation in T. (a) Output load power (b) Output load voltage (c) Operation Solar Radiation Power (c) Operation temperature. ....	75
<b>Figure 5.7:</b> Connection simulation circuit of PV system with FLC based MPPT control. ...	76
<b>Figure 5.8:</b> Case 3 simulation results with variation in G. (a) Output load power. (b) Output load voltage. (c) Operation Solar Radiation Power (c) Operation temperature. ....	77
<b>Figure 5.9:</b> Case 3 simulation results with variation in T. (a) Output load power. (b) Output load voltage. (c) Operation Solar Radiation Power (c) Operation temperature. ....	78
<b>Figure 5.10:</b> Simulation connection circuit of PV system with ANN based MPPT controller. ....	79
<b>Figure 5.11:</b> Case 4 simulation results with variation in G. (a) Output load power. (b) Output load voltage. (c) Operation Solar Radiation Power (c) Operation temperature. ....	80
<b>Figure 5.12:</b> Case 4 simulation results with variation in T. (a) Output load power. (b) Output load voltage. (c) Operation Solar Radiation Power (c) Operation Temperature.....	81
<b>Figure 5.13:</b> Simulation connection circuit of PV system with FLC based ANFIS training based MPPT .....	82
<b>Figure 5.14:</b> Case 5 simulation results with variation in G. (a) Output load power. (b) Output load voltage. (c) Operation Solar Radiation Power. (c) Operation Temperature. ....	83
<b>Figure 5.15:</b> Case 5 simulation results with variation in T. (a) Output load power. (b) Output load voltage. (c) Operation Solar Radiation Power. (c) Operation temperature. ....	84
<b>Figure 5.16:</b> Output power of all simulations results for variation in G in one plot. ....	85
<b>Figure A.2.1:</b> Simulation circuit of Photon current ( $I_{ph}$ ) .....	95
<b>Figure A.2.2:</b> Simulation circuit of saturation current ( $I_o$ ).....	95
<b>Figure A.2.3:</b> Simulation circuit of the reverse saturation current ( $I_{rs}$ ) .....	96
<b>Figure A.2.4:</b> Simulation circuit of the PV Output current( $I_{pv}$ ).....	96
<b>Figure B.1:</b> Simulation circuits for analyzing the effect of varying G and T on the $P_{mpp}$ and $V_{mpp}$ .....	97

<b>Figure B3:</b> MATLAB function block based P&O MPPT algorithm.....	102
<b>Figure C.3.1:</b> Loading training data using neuro fuzzy designer. ....	108
<b>Figure C.3.2:</b> ANFIS structure with 16 rule bases.....	109
Training process reaches minimum error of 0.0065 in Epoch 68. see figure below:.....	109
<b>Figure C.3.4:</b> Mean square error of the output during the ANFIS training process.....	109
<b>Figure C.3.5:</b> Comparing output of trained ANFIS with training data. ....	110
<b>Figure C.4:</b> Simulation circuit for testing ANN and FLC based ANFIS.....	110



**IMPLEMENTATION AND EVALUATION MAXIMUM POWER POINT  
TRACKING (MPPT) BASED ON ADAPTIVE NEURO FUZZY INFERENCE  
SYSTEMS FOR PHOTOVOLTAIC PV SYSTEM**

**ÖZET**

Photovoltaik (PV) olarak adlandırılan elemanlarla yapılan güneş enerjisinin elektrik enerjisine dönüşümü önemli bir uygulama alanıdır. Bu çalışmada PV sistemlerinin performanslarının en büyük güç izleme açısından (MPPT) Adaptive Neuro Fuzzy Interference System (ANFIS) tekniğinin incelenmesi ve diğer yaygın algoritmalar olan Perturb and Observe (P&O), Fuzzy Logic Control (FLC) ve Artificial Neural Network (ANN) algoritmaları ile karşılaştırılmaları amaçlanmıştır. Bu algoritmalar güneş panelinden en büyük güç elde edilmesi için DC-DC çeviriciden alınan işaretler, çalışma oranı ile kontrol edilmiştir. MMMPT uygulaması sabit direnç yükünde Boost çevirici kullanılarak yapılmıştır. İlave olarak ile benzetişim, gerçek elektriksel veriler kullanılarak ayarlanabilen parametreler ile yapılmıştır. Radyasyon ve ısı parametreleri değiştirilerek PV çıkış gücü incelenmiştir. Tüm sistemin analiz ve benzetişimi MATLAB Simulink ile gerçekleştirilmiştir. Benzetişim sonuçları; MPPT n temel alınarak ANFIS and ANN teknikleri, MPP tekniğine göre cevabının daha hızlı ve Fuzzy Logic MPPT'ye göre ve bilinen P&Q tekniklerine göre çalışma koşullarının hızlı değişimleri açısından veriminin daha yüksek olduğu saptanmıştır.

**Anahtar Kelimeler:** - Photovoltaic (PV) Cell, P&O Maximum Power Point Tracking (MPPT), Boost DC –DC Converter, Fuzzy logic control (FLC), Artificial Neural Network (ANN) and Adaptive Neuro-Fuzzy Inference Systems (ANFIS).





**IMPLEMENTATION AND EVALUATION MAXIMUM POWER POINT  
TRACKING (MPPT) BASED ON ADAPTIVE NEURO FUZZY INFERENCE  
SYSTEMS FOR PHOTOVOLTAIC PV SYSTEM**

**ABSTRACT**

Convert solar energy to electrical energy is one of its important applications which is done by devices called Photovoltaic (PV) cell. This study was aimed to compare, investigate, and evaluate the performance of PV system operating with Maximum Power Point Tracking (MPPT) that work by Adaptive Neuro Fuzzy Interference System (ANFIS) technique. It is appraised with other MPPT algorithms like the most common Perturb and Observe (P&O) algorithm, Fuzzy Logic Control (FLC) algorithm, and Artificial Neural Network (ANN) algorithm. These algorithms work for controlling the duty cycle (D) of the plus signal that goes to switch of the DC-DC converter for maximizing the power generated by solar panel. Implementation of MPPT is made by using boost DC-DC converter with constant resistive load. In addition, it was conducted to introduce for simulating and modeling general PV panel with some adjustable parameters that modelling any real PV panel using its electrical data. And testing the simulated model for showing the effects of changing in the solar irradiation and the operation temperature on the output power of the PV. All systems were analyzed and simulated by using MATLAB Simulink program.

The simulation results show that the ANFIS and ANN based MPPT method gave faster response to achieve the MPP and more efficient than fuzzy logic MPPT and the conventional P&O methods under rapid variations of operating conditions.

**Key Words:** - Photovoltaic (PV) Cell, P&O Maximum Power Point Tracking (MPPT), Boost DC –DC Converter, Fuzzy logic control (FLC), Artificial Neural Network (ANN) and Adaptive Neuro-Fuzzy Inference Systems (ANFIS).



# **1 INTRODUCTION**

## **1.1 Background**

The evolution of renewable energy systems such as wind, sea wave and solar energy systems have been made over the last few years and still running by researchers. One of these sources is solar energy that is considered nowadays as reliable, daily accessible for free, and environmentally harmless. It has no harm effect on the natural environment compared with other traditional energy sources such as Coal, gas, oil and nuclear. These sources have bad affection in the environment and the weather which are producing Gases such as CO<sub>2</sub> and contribute significantly to increase the temperature of the atmosphere that leading to increase global warming phenomena and problems of climate change [10]. With developing of technologies, the using of solar energy source is considered as a noble mission. Many countries have adopted many policies to support renewable energy such as solar energy [1,13].

The amount of energy that comes from the sun to the earth during a day can feed the total energy that earth needs for one year [2].

Solar radiation can be used in two ways as following:

- i) It can be convert to electricity by devices called solar cells.
- ii) It can be convert to heat by collectors which reflect the solar light to generate heat.

Transform solar radiation power to electrical power is common application of the solar energy, which is done by semiconductor device called Photovoltaic (PV) that produces electricity in a direct electricity generation way through photoelectric phenomenon. A PV consists of an arrangement of several cells connecting with each other electrically in one board or in arrays see figure 1.1 [20].



**Figure 1.1:** A large array of PV modules on a rooftop in Switzerland.

Table 1.1 shows lists some of the advantages and disadvantages of PV system. Note, that they include both technical and nontechnical issues [13].

**Table 1.1:** Advantage and disadvantage of photovoltaic.

---

**Advantages of photovoltaics**

- Fuel source is vast, widely accessible and essentially infinite
- No emissions, combustion or radioactive waste (does not contribute perceptibly to global climate change or air/water pollution)
- Low operating costs (no fuel)
- No moving parts (no wear); theoretically everlasting
- Ambient temperature operation (no high-temperature corrosion or safety issues)
- High reliability of solar modules (manufacturers' guarantees over 30 years)
- Rather predictable annual output
- Modular (small or large increments)
- Can be integrated into new or existing building structures
- Can be very rapidly installed at nearly any point-of-use

**Disadvantages of photovoltaics**

- Fuel source is diffuse (sunlight is a relatively low-density energy)
  - High initial (installed) costs
  - Unpredictable hourly or daily output
  - Lack of economical efficient energy storage
-

Unfortunately, PV source is non-linear source and the conversion efficiency is about 10% to 25% from the total power moreover effected with operation temperature ( $T$ )  $C^\circ$  and solar radiation( $G$ )  $Kw/m^2$  [21]. Therefore, to increase the operation's efficiency, it is necessary to use Maximum Power Point Tracking (MPPT) algorithm to feed the load with maximum available power from PV at different operating points. MPPT system is a power electronic device contains DC-DC converter with controller work with one of MPPT algorithm.

Increasing efficiency of a PV panel is done by MPPT algorithms, which is implemented for controlling the duty cycle ( $D$ ) of the pulse width modulation(PWM) that goes to the switch of the DC converter. Many MPPT algorithms have been developed as they are seen in the Literatures, and many researches carried out to optimize many various MPPT techniques [7,3]. In this study, some of MPPT algorithms will be enlightened.

## **1.2 Problem Statement**

The output power characteristics PV cell are changing by amount of the solar radiation ( $Kw/m^2$ ) and the operation temperature ( $C^\circ$ ). These parameters vary with the time of the days and season of the year causing changing in Current-Voltage (I-V) and Power-Current (P-V) curves of photovoltaic cells. Consequently; operation point of the PV system will not be at its maximum power (see section 2). Many researches have been done to overcome this problem [5].

PV systems are required to operate as efficiently as possible. Therefore, MPPT is used with photovoltaic PV systems. These technique is used to maximize the output power of PV systems as well as improve the performance of system.

A DC – DC converter working with MPPT technique is used to control the  $D$  of pulse signal that goes to switch of the converter [3]. System with this technique will force the PV cells work at maximum power point (MPP) [4]. Many researches carried out to optimize the various techniques [7,3]. The popular one that is widely used perturb and observe algorithm is conventional algorithm that track the MPP with constant step of duty cycle increasing and decreasing till it achieves the MPP. The time response to reach the MPP is depends on the value of  $D$ . If it is too small the time response will be large and vice versa. With intelligent control systems such as Fuzzy Logic Control (FLC), Artificial Neural Network (ANN) and the hybrid of the two of them, the

performance of the system can be better than the conventional algorithm. The aim of this study is to cure the shortcoming of the long-time response with these intelligent systems, to focus on some intelligent MPPT control algorithms for PV system, to optimize the performance over the widest range of operating conditions.

### **1.3 Organization of The Thesis**

In this thesis, there are five sections:

Section one introduces the statement of the thesis's subject.

Section two makes a literature review on solar PV cell with its equivalent circuits and electrical characteristics equations.

Section three discusses and makes a literature review on MPPT in details and shows different MPPT methods and the proposed control schemes are explained. Four MPPT techniques are discussed (P&O, FLC, ANN and the proposed ANFIS) and show the basic working mechanism of them also explains the role of DC-DC boost converter.

Section four introduces simulating general PV model for simulating any PV model by its manufacture data. In addition, studies and analyze affection of changing operation temperature and solar irradiating power on output power of the PV that by testing the PV model whose electrical characteristics data is taken from real PV model. testing simulation model is done by using MATLAB-Simulink. Also in this chapter, full PV system simulated with MPPT controllers work by these techniques P&O, FLC, ANN and the proposed algorithm ANFIS method for controlling D of switch of DC-DC boost converter and run the system under variable operation condition to deliver maximum power to resistive load. All the simulations are made using MATLAB-Simulink Computer Program. Results are recorded and listed in chapter 5 and showing reasons of using MPPT based on these results.

Section five, a total results and conclusions and all the outcomes of the study are state

## 2 PHOTOVOLTAIC CELL

### 2.1 Introduction

Electrical energy can be obtained directly from sunlight using PV devices (cells). The PV cell converts solar power to electrical power under the photovoltaic effect [6]. PV cell is made using semiconductor materials with at least two-semiconductor layers one positive and one negative [1].

Energy of the sunlight comes from a little particle called photons (figure 2.1). As a PV cell is exposed to this sunlight, the photons pass and absorbed by the solar cell. The free the electrons pass through the closed-circuit constitutes electrical current with electrical voltage on the load. Usually the amount of the current for one cell in (mA) and the voltage about 0.6 V [1].

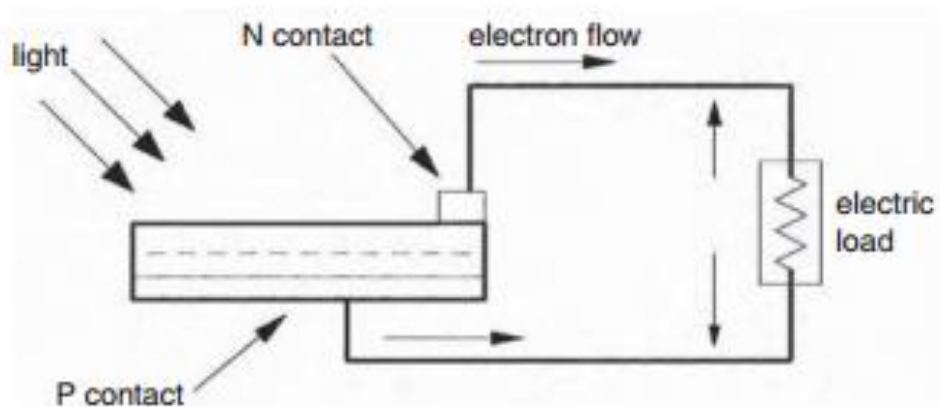


**Figure 2.1:** Principle work of photovoltaic cell.

To obtain the desired voltage and power, cells are connected in series and parallel [8]. To increase the output voltage, increase the connected series cells (figure 2.2 (b)). Connection of solar cells make the same current flow through every solar cell. The total voltage is the sum of the each cell's voltage and the total output voltage is calculated as following:

$$V_{out} = V_1 + V_2 + V_3 + \dots + V_n$$

since the cells voltage are equal the equation can be rewritten as :

$$V_{out} = V * N_s \tag{2.1}$$

Where :  $N_s$  is the cells number that is connected in series .

$V$ = cell voltage

To increase the power output, increase the output current by increase the parallconnected cell (figure 2.2 (a) ). The voltage across each cell is equal, so the total current is summation of all currents of each cell and the totel output current is calculated as following:

$$I_{out} = I_1+I_2+I_3+\dots\dots I_n .$$

senice the cells current is equal and collected in node the output current is :

$$I_{out} = I * N_p \tag{2.2}$$

Where :  $N_p$  is the number of cells connected in parall.

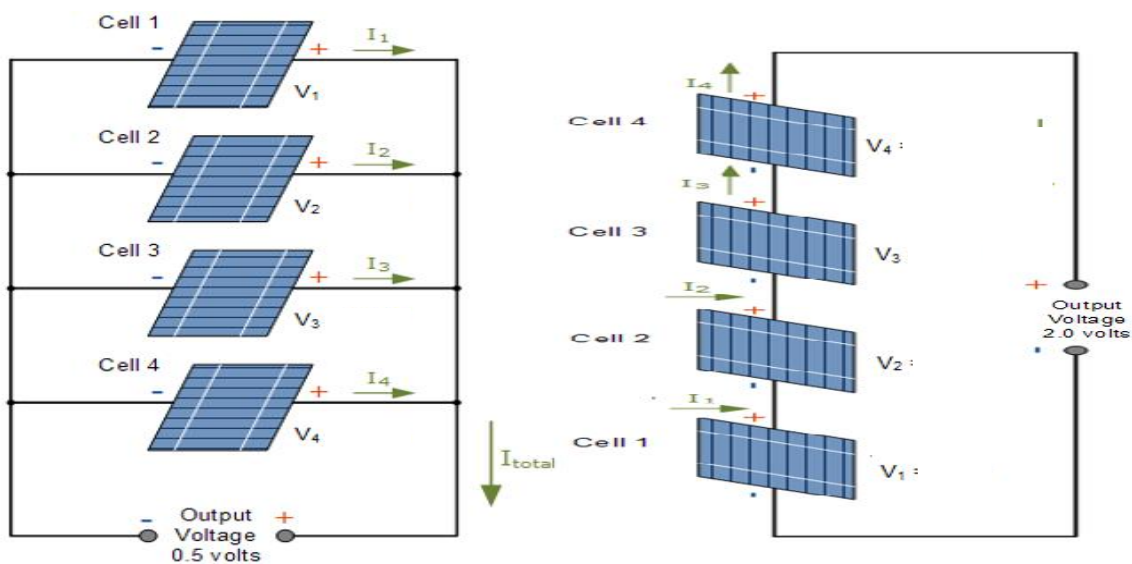


**Figure 2.2:** Solar cell connections. (a) Parball connection. (b) Series connection of solar cell.

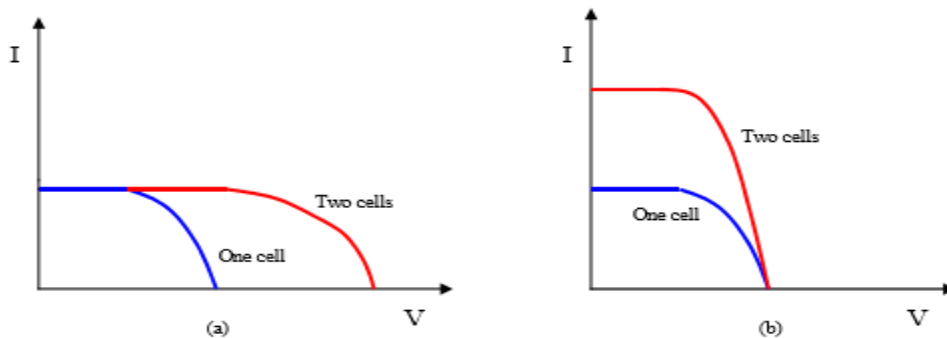


**Figure 2.3:** Effect of adding cells on I-V PV curve. (a) Series. (b) Parallel [40].



The PV solar cell can be one of the following form

- **Solar cell:** A single PV cell converts light to electricity.
- **PV module:** A PV module contains several solar cells connected serially and parallely and Fixed on one board called module.
- **PV array:** Connection of PV modules serially and parallely is called PV array.

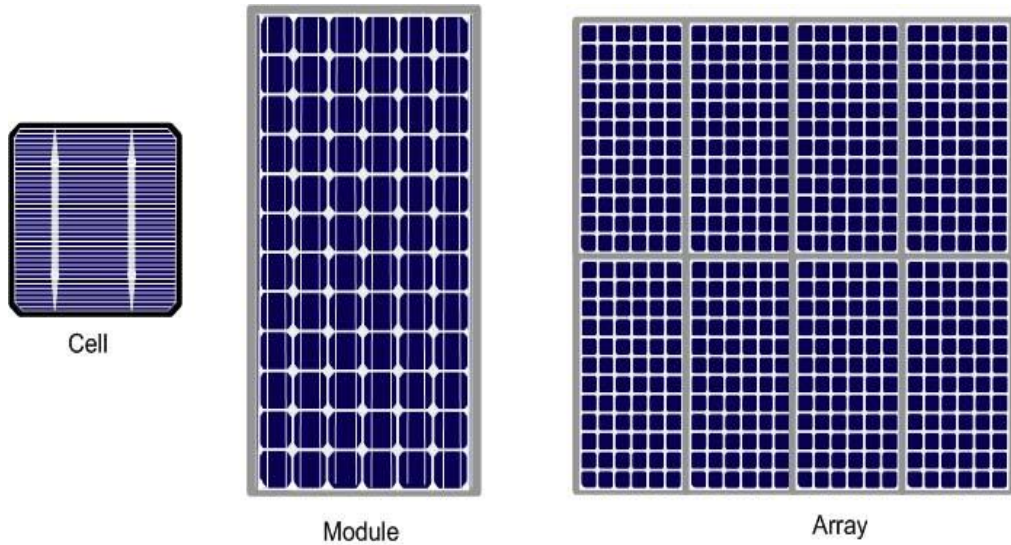


**Figure 2.4:** Forms of the photovoltaic panels.

## 2.2 Photovoltaic Cell'S Equivalent Circuit

Equivalent circuit of PV cell can be considered as p-n semiconductor junction. When the cell visible to the solar, the cell's terminal generates DC current. The generated current influenced by solar irradiance, temperature and load current [15]. The equivalent electrical circuit of the cell can represent as it shown in figure 2.5. Moreover, the output current characteristic is expressed in the following equations:

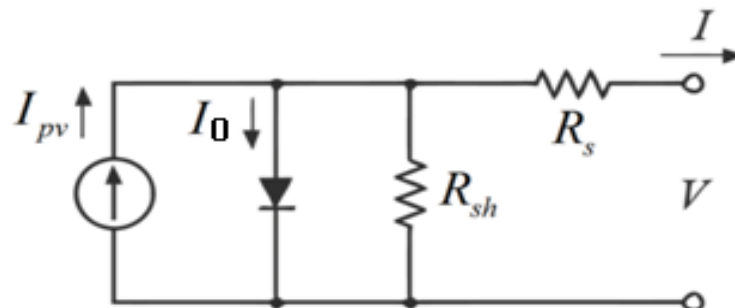


**Figure 2.5:** Electrical equivalent circuit of a Single PV cell.

$$I_{pv} = I_{ph} - I_0 * [e^{\left(\frac{V_{pv} + I_{pv} * R_s}{A * K * T_{ak}}\right)} - 1] - \left(\frac{V_{pv} + I_{pv} * R_s}{R_{sh}}\right) \quad (2.3)$$

$$I_{ph} = I_{scr} + K_i * (T_{ak} - T_{rk}) * G \quad (2.4)$$

$$I_0 = I_{rs} * \left(\frac{T_{ak}}{T_{rk}}\right)^3 * e^{\left[\left(\frac{q * E_g}{A * k}\right) * \left(\frac{1}{T_{ak}} - \frac{1}{T_{rk}}\right)\right]} \quad (2.5)$$

$$I_{rs} = \frac{I_{scr}}{\left[e^{\left(\frac{q(V_{oc} + I_{pv} * R_s)}{A * K * T_{ak}}\right)} - 1\right]} \quad (2.6)$$

For large arrays model of  $N_s \times N_p$  series and parallel cells the equation become:

$$I = I_{ph} * N_p - I_0 * N_p * \left(e^{\left(\frac{q(V_{pv} + I_{pv} * R_s)}{N_s * K * A * T_{ak}}\right)} - 1\right) - \frac{V_{pv} \frac{N_s}{N_p} + I_{pv} * R_s}{R_p} \quad (2.7)$$

### 2.3 Characteristic of the PV Cell Output

- $T_{rk}$ : Reference temperature at 298 K.
- $I_{ph}$ : photocurrent (A)
- $A$ : Ideality factor = 1.6.
- $q$ : Electron charge =  $1.6 \times 10^{-19}$  C
- $I_{scr}$ : The PV module short-circuit current
- $K_i$ : The short-circuit current temperature coefficient
  
- $E_g$ : Band gap for silicon = 1.1 eV
- $V_{oc}$ : Open-circuit voltage (V)
- $V_{pv}$ : Output voltage of the PV cell (V)
- $I_{pv}$ : Output current of the PV cell (A)
- $I_{rs}$ : Reverse saturation current at  $T_{rk}$  (A)
- $K$ : Boltzmann constant =  $1.3805 \times 10^{-23}$  J/K
- $R_s$ : Internal series resistance of the PV cell
- $R_p$ : Internal parallel resistance of PV cell
- $G$ : PV module illumination ( $W/m^2$ )
- $N_s$ : Number of cells serially connected
- $N_p$ : Number of cells parallelly connected
- $I_0$ : PV cell's saturation current
- $T_{ak}$ : Ambient temperature

The relationship between Current and voltage is used to define the characteristics of PV cell and it is described as curve. If the cell's terminal relates to a variable resistance  $R$ , the operating point is determined by the Current-Voltage (I-V) characteristic in the

load (Figure 2.6). The load characteristic can be as a straight line with a slope  $1/R$ . Only the value of the resistance determines the power delivered to the load. Therefore, when the load  $R$  is small, then cell will operate in the region between M and N on the curve, where the cell acts as constant current almost equal to the cell's  $I_{sc}$ . Furthermore, when the load  $R$  is large, the cell will operate on the region between P and S on the curve, where the cell acts as a constant voltage source its value almost equal to  $V_{oc}$  [40].

PV cell's I-V and cell's P-V curves have the form shown in Figure 2.5, power is obtained for a given radiation level [2].

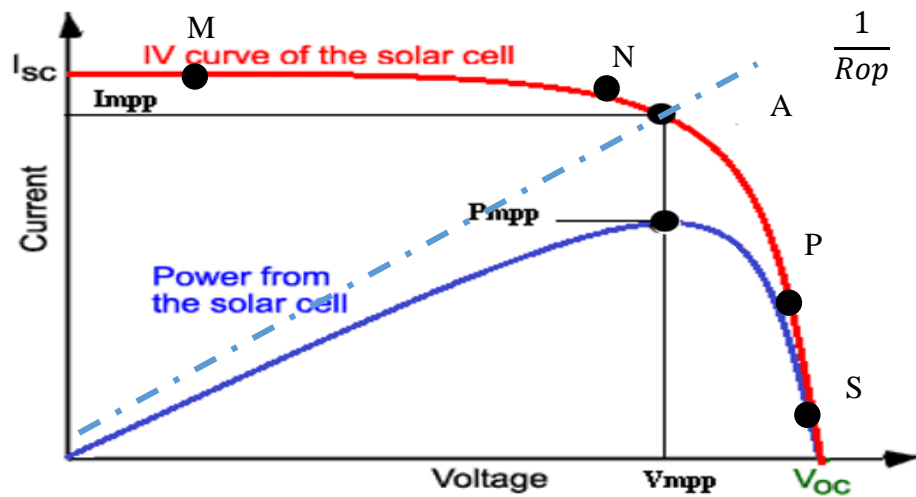


**Figure 2.6:** Power curves and maximum power point (MPP).

Actual PV cell can be described by the following fundamental parameters [40], which are drawn in previous figure:

**Short-circuit current ( $I_{sc}$ ).** A short circuit condition generates the  $I_{sc}$  current.

**Open-circuit voltage ( $V_{oc}$ ).** The voltage across the diode when there is no load relates to the cell.

**Maximum power ( $P_{MPP}$ ).** It is the maximum power extracted by the load when cell operate at point P ( $I_{MPP}$ ,  $V_{MPP}$ ) at which power dissipated in the load is maximum:

$$P_{MPP} = I_{MPP} * V_{MPP} \quad (2.9)$$

**Maximum power operating current ( $I_{MPP}$ ).** The current generated by the cell or module when it is matching the MPP on (I-V) curve.

**Maximum power operating voltage ( $V_{MPP}$ ).** The voltage generated by the cell module when it is matching the MPP on (I-V) curve.

## 2.4 Cell Efficiency

Efficiency conversion of the cell is important property of a PV cell. It is defined as the ratio of the cell output power to the radiation power falling on it:

$$\eta = \frac{I_{MPP} * V_{MPP}}{G} = \frac{FF * I_{sc} * V_{oc}}{G} \quad (2.10)$$

where:

FF (fill factor) is the ratio of MPP that can be distributed to the load and the product of  $I_{sc}$  and  $V_{oc}$  [40]. Its value mostly higher than 0.7. The fill factor can be written as following:

$$FF = \frac{I_{MPP} * V_{MPP}}{V_{oc} * I_{sc}} \quad (2.11)$$

Efficiency of cell is specified under standard test conditions (STC) that when the T is 25C° and G is 1000KW/m<sup>2</sup>.

## 2.5 Temperature and Solar Radiation Affection on PV Output

changing in operation G and T cause change in the output power of the PV solar cell (figure 2.7). When the amount of the radiation increases the  $I_{sc}$  and  $V_{oc}$  of the solar cell increase. from equation (2.2);  $I_{ph}$  is almost in a linear relationship with G. As the T increases, the  $V_{oc}$  decreases and  $I_{sc}$  increases [1]. The influence of the varying G and T on the cell characteristics is present in figure 2.6.

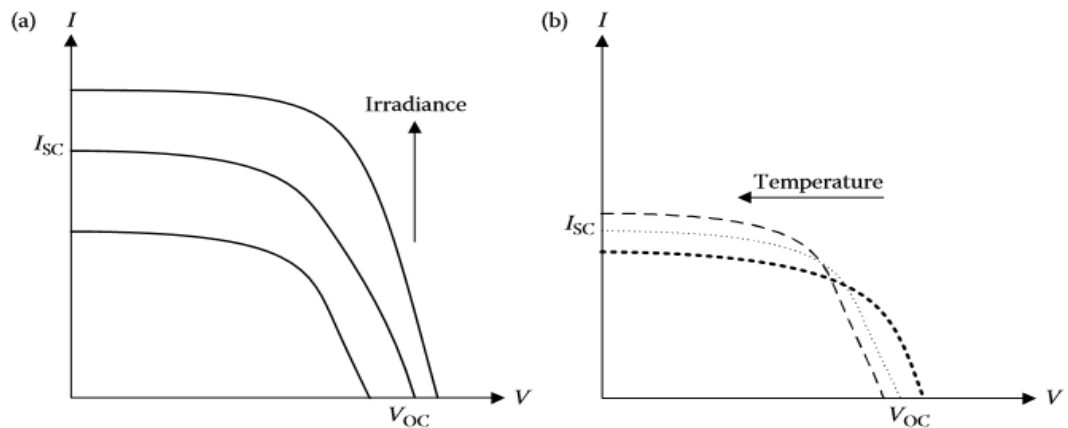


**Figure 2.7:** Influences of radiation and temperature on the cell I–V characteristics.  
 (a) Influence of the irradiance. (b) influence of temperature [1].

In section 4; a PV model is simulated using MATLAB Simulink and will see the effects of varying on T and G on the I-V and P-V curves.

## 2.6 Formats of PV system

Photovoltaic PV system has one of the following forms:

Stand-alone or Off-Grid systems PV system without any contact with grid network usually used for isolated area and has many applications street lighting, charging batteries, inverters...act.

- The grid-connected system form connects directly to the power grid and without batteries that for working in night from the grid network.
- A hybrid system combines the grid system with a battery backup, when grid power is missing the battery is used as source (Same as grid system but with battery).



### 3 MAXIMUM POWER POINT TRACKING

#### 3.1 Introduction

MPPT algorithms are needed in PV applications. As it is seen in literatures; the MPP and I-V of the PV cell changes with the variation of the atmospheric conditions (G and T) as it showed in figure 2.6. Scientists and researchers have been worked to overcome this problems by add intelligent power electronic systems connected to the PV system to force the PV system run at maximum efficiency at the point (MPP).

MPPT is a technique used to maximize power extraction available power from PV module under all conditions. Operating a DC-DC converter with MPPT algorithm is used to maximize the PV generated power (figure 3.1). This chapter presents and discusses some MPPT techniques which are used in this study for evaluating the tracking performance of MPP.

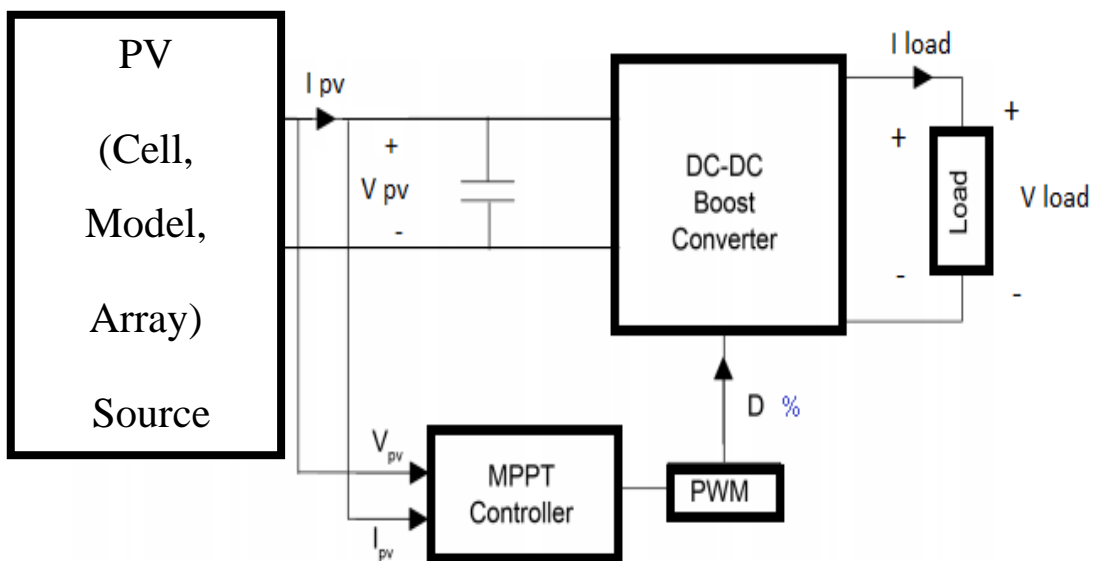
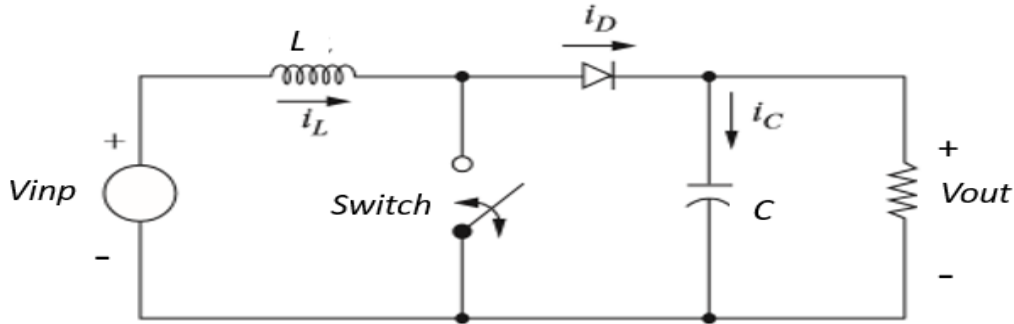


Figure 3.1: The Proposed PV system with MPPT.

#### 3.2 Boost DC-DC Converter

Converts a DC voltage to another DC voltage level is done using Dc-Dc converter which is electronic device. It consists of an inductor, a power electronic switch, a diode and a filter capacitor to feed the output load. Function of the Boost convertor is to step up the input DC voltage to feed it to the output with a desired voltage level. Figure 3.2

shows electrical circuit of a boost converter. It operates by opening and closing an electronic switch. output voltage of the convertor is larger than the input [22].



**Figure 3.2:** The boost converter circuit.

The output voltage level is controlled by adjusting the ratio duty cycle (D) on/off time of the switch using Pulse-width modulation (PWM) that works to control and regulate of the output voltage.

Generally, the operation of the converter has two modes:

**Mode-1:** When the switch is closed, the diode is opened and whole circuit will be as two loops, one in the output and another on in the input. The DC input voltage applied across the inductor (figure 3.2(a)) for a period of time (usually from 20 kHz to 5 MHz) which charges the inductor with the current flowing through the closed loop. This current will increase while loop is in closed condition. In the same time. The equivalent circuit that represents mode 1 is shown in figure 3.2 (a) [22]. by Applying Kirchoff's voltage, the voltage across inductor can be calculated:

$$V_L = V_0 = L \frac{\partial i_L}{\partial t} \quad (3.1)$$

the current increases linearly while the switch is closed, as shown in Figure 3.4(b). The change in inductor current is given from:

$$\frac{\Delta i_L}{\Delta t} = \frac{\partial i_L}{\partial t} = \frac{Vs}{L}$$

By solving the previous equation we can get the charging current when the switch closed

$$\Delta i_{L(Closed)} = \frac{Vs \cdot DT}{L} \quad (3.2)$$



**Mode-2:** When the switch opened, diode becomes close which makes one closed loop consisting source, inductor and capacitor that connected to the load. The charged inductor during closed switch mode discharge its store energy to the RC load through this mode. The inductor current charging the capacitor at the load side and will decrease while the switch is in closed state (figure 3.2 (b)), [22]. The voltage across the inductor is:

$$V_L = V_s - V_0 = L \frac{\partial i_L}{\partial t}$$

$$\frac{\partial i_L}{\partial t} = \frac{V_s - V_0}{L}$$

The change in inductor current while the switch is open is:

$$\frac{\partial i_L}{\partial t} = \frac{\Delta i_L}{(1-D)T} = \frac{V_s - V_0}{L}$$

Solving for  $\Delta i_L$ ,

$$\Delta i_{L(Open)} = \frac{(V_s - V_0)(1-D)T}{L} \quad (3.3)$$

For steady-state operation the change in inductor current must be zero using equation. (2.4) and (2.3):

$$\begin{aligned} \Delta i_{L(Closed)} + \Delta i_{L(Open)} &= 0 \\ \frac{V_s DT}{L} + \frac{(V_s - V_0)(1-D)T}{L} &= 0 \end{aligned}$$

By solving the previous equation to get

$$V_s (D+1-D) - V_0 (1-D) = 0$$

The output voltage will be :

$$V_0 = \frac{V_s}{(1-D)} \quad (3.4)$$

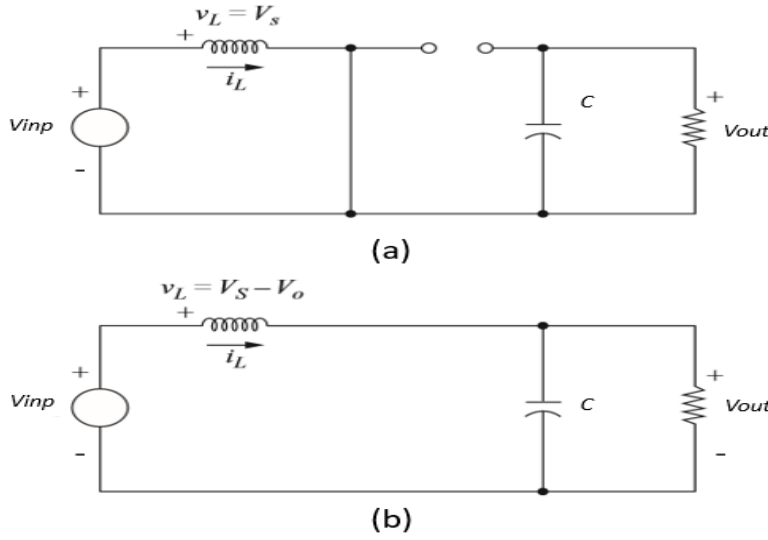


**Figure 3.3:** The Equivalent circuit of the boost converter. (a) closed switch mode.  
(b) open switch mode.

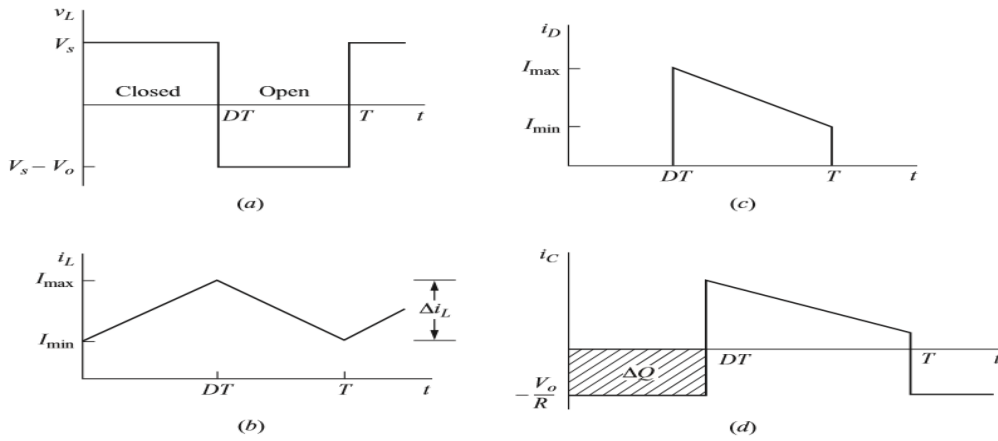


**Figure 3.4:** waveform of the Boost converter. (a) Inductor voltage. (b) Inductor current. (c) Diode current. (d) Capacitor current.

The power in the load resistor is:

$$P_{Out} = \frac{V_o^2}{R} = \frac{V_o^2 * R}{(1-D)^2} = V_{inp} I_L \quad (3.5)$$

By solving for average inductor current  $I_L$  can be expressed as :

$$I_L = \frac{V_o}{R * (1-D)^2} = \frac{V_o^2}{V_s * R} = \frac{V_o * I_o}{V_s}$$

The minimum inductance for continuous current mode (CCM) in the boost converters should be:

$$L_{min} = \frac{D*(1-D)^2*R}{2f} \quad (3.6)$$

For Designing boost converter working in CCM mode the inductor value should be greater than  $L_{min}$  [22].

The change in capacitor charge can be calculated from:

$$\Delta V_0 = \frac{V_0 * D * T}{R * C} = \frac{V_0 * D}{R * C * f}$$

$$\frac{\Delta V_0}{V_0} = \frac{D}{R * C * f} \quad (3.7)$$

Where  $f$  is the frequency of open and close switching. The minimum output capacitor is:

$$C_{min} = \frac{D * V_0}{R * \Delta V_0 * f} \quad (3.8)$$

For designing boost converter  $C$  is selected greater than  $C_{min}$ . Efficiency of the boost converter can be calculated by this expressing:

$$\eta = \frac{P_0}{P_0 + P_{loss}} = \frac{V_0^2 / R}{V_0^2 / R + R_L * I_0^2} \quad (3.9)$$

where,  $R_L$ : The internal resistance of the inductor *and*

$P_{loss}$ : losses power.

$R$ : Resistive load.

$I_0$ : Load current.

$P_0$ : Output power.

The relation between the duty cycle (D) and the efficiency can be seen in figure 3.5. Actually, efficiency of 71% to 97% are typically obtained.

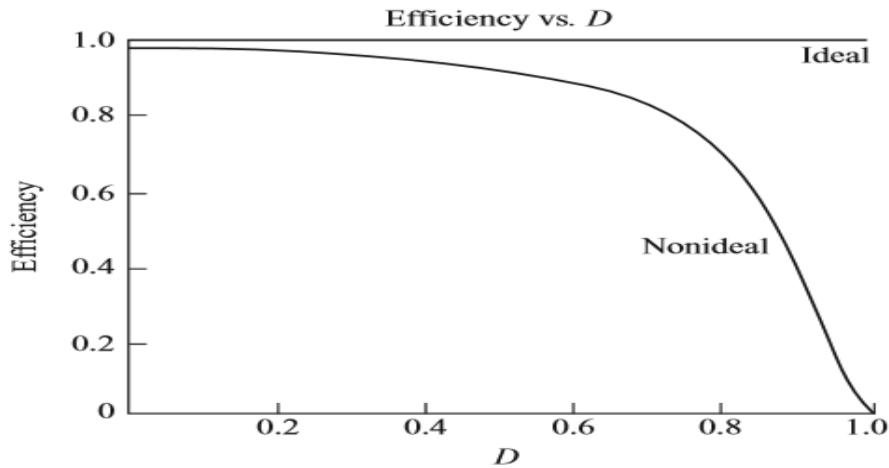


**Figure 3.5:** Boost converter efficiency.

### 3.3 MPPT Algorithms

The literatures are rich with many type of MPPT techniques and with variable complexity [11, 12,24,25]. The most popular MPPT method is P&O algorithm which is most used for evaluates the performance of MPPT comparing with other MPPT algorithms. The algorithms that will be presented in this study are:

1. P&O MPPT algorithm.
2. FLC based MPPT algorithm.
3. ANN based MPPT algorithm.
4. ANFIS based MPPT algorithm.

#### 3.3.1 Perturb and Observe Method

The perturb and observe MPPT technique is most common used method of MPPT that for its ease of implementation and simple structures and highly competitive against other MPPT methods [24,25,23]. The main idea of this method increases the  $D$  with initial value mostly 0.01 and observes the power perturbation of the PV. If it is positive then it runs in right direction and the operating point will be close to the MPP. As a result of this, new value added to the current value of  $D$  in the same direction. If the power perturbation of the PV is negative, the operation point goes far from the MPP. Therefore,  $D$  should be decreased [26].

Figure 3.4 show the flow chart of the P&O algorithm. The MPPT control system increment and decrement the PV voltage periodically. First step is measuring the

$I_{pv}(k)$  current and voltage  $V_{pv}(K)$  at current iteration  $k$  and calculate  $P(k)$  by following:

$$P_{pv}(k) = I_{pv}(k) * V_{pv}(k)$$

$$P_{pv}(k-1) = I_{pv}(k-1) * V_{pv}(k-1)$$

$$\Delta P_{pv} = P_{pv}(k) - P_{pv}(k-1) \quad (3.10)$$

$$\Delta V_{pv} = V_{pv}(k) - V_{pv}(k-1) \quad (3.11)$$

$$D = D(k) - \Delta D \quad (3.12)$$

where:

( $k-1$ ): mention to previous iteration.

$\Delta D$ : constant value mostly less than 0.05.

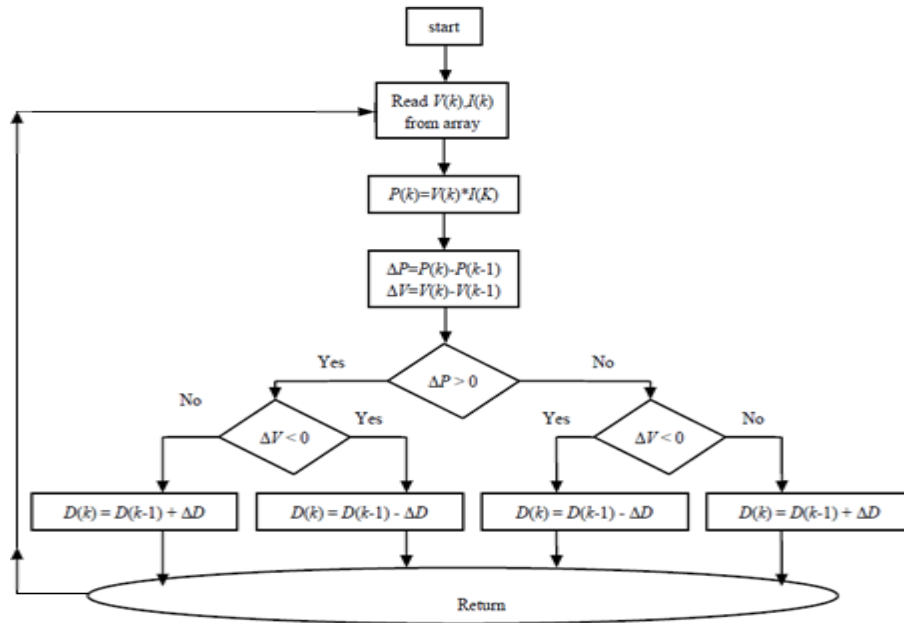


**Figure 3.4:** P&O MPPT Algorithm flowchart.

As shown in Figure 3.5, if the operating point is in the left of MPP, then the increasing in the voltage gives positive power drawn from the PV array and the operating point becomes closer to the MPP. If the current is negative perturb, that causes decreasing in the power of the PV. This means that the operation point is moving away from the MPP. Therefore, the perturbation of the operating current should be reversed [32].

One of the disadvantage of this algorithm is that the time response depends on the step size of the  $\Delta D$ . So, if  $\Delta D$  is large value, the time response will become fast to reach

MPP. However, the operation point is not actually at MPP because of large perturbation.

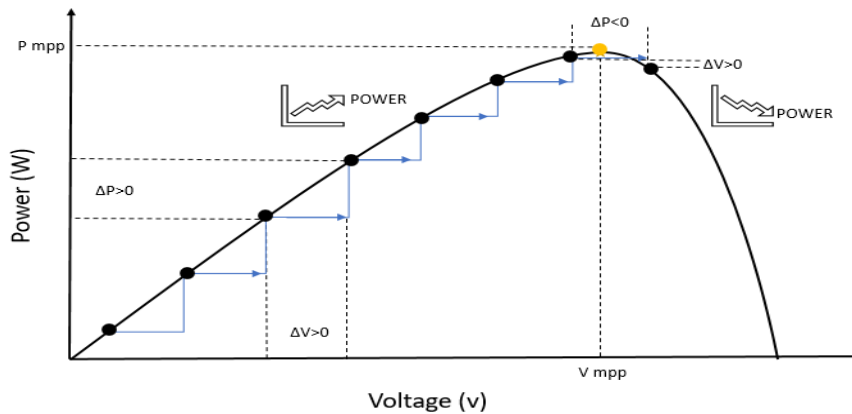
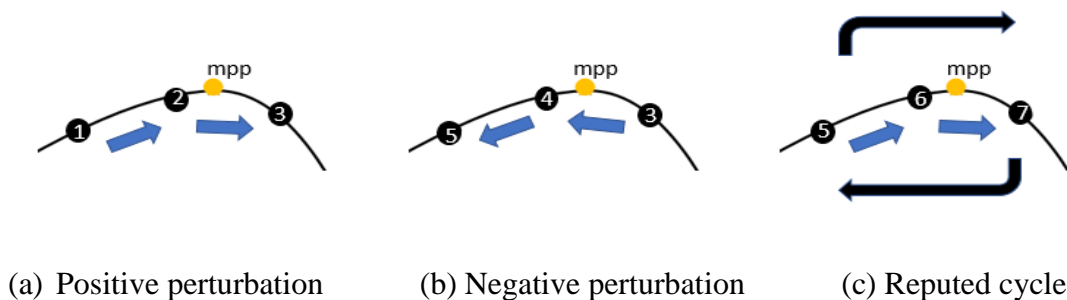


**Figure 3.5:** Understanding P&O running on I-V curve of the PV.

In contrast, if the step size of  $\Delta D$  is small value, the time response will become slow to reach MPP. However, the operation point is very close to actual MPP and perturbation is small. Assume that the operation point is at point 1 and by increasing  $D$  with positive  $\Delta D$ , the voltage will increase and power with positive perturbation will be at point 2 close to actual MPP, but the value is less than MPP (figure 3.6 (a)). Therefore, the algorithm will increase  $D$  with same value of  $\Delta D$  that will increase voltage, but the operation will move away from the actual MPP at point 3 (figure 3.6 (b)). In addition, the perturbation will be negative then the next step will be back to point 4, to point 5, and from point 5 to point 6 and so on. This process makes the operation point increasing and decreasing around the actual MPP. This cycle repeats while the system is running (Figure 3.6(c)) [17,18].



(a) Positive perturbation

(b) Negative perturbation

(c) Repeated cycle

**Figure 3.6:** Perturbation of operation point around actual MPP.

The process of increasing and decreasing  $D$  is written as it shown in Table 3.1.

**Table 3.1:** Truth table of the P&O MPPT algorithm

Sign of $\Delta V$	Sign of $\Delta P$	Direction of next step
+	+	$+\Delta D$
-	-	$+\Delta D$
-	+	$-\Delta D$
+	-	$-\Delta D$

P&O controller output decision is  $\Delta D$  that will be added to current operation  $D$  increasing and decreasing with constant step size based on Table 3.1.

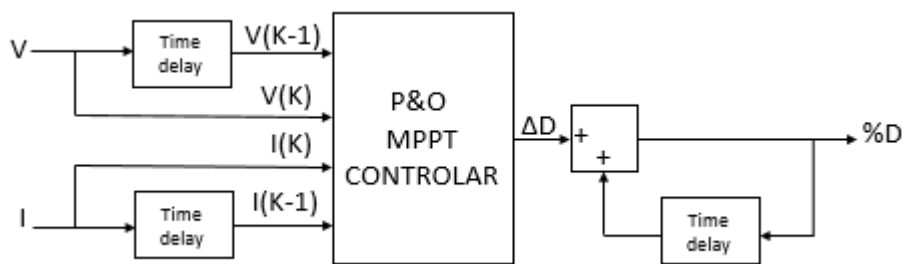


**Figure 3.7:** Block diagram of P&O MPPT algorithm.

### 3.3.2 Fuzzy Logic Control based MPPT

The Fuzzy Logic tool was presented in 1965 by Professor: L. A. Zadeh in his famous paper fuzzy set. Fuzzy Logic is a form of logic used to express expert systems. It has been used in many fields, from control theory to artificial intelligence applications. It deals with uncertainty between sets. In classical logic, the relationship between two sets could be true or false, 0 or 1 and Belong not belong. but in fuzzy logic sets are overlapped and the relationship between two sets could be Belonging partially with value between 0 and 1. Fuzzy logic deals with degrees of membership between sets and allows for its members to have degrees of membership.

To understand what is the different between classic logic and fuzzy logic. From the practical concept of the P & O method and from Table 3.1, there are two possibilities for changing the duty cycle either forward or backward with a fixed step size with two cases:

If the operation point located in the left of MPP, then the method increases the duty cycle. If the operation point located in the right then the method decreases the duty cycle (figure 3.8). That means all operation point in the left of the MPP will be

considered as in the left whether its location far or close from MPP. Therefore, the reaction will be go forward with same fixed initial duty cycle [26].

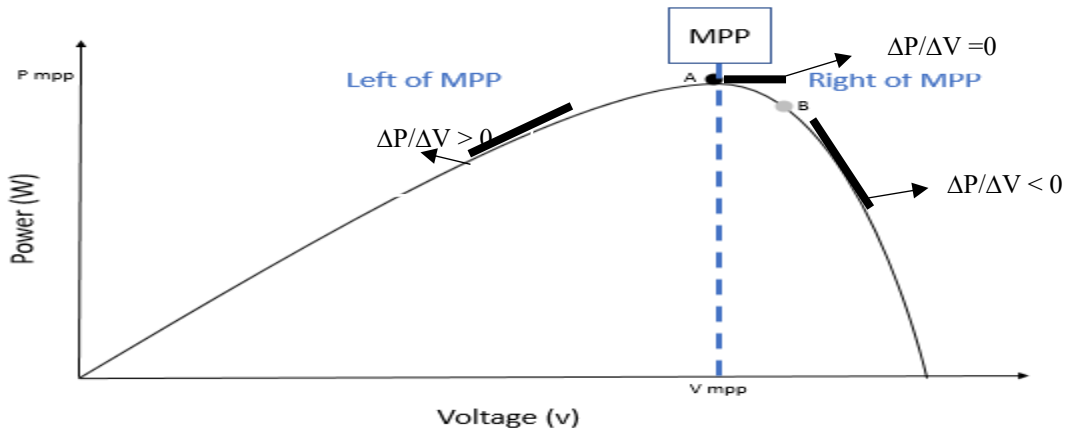


**Figure 3.8:** Situations of the operation point on the P-V curve.

Consider the location of the operating point is located at B point in I-V (figure 3.8). In classical set, it belongs to the right set only. But by using fuzzy sets, it can be seen that point considered as right set with membership degree 0.7. also, it can be considered as it belongs to the left set with membership degree 0.3. Fuzzy sets allow their members to have degrees of membership (figure 3.9). The x axis represents the crisp value of the power and y axis represents the belonging degree.

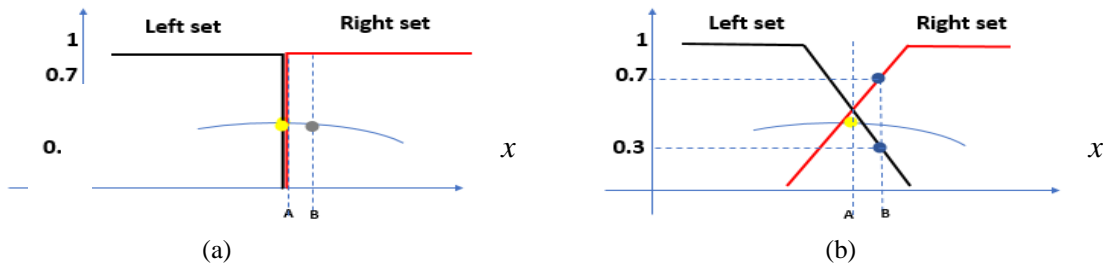


**Figure 3.9:** (a) Classical sets. (b) Fuzzy sets.

Fuzzy logic system has fast, smooth response and less complexity than traditional systems [13]. Fuzzy logic has a simple rule-based IF X AND Y THEN Z approach to a solving control problem rather than attempting to model a system mathematically [18].

### 3.3.2.1 Fuzzy Logic Control Cine Steps

To implement fuzzy logic technique to a real application requires the following three steps:



**Fuzzification** – convert input value into fuzzy value by using one of fuzzy sets and Membership functions (MFs) form mostly triangle sets are used (figure 3.10).

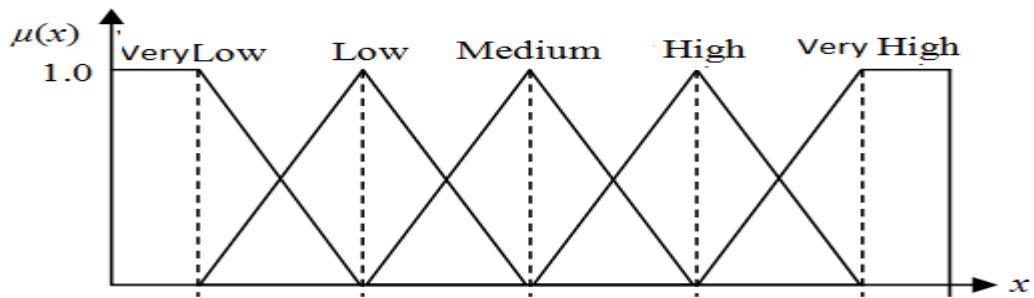


**Figure 3.10:** Triangle fuzzy sets.

Where X axis represents the crisp input and each set has its linguistic variable. Y axis represent the membership degree. Linguistic variable of each set describes the range situation of the crisp input X.

1. **Fuzzy Inference Process (Rule)** – deriving the membership function from the control rules to derive the fuzzy output. This process determines one set from group sets by using operation (And, Or and Not) and determines its membership degree. It easy to build rule base because it is close to human languages, IF input high THEN output is low.
2. **Defuzzification** – after defining the set with its membership degree that between 0 to 1. The process in the output fuzzy sets defines the area under this degree. this area is fuzzy output as it shown in figure 3.11. by calculating centroid of the area or center of gravity, the fuzzy output converts to crisp output. There are three defuzzification techniques are commonly used [14]: Mean of Maximum method, Center of Gravity method and the Height method. The following section will explain the design of each step based on P&O algorithm concept [26].

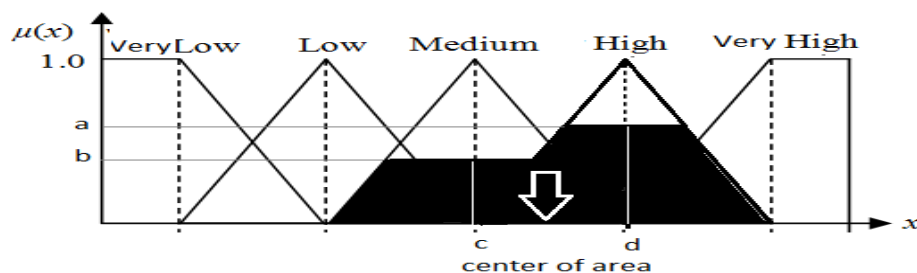


**Figure 3.11:** DE fuzzification converts fuzzy output to crisp output.

### 3.3.2.2 Fuzzy Controller Based MPPT

To implement table 3.1 based fuzzy logic, we must find where the operation point is .is it in the left or in right or is it at MPP.

As it is shown from previous figure 3.9 P-V curve:

- If  $\Delta P/\Delta V = 0$ : that means the point at MPP on the curve. So, there is no reaction comes from the controller.
- If  $\Delta P/\Delta V < 0$ : that mean the point in the right MPP on the curve. The reaction should be decreasing the voltage by decreasing D% duty cycle of the boost converter until reaching MPP at  $\Delta P / \Delta V = 0$  that means controller stop decreasing the voltage.
- If  $\Delta P / \Delta V > 0$ : that means the point on the left MPP the reaction should be increasing the voltage until reaching MPP at  $\Delta P / \Delta V = 0$ . At this point the controller stops increasing the voltage.

By these concepts, fuzzy controller takes samples from the output of the PV current ( $I_{pv}$ ), voltage ( $V_{pv}$ ) at time or iteration (k), calculate the result power  $P_{pv}(k)$  with the previous sample at previous time (k-1), calculate the error E(k) and the change in error  $\Delta E(k)$  :

$$P_{pv}(k) = I_{pv}(k) * V_{pv}(k).$$

$$P_{pv}(k-1) = I_{pv}(k-1) * V_{pv}(k-1).$$

$$\Delta P_{pv} = P_{pv}(k) - P_{pv}(k-1).$$

$$\Delta V_{pv} = V_{pv}(k) - V_{pv}(k-1).$$

$$E(k) = \frac{\Delta P_{pv}}{\Delta V_{pv}} \quad (3.13)$$

$$\Delta E(k) = E(k) - E(k-1) \quad (3.14)$$

The first step the controller dose, the fuzzification process. process the crisp input to get the linguistic variables using the membership functions. In this case, there are five fuzzy sets with linguistic variable name: NB (negative big), NS (negative small), ZE (zero), PS (positive small), and PB (positive big). Controller has two inputs and one output. the numeric variables are E(K) and  $\Delta E(K)$  for inputs and D duty cycle for output. Each input has its MFS and same for the output (figure 3.12). The value of a and b in the are selected by experience to get best performance [1,26].

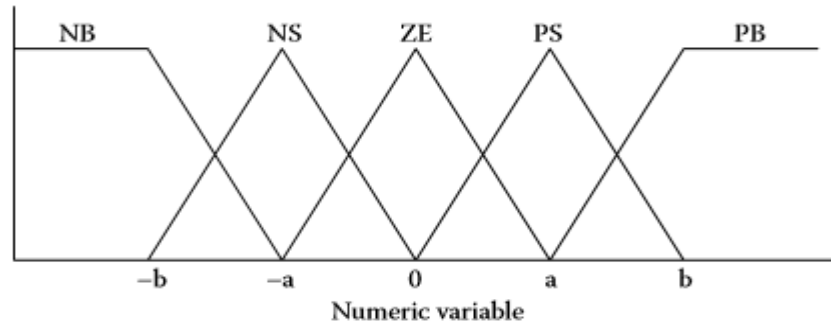


**Figure 3.12:** Membership function for inputs and outputs of MPPT based FLC [1]

See figure 3.13 Fuzzy logic controller output diction is  $\Delta D$  that will be added to current operation  $D\%$  increasing and decreasing with variable step size based on defuzzification process in the output membership functions and rules in Table 3.2.

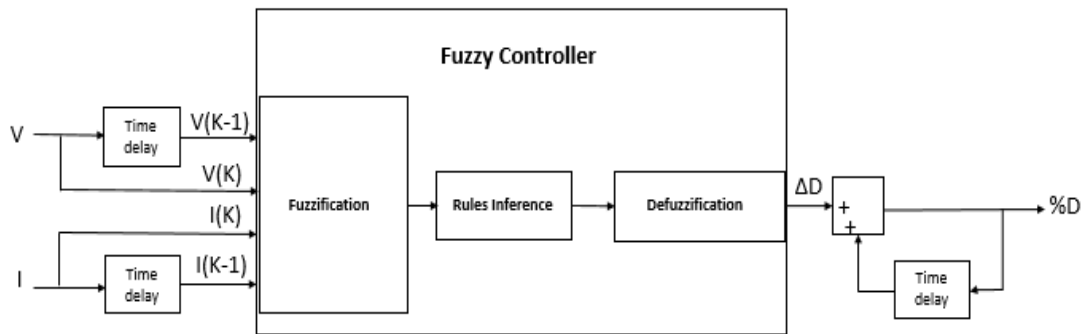


**Figure 3.13:** MPPT based fuzzy logic control Block diagram.

The rules base of this fuzzy logic controller is written as in this table 3.2. [1].

**Table 3.2:** Rule base of fuzzy logic controller based MPPT.

$E(K)$ $\Delta E(K)$	<i>PB</i>	<i>PS</i>	<i>ZE</i>	<i>NS</i>	<i>NB</i>
<i>PB</i>	<i>ZE</i>	<i>ZE</i>	<i>NB</i>	<i>NB</i>	<i>NB</i>
<i>PS</i>	<i>ZE</i>	<i>ZE</i>	<i>NS</i>	<i>NS</i>	<i>NS</i>
<i>ZE</i>	<i>ZE</i>	<i>ZE</i>	<i>ZE</i>	<i>ZE</i>	<i>ZE</i>
<i>NS</i>	<i>PS</i>	<i>PS</i>	<i>PS</i>	<i>ZE</i>	<i>ZE</i>
<i>NB</i>	<i>PB</i>	<i>PB</i>	<i>PB</i>	<i>ZE</i>	<i>ZE</i>

For example, to understand the rules in Table 1, IF  $\Delta E(K)$  is PB and  $E(K)$  is NS THEN  $\Delta D$  is NB. This means that if the operating point is far from MPP towards right hand side and the change in  $E(K)$  is small, then the controller should decrease the duty ratio largely for reaching MPP [1].

IF  $\Delta E(K)$  is PS and  $E(K)$  is NS THEN  $\Delta D$  is PS. This means that the operating point is close to MPP towards left side and the change in voltage is positive, then the controller should increase the duty ratio by small value for reaching the MPP. When both the  $\Delta E(K)$  and  $E(K)$  are changing by small value, it means that the system close to MPP [1].

### 3.3.3 Neural Networks Based MPPT

MPPT based neural network is an intelligent control technique [27,1]. Artificial Neural Networks (ANN) is a network that imitates the biological neural of the human system which contains a large parallel interconnection of massive number of neurons. that do many different tasks in very small time even as comparing today to high speed of computers. networks behavior, widely used in modeling complex relationships between inputs and outputs in linear and nonlinear systems and to data mapping. Network structure of three layers can be as following:

- input layer: it contains the input features represented by nodes. Each node is connected to every single node in the hidden layer. The connections have their weightiness that will be adjusted in the training process.
- hidden layer: first it takes summation of the multiplication of each input node with connected weights than the output of hidden node is calculating by apply the activation function. function typically ramp, threshold or sigmoid.
- output layer: is repeated the same process that in the hidden layer to get the output. Figure 3.12 shows these layers.

There are many structures of networks [29]. The structure type of neural network that is used for build MPPT controller is multi-layer feed forward networks. Inputs of the MPPT controller in the input layer are generally two-node PV set parameters, such as radiation (G), temperature (T) and single output nodes in the output layer represents the output decision. By processing these inputs, controller determines the adapter operation duty cycle  $D$  as output resolution. Sigmoid function usually is used as activation function for each node. ANN must be trained off line before using it in the

system. Figure 3.14 shows network has three-layer. input layer **i** contains two nodes represent the two inputs ( $x_1, x_2$ ), hidden layer **j** contains three nodes and one output layer **y** contains one neuron connected to the previous neurons in the hidden layer [29].

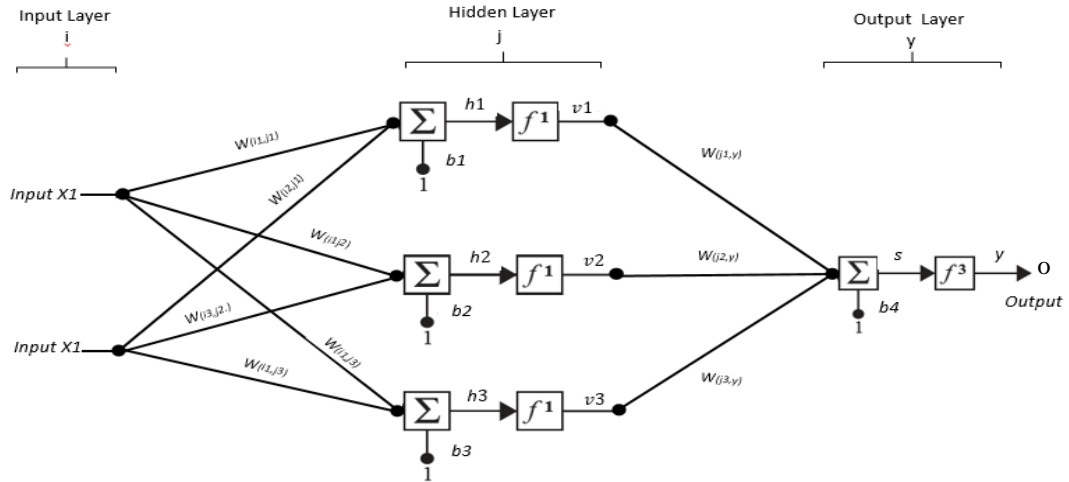


**Figure 3.14:** Three layer of multi-layer feed forward network.

From figure above the output of the network can be calculated by:

First calculate  $h_1, h_2$  and  $h_3$

$$h_1 = x_1 * W_{(j_1,i_1)} + x_2 * W_{(j_2,i_1)} + b_1$$

$$h_2 = x_1 * W_{(j_2,i_1)} + x_2 * W_{(j_2,i_2)} + b_2$$

$$h_3 = x_1 * W_{(j_3,i_1)} + x_2 * W_{(j_3,i_2)} + b_3$$

where:

$W_{(j,i)}$  are the weights of connections between input node **i** and the hidden neuron **j**.

$b_1, b_2, b_3$  and  $b_4$  : Bias parameters like the weights usually have constant of 1.

The node output in the hidden layer is calculating by applying the activation function ( $f$ ) sigmoid function is usually used as transfer function.

$$v_1 = f(h_1)$$

$$v_2 = f(h_2)$$

$$v_3 = f(h_3)$$

Calculate the summation of the multiplications of the output of the hidden neurons to their weights.

$$s_0 = v_1 * W_{(j_1,y)} + v_2 * W_{(j_2,y)} + v_3 * W_{(j_3,y)} + b \quad (3.15)$$

Then the output of the network  $y$  can be calculated by applying the activation function on  $s$ .

$$y = f(v_1 * W_{(j_1,y)} + v_2 * W_{(j_2,y)} + v_3 * W_{(j_3,y)} + b_4) = f(s) \quad (3.16)$$

where:

$W_{(j,y)}$  : weight connections between the node  $j$  and the output node  $y$ .

$f_1, f_2, f_3$  and  $f_4$  : transfer function usually sigmoid function is used it takes form:

$$y = f(s_0) = \frac{1}{1 - e^{-s_0}}$$

Note: all weights are adjustable parameters when the process of training is applied to the network. During the training process, all weights will be changed until the best fit is reached for the input and output shapes from training data set based on the minimum errors that are selected.

### 3.3.3.1 Backpropagation Learning Algorithm

Any ANN network must learn the tasks first before putting it in the system [29,30]. The type of learning that is used here is supervised learning algorithm which incorporates an external teacher and makes network learn from examples from training data. The teach way is by setting and adjusting weights between nodes during the training process. Firstly, weights are selected randomly. Supervisor Backpropagation learning algorithm is used for training the multilayer feed-forward network, it works to decrease the output error between the desired and calculated values. That by propagate the error from the output to input nodes. During this process and determine a new set of weights which makes the error become small. The general learning procedure in backpropagation algorithm is by following the steps and equations below:

Calculate the summation of the node in the hidden layer of network as following:

$$h_j = \sum(W_{(j,i)} * x_j) \quad (3.17)$$

apply activation function to get output of the hidden neuron is:

$$v_j = f(h_j) = \frac{1}{1 - e^{-h_j}} \quad (3.18)$$

Calculate Summation of the node in the output layer.

$$s_o = \sum(W_{(j,y)} * v_j) \quad (3.19)$$

apply activation function to get output of the output neuron.

$$y = f(s_o) = \frac{1}{1 - e^{-s_o}} \quad (3.20)$$

Then compute the cost function which is the mean square error in the output.

$$E = \frac{1}{2} \sum (y^d - y)^2 \quad (3.21)$$

where:

$y^d$  : desired output,  $y$  is calculated output.

E: Is the mean square error in the output.

Then update the old weight  $W_{(j,y)}$  in iteration  $k$  by:

$$W_{(j,y)(k+1)} = W_{(j,y)(k)} + \int * \frac{\partial E}{\partial W_{(j,y)}} \quad (3.22)$$

$$W_{(i,j)(k+1)} = W_{(i,j)(k)} + \int * \frac{\partial E}{\partial W_{(i,j)}} \quad (3.23)$$

where:

$\int$  : learning rate or correction factor constant effects on the step size of the minimizing the square error and it determine the speed learning if it is small the network learns slow.

Calculate the propagation error between hidden and output layer by finding the derivative of the error respect to the weights. Solve the partial derivatives of the error can be gotten using chain rule.

$$\frac{\partial E}{\partial W_{(j,y)}} = \frac{\partial E}{\partial y} * \frac{\partial y}{\partial W_{(j,y)}}, \text{ equation's derivative (3.21) respect to weight } W_{(j,y)}$$

$$\frac{\partial E}{\partial W_{(j,y)}} = -(y^d - y) * \frac{dy}{\partial W_{(j,y)}}$$

$$\frac{\partial y}{\partial W_{(j,y)}} = \frac{\partial y}{\partial s_o} * \frac{\partial s_o}{\partial W_{(j,y)}}, \text{ equation's derivative (3.20) respect to weight } W_{(j,y)}.$$

$$\frac{\partial y}{\partial s_o} = y(1 - y), \text{ equation's derivative (3.20) respect to } S_o \text{ equation (3.18)}$$

$$\frac{ds_o}{\partial W_{(j,y)}} = v_j, \text{ equation's derivative (3.19) respect to weight } W_{(j,y)}$$

$$\frac{\partial E}{\partial W_{(j,y)}} = y(1 - y) * v_j, \text{ equation's derivative (3.21) respect to weight } W_{(j,y)}$$

The new weight is:

$$W_{(j,y)(k+1)} = W_{(j,y)(k)} + \int * y * (1 - y) * v_j * -(y^d - y)$$

$$W_{(j,y)(k+1)} = W_{(j,y)(k)} + \int * \delta_j * v_j, \quad (3.24)$$

where:  $\delta_j = -y * (1 - y) * (y^d - y)$

Now calculate the propagation error to update  $W_{(i,j)}$  by calculate the derivative of the error respect to weights.

Solve:

$$\frac{\partial E}{\partial W_{(i,j)}} = \frac{\partial}{\partial W_{(i,j)}} \left( \frac{1}{2} \sum (y^d - y)^2 \right), \text{ equation's derivative (3.21) respect to the weight } W_{(i,j)}.$$

$$\frac{\partial E}{\partial W_{(i,j)}} = -(y^d - y) * \frac{\partial y}{\partial W_{(i,j)}}$$

$$\frac{\partial y}{\partial W_{(i,j)}} = \frac{\partial y}{\partial s_o} * \frac{\partial s_o}{\partial W_{(i,j)}}, \text{ equation's derivative (3.20) respect to the weight } W_{(i,j)}.$$

$$\frac{\partial s_o}{\partial W_{(i,j)}} = \frac{\partial s_o}{\partial h_i} * \frac{\partial h_i}{\partial W_{(i,j)}}, \text{ equation's derivative (3.19) respect to the weight } W_{(i,j)}.$$

$$\frac{\partial s_o}{\partial h_i} = \frac{\partial s_o}{\partial v_j} * \frac{\partial v_j}{\partial h_i}, \text{ equation's derivative (3.19) respect to } h_i \text{ equation (3.16)}$$

$$\frac{\partial y}{\partial W_{(i,j)}} = \frac{\partial y}{\partial s_o} * \frac{\partial h_i}{\partial W_{(i,j)}} * \frac{\partial s_o}{\partial v_j} * \frac{\partial v_j}{\partial h_i} = x_i * W_{(i,y)} * v_j * (1 - v_j) * y(y^d - y)$$



Finally find the new  $W_{(i,j)}$  using equation:

$$W_{(i,j)(k+1)} = W_{(i,j)(k)} - \int * x_i * W_{(i,y)} * v_j * (1 - v_j) * (y^d - y) * y(y^d - y)$$

$$W_{(i,j)(k+1)} = W_{(i,j)(k)} + \int * \delta_i * v_j \quad (3.25)$$

Where:

$$\delta_i = -\delta_j * v_j * (1 - v_j) * y(y^d - y)$$

These steps should be done for one samples from the training data. Firstly, all weights are selected randomly and select the minimum error that is allowable. Then feed the network forward to calculate the actual output. If the result is not same to the desired output that means the mean square error is bigger than the allowable error [30]. In this case, the previous steps are followed to adjust the weights to minimize the error and done continuously until error becomes small. So, algorithm learn through iterations. Number of iterations in typical network can be any number from five to ten thousand. So, learning it can be done by hand for very small amount of training data, but for large training date computer is used to train the network. **MATLAB** program has neural network tools which make it easily to build the network and train it, using any training data.

Neural network will be built in this study and trained in the next chapter using data contains all possible operation temperature and solar irradiation and their best decision of D to work as MPPT controller to control D% signal that goes to the switch of the boost converter for guiding the system to work at MPP state (figure 3.15). Well trained network gives superior performance of the ANN based MPPT controller.

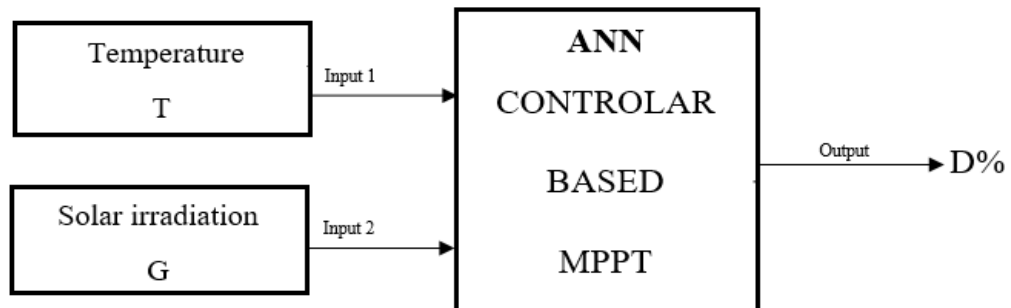


**Figure 3.15:** Block diagram of ANN based MPPT algorithm.

### 3.3.4 Adaptive Neuro-Fuzzy Inference System Based MPPT

Another MPPT algorithm used artificial intelligence technique called ANFIS which is efficient algorithm to work with MPPT concept, and has been applied and proved its efficient [35,38].

Fuzzy logic system is useful tool for building system based human thinking and doesn't need to model the system mathematically. Output decision of FLC is based on written rules and making defuzzification on the output membership functions parameters. these parameters are designed by an expert or by experiences and adjusting many time to improve the performance of the controller for approximating nonlinear functions. Artificial neural network system has capabilities of learning from examples or learning from data using training algorithm as it seen in the previous section.

An adaptive neuro-fuzzy inference system or adaptive network-based fuzzy inference system has been introduced by Jang in [33] to construct a fuzzy logic controller. ANFIS is form of ANN that is uses learning capabilities with hybrid learning of ANN to generate fuzzy IF-THEN rules and select the MFs parameters of the Takagi–Sugeno fuzzy inference system a set of input and output samples from training data to mapping or approximating any nonlinear system. The architecture of ANFIS is as shown below [36].

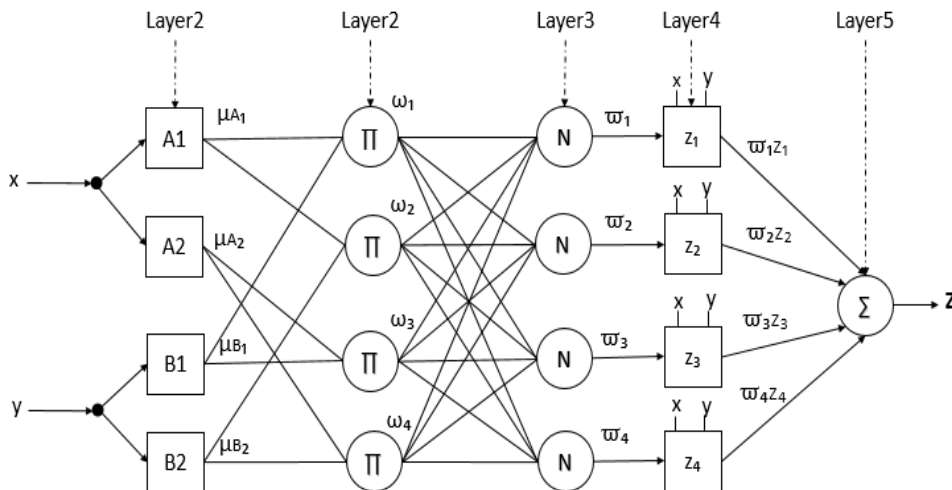


**Figure 3.16:** Architecture of ANFIS with four rules and two membership function.

ANFIS in figure has two inputs  $x$  and  $y$  and one output  $z$ . the fuzzy if-then rules can be expressed as:

Rule: If  $x$  is  $A$  and  $y$  is  $B$ , then  $z = p x + q y + r$ .

where  $A_i$  and  $B_i$  are the fuzzy sets in the antecedent, and  $p_i$ ,  $q_i$ , and  $r_i$  are parameters which are determined during the training process.

### 3.3.4.1 Structure of ANFIS

ANFIS consists five layers. There are nodes in each layer depends on number of inputs, membership function and rules and usually, one output as it is seen in figure 3.14:

- **Layer 1:** this layer consists number of nodes  $i$  and represents inputs membership functions.

$$O_{(1,i)} = \mu_{A_i(x)}, \quad i = 1, 2 \quad (3.26)$$

$$O_{(1,i)} = \mu_{B_i(x)}, \quad i = 3, 4 \quad (3.27)$$

where:

$\mu_{A_i(x)}$  and  $\mu_{B_i(x)}$  are Membership functions. They can be obtained by fuzzification process for example Triangular membership function mostly used has equation of:

$$\text{Triangle}(x; a, b, c) = \begin{cases} 0, & x \leq a \\ \frac{x-a}{b-a}, & 0 \leq x \leq b \\ \frac{c-x}{c-b}, & b \leq x \leq c \\ 0, & b \leq x \leq c \end{cases} \quad (3.28)$$

where  $\{a, b, c\}$  are the parameters set that changes the shapes of the MFs and Parameters in this layer are called premise parameters

- **Layer 2:** each node in this layer receives the linguistic variables with MF degrees and calculates the firing strength of a rule via multiplication and sent it to next layer send the firing. or T-norm operators can be used as AND function to rule firing [32].

$$O_{(2,k)} = \omega_k = A_i(x) * B_i(x), \quad i=1, 2; j=1, 2; k=2(i-1) + j \quad (3.29)$$

Where  $k$ : represents the output number.

- **Layer 3:** Outputs are called normalized firing strengths that by calculate the ratio of firing strength rule in the  $i$  node that comes from previous node to the sum of all rule's firing strengths.

$$O_{(3,i)} = \bar{\omega}_i = \frac{\bar{\omega}_i}{\omega_1 + \omega_2 + \omega_3 + \omega_4}, \quad i=1,2,3,4 \quad (3.30)$$

- **Layer 4:** Output of each node in this has the following function:

$$O_{(4,i)} = \bar{\omega}_i z_i = \bar{\omega}_i (p_i x + q_i y + r_i), \quad i=1,2,3,4 \quad (3.31)$$

where  $\bar{\omega}_i$ : is referred to as the normalized firing strength from layer 3

$p_i, q_i$  and  $r_i$ : is the parameter set of  $i$  node. These are referred to as consequent parameter

- **Layer 5:** The output node in this layer computes the overall output as the summation of all incoming signals divided summation of all weights or all rule's firing strengths from layer 2. expressed as:

$$\begin{aligned} O_5 &= \frac{\omega_1 z_1 + \omega_2 z_2 + \omega_3 z_3 + \omega_4 z_4}{\omega_1 + \omega_2 + \omega_3 + \omega_4} = \sum_{i=1}^4 \bar{\omega}_i z_i = \sum_{i=1}^4 \bar{\omega}_i (p_i x + q_i y + r_i) \quad (3.32) \\ &= \bar{\omega}_1 (xp_1 + yq_1 + r_1) + \bar{\omega}_2 (xp_2 + yq_2 + r_2) + \bar{\omega}_3 (xp_3 + yq_3 + r_3) \\ &\quad + \bar{\omega}_4 (xp_4 + yq_4 + r_4) \end{aligned}$$

### 3.3.4.2 Basic ANFIS Learning Algorithm

The structure of a ANFIS is like a multi-layer neural network. The square nodes in figure 3.14 have adjustable parameters and the circle nodes has fixed parameters. The basic learning algorithm to optimize ANFIS parameters are backpropagation gradient descent algorithm which has been used to learn the multi-layer ANN (see section 3.3.3.1) [37]. During the learning process, the premise parameters ( $a, b, c$ ) in the layer 2 and the consequent parameter ( $p_i, q_i, r_i$ ) in the layer4 are updated based to training data and trained until the desired output is gotten.

first things, the training data set should be available to feed the inputs. ANFIS network mostly has two inputs. Second thing, is selecting the number of the MFs for each input that define the kind of functions. The triangular MFs are selected in this study which has parameter ( $a, b, c$ ) see equation (3.27). These parameters are named premise parameters. number of rules can be determined by multiplication of number of sets of each inputs with number of set in the input 2. Then it calculates the final output and total square error by:

$$E = \frac{1}{2} \sum (O^d - O_a)^2 \quad (3.32)$$

Where  $O^d$  : desired output.

$O_a$ : actual output.

The general equation of backpropagation for updating both the premise and consequent parameters is:

$$\alpha_{(k+1)} = \alpha_{(k)} + \eta * \frac{\partial E}{\partial \alpha} \quad (3.33)$$

Where:

$\alpha$  : is any update wanted parameter

$\eta$ : learning rate

$\alpha$  : is any update wanted parameter

k: iteration number.

There is another learning algorithm called the hybrid learning algorithm, which uses the least square method and the backpropagation algorithm. This algorithm has a twostep process.

1. Forward pass: the consequent parameters are updated by least square method which assume the parameters in equation (3.31) as linear combination.
2. Backward pass: the premise parameters are updated by backpropagation gradient descent method. In this study, we just used pack propagation method.

From training data, which is contains vector of inputs represent the operation temperature, operation solar irradiation and vector represent the best decision of duty cycle that will be given to the system to run at MPP. MPPT based ANFIS have been seen the literatures [35,34]. MATLAB program has ANFIS tool which will be used to build ANFIS controller and will learned. The proposed ANFIS controller based MPPT black diagram is shown in figure below.

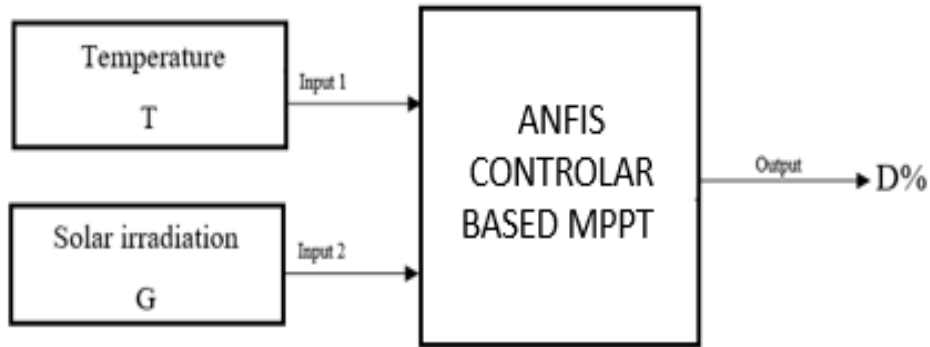


**Figure 3.17:** Black diagram of ANFIS based MPPT

### 3.4 MPP Tracking efficiency

The tracking efficiency of the MPPT algorithm can be calculated by the following:

$$\eta\text{-MPPT} = (P_{out}) / (P_{mpp}) \quad (3.34)$$

where:

$P_{mpp}$ : the maximum theoretical power.

$P_{out}$ : the power extracted from the PV that work with MPPT algorithm [39].

Note that the  $\eta$  -MPPT is physical efficiency of the converter.

Next section will be implementation all presented MPPT algorithms in this chapter using MATLAB program. In addition, will be run each algorithm with PV system in Simulink environment to analyze the performance of each case.

## 4 PV MODEL AND CASE STUDIES SIMULATIONS

### 4.1 Introduction

This section shows all systems simulations: The Photovoltaic PV model, boost converter, MPPT controller based P&O, FLC, ANN, and the proposed ANFIS. All the circuit simulations are made using MATLAB/Simulink Program. In this chapter; The case studies and simulation results for the complete system is discussed. Next section contains modeling a general PV panel and shows some of results about effects of T and G on PV output power and MPP operation. Figure 4.1 shows the block diagram connections of purposed MPPT controllers with PV system.

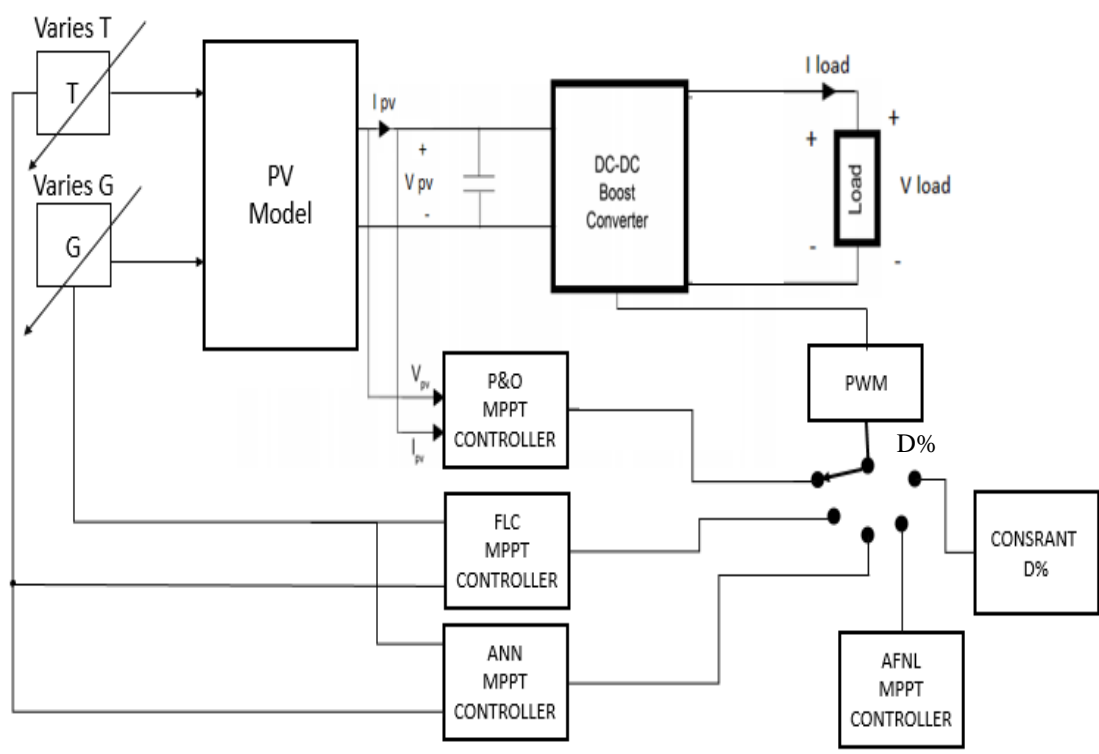


**Figure 4.1:** Block diagram for all system connections.

### 4.2 PV Model Simulation

The first objectives of this study, is to simulate a PV model and to estimate the I-V characteristic curves of PV under different operation of T and G, and to use simulated model for testing the dynamic performance of MPPT later.

The simulation is done by MATLAB Simulink and by modeling the equations (2.1), (2.2), (2.3) and (2.4). Using subsystem blocks and building general system that can model any PV system contained one model or more than one model as array (figure 4.2). For more information subsystem blocks see Appendix A.

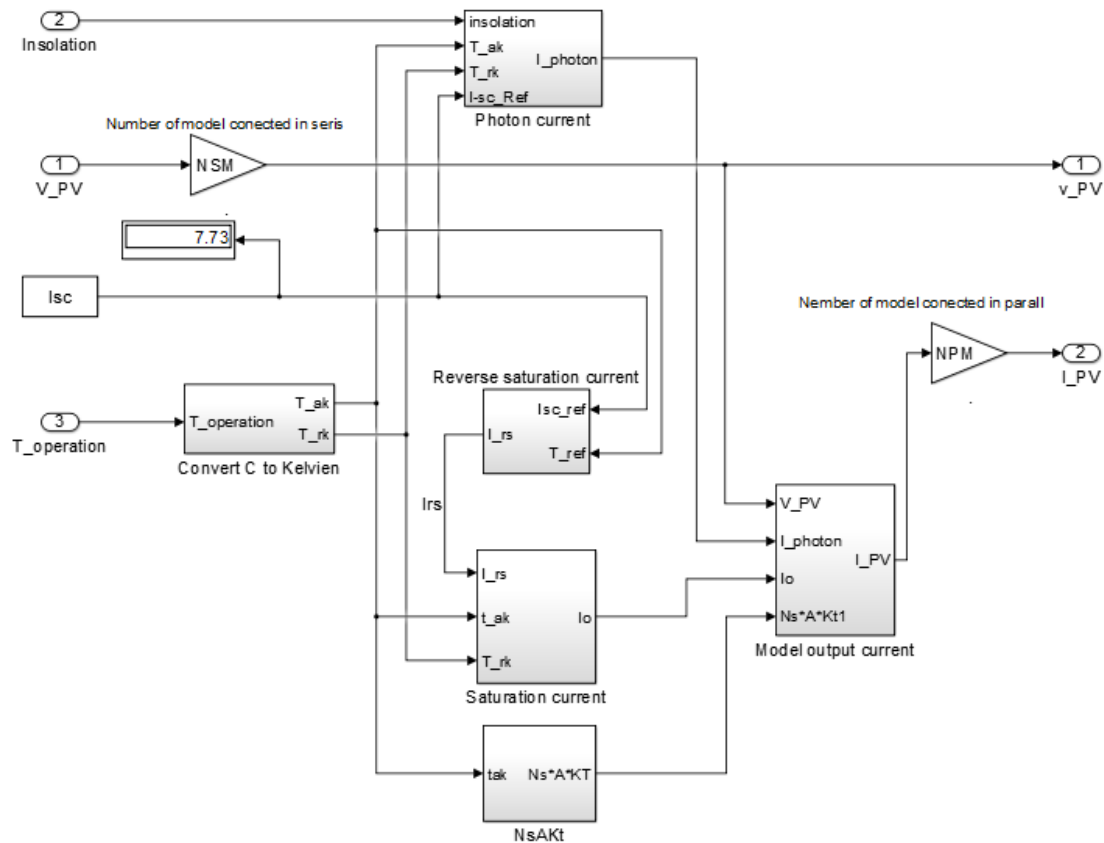
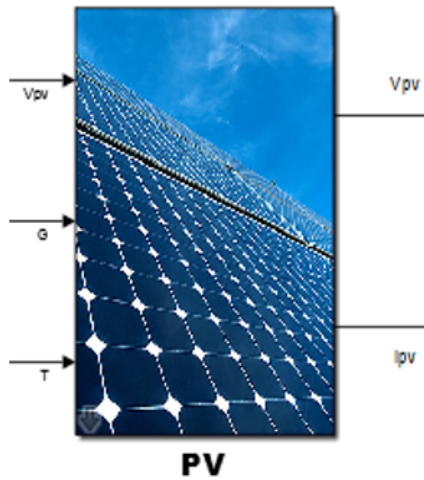


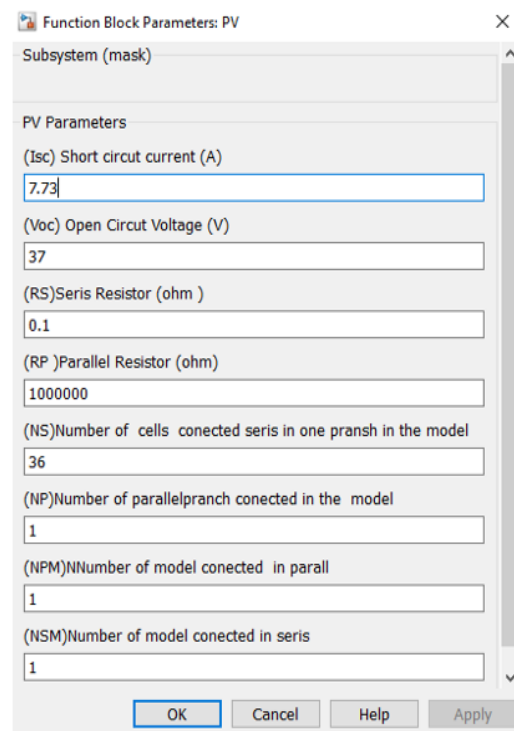
**Figure 4.2:** Internal subsystems of the PV model.

The previous subsystems are shortened in one block ( Figure 4.3 (a)). There are some parameters is designed to be adjustable (Figure 4.3 (b)) by using mask parameter property. The PV model contains temperature (T) and solar irradiance (G) input which will use as adjustable values for testing and analysis the performance of the PV model (figure 4.3 (a)). For more details see appendixes A.





(a)



(b)

**Figure 4.3:** The main model of the PV. (a) PV model block. (b) Subsystem mask parameters of the PV model.

#### 4.2.1 Temperature and Solar Irradiation Affection on I-V curve

Photovoltaic PV cell has nonlinear characteristics as the I-V curve profs that, and output power are affected with the change of the operating conditions (T and solar G), (figure 2.6), [9, 8].

#### 4.2.2 Simulation Testing

A PPS130W AS8118 PV module that has characteristic data is shown in Table 1. It has taken as the reference for simulation and analyzing temperature and solar irradiance affections on the output power.

Note: The electrical data are STC when G equal to of 1 kW/m<sup>2</sup>, and T equal to 25 C°. see appendix A for more information.

**Table 4.1:** Electrical Data of PPS130W AS8118 PV Module

<i>Electrical Data Under STC</i>	<i>Value</i>
<i>Maximum Power (<math>P_{max}</math>)</i>	130W
<i>Maximum power voltage (<math>V_{mpp}</math>)</i>	18V
<i>Maximum Power current (<math>I_{mpp}</math>)</i>	7.23A
<i>Open Circuit Voltage (<math>V_{oc}</math>)</i>	22.5V
<i>Short Circuit Current (<math>I_{sc}</math>)</i>	7.81A
<i>Number of Cells</i>	36 pcs
<i>Temperature coefficient of (<math>I_{sc}</math>)</i>	0.055% /°C

Testing the model is done by connect it with variable resistor load. This resistor is controlled to start from short circuit to open circuit and to plot relationship between current and voltage; which represent I-V curve and power and voltage; which represent P-V Curve. The block diagram of the testing circuit is below.

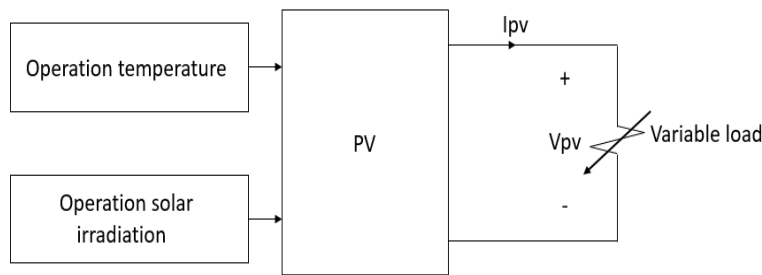


**Figure 4.4:** Block diagram testing of the PV mode.

In addition, importing the result of G, T, P, V and I to MATLAB to work-Space to find out the PMPP and VMPP for each case and plot the relations using program code is written in MATLAB M.file (Appendix B) . The simulation circuits are show below.

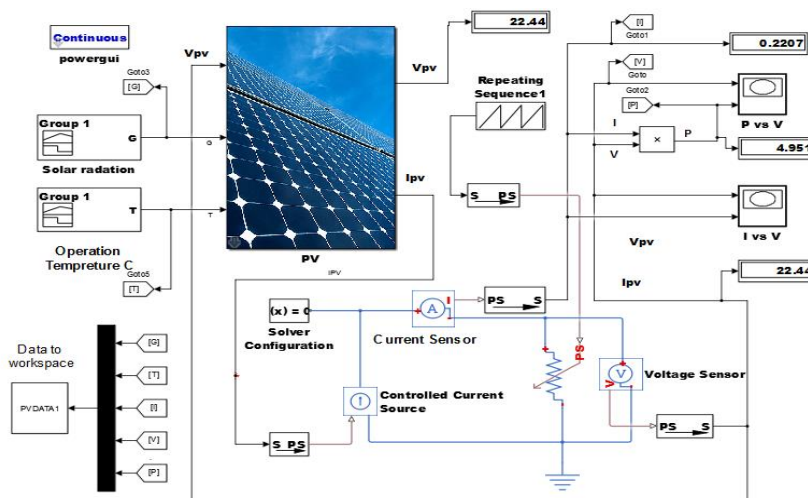


**Figure 4.5:** MATLAB simulation circuit for testing PV simulation model.

### 4.2.3 Simulation Results of PV model Testing and Conclusion

The first test was done by Applying Constant  $G$  1000  $\text{kw}/\text{m}^2$  with the changing in  $T$  from  $5\text{ C}^\circ$  to  $40\text{ C}^\circ$  with step of  $5\text{ C}^\circ$ . The results in figure 4.6 show that Whenever the temperature increases, the voltage and power output decreases and vice versa.

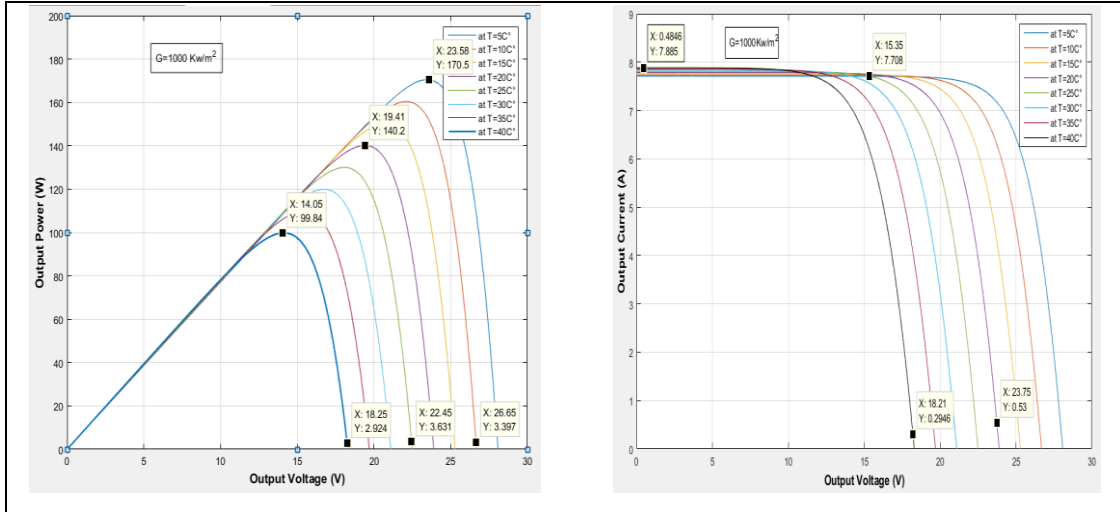


**Figure 4.6:** Influence of the temperature on  $V$ - $I$  and  $P$ - $V$  curves.

The second simulation test is done by applying constant  $T$   $25^\circ$  with changing in  $G$  from  $650\text{ kw}/\text{m}^2$  to  $700\text{ kw}/\text{m}^2$  with increasing step of  $50\text{ kw}/\text{m}^2$ . The results in the figure 4.7 show that whenever the solar radiation increases, the short current operation and power output increase. And vice versa with small changing in voltage.

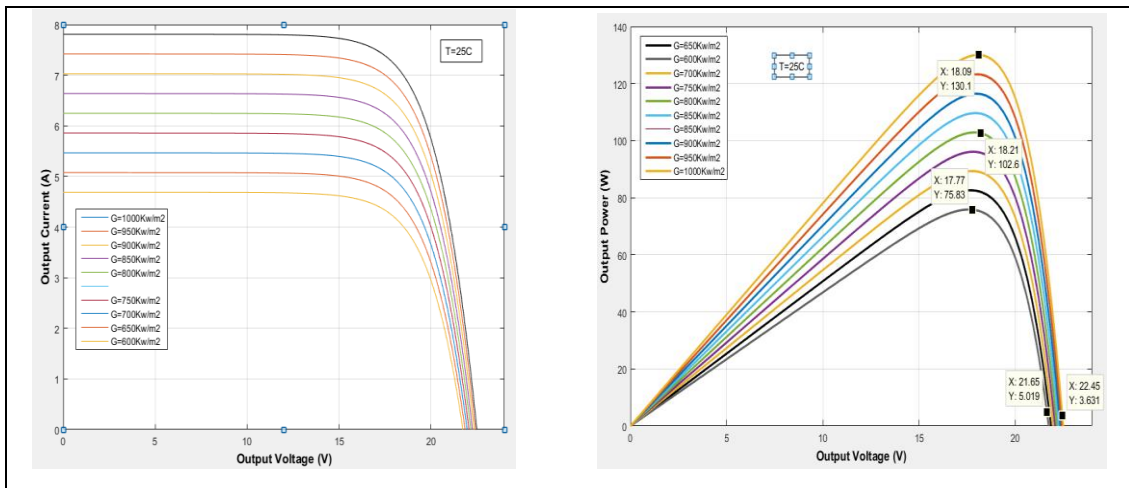


**Figure 4.7:** Influence of the solar radiation on  $V$ - $I$  and  $P$ - $V$  curves.

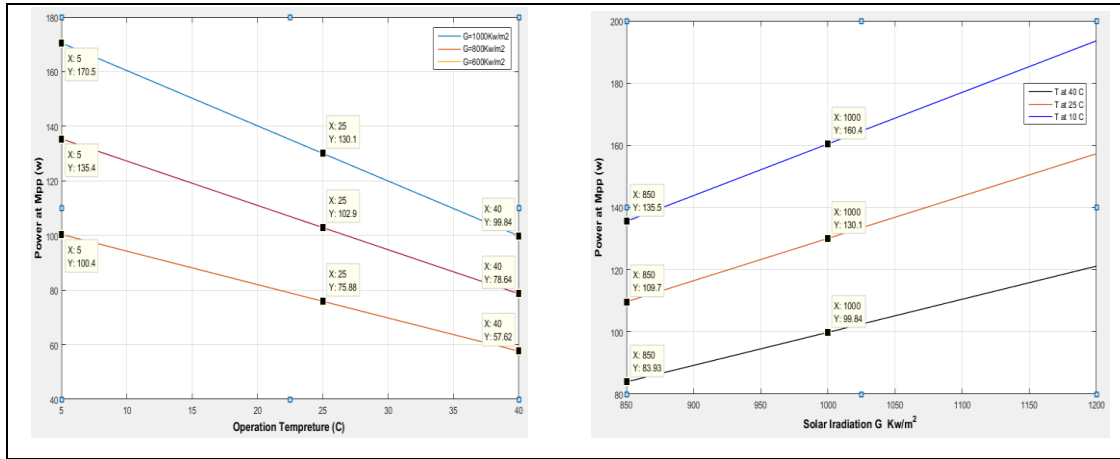


**Figure 4.8:** Influence of solar radiation and temperature on  $P_{mpp}$ .

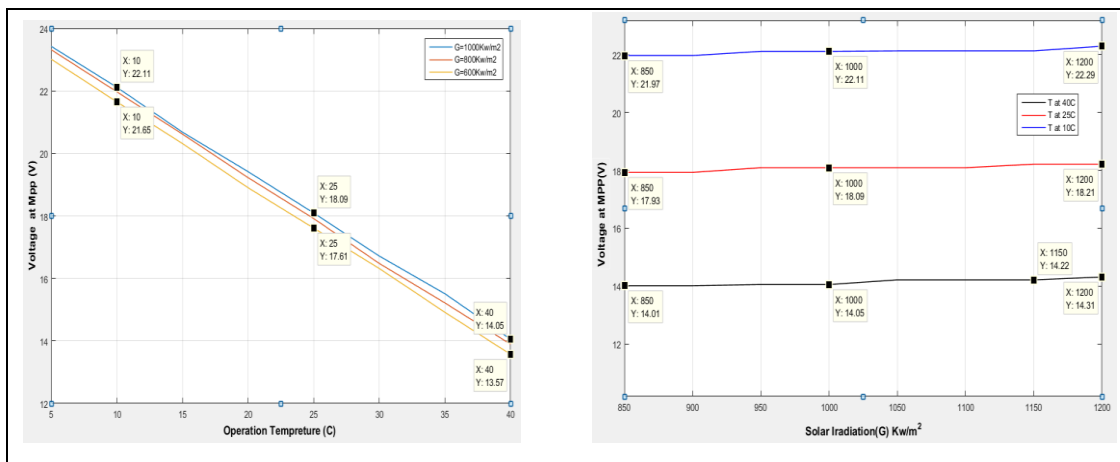


**Figure 4.9:** Influence of solar radiation and temperature on  $V_{mpp}$ .

From figure 4.8, when the radiation increases the  $P_{mpp}$  operation increase and vice versa with the temperature increase. and when the temperature decreases the  $V_{mpp}$  increases and approximately be constant when the radiation change (figure 4.9).

These results prove that operation point and MPP in the V-I curve and P-V curve are changing with any change in solar irradiation and temperature. As it known, these factors vary with time and the weather situation and the seasons of the year. For more information see Table B.1 and B.2 in appendix B.

A DC-DC convertor controlled with MPPT technique is used to maximize the PV power and delivers it to the load. Next section shows the simulation circuit for boost DC-DC converter which is used to analyze the performance of the proposed MPPM algorithm.

### 4.3 Boost Convertor Model

The parameters for the DC-DC boost converter are shown in table 4.2. The switching frequency ( $f_s$ ) is selected as 200KHz. The inductor value ( $L_1$ ) were selected greater than  $L_{min}$  in equation (3.6). Also, the capacitor values ( $C_1, C_2$ ) was chosen in order to obtain a fast response for the MPPT algorithms. The simulation circuit of the convertor is shown in figure 4.10.

**Table 4.2:** Boos DC-DC convertor simulation parameters.

<i>Parameter</i>	<i>Value</i>
<b>Inductance <math>L_1</math></b>	<b>1 mH</b>
<b>Capacitor <math>C_1</math></b>	<b>1<math>\mu</math>F</b>
<b>Capacitor <math>C_2</math></b>	<b>200<math>\mu</math>F</b>
<b>Load resistor <math>R</math></b>	<b>10<math>\Omega</math></b>
<b>Switching Frequency <math>F_s</math></b>	<b>200kH</b>
<b>Switching Type</b>	<b>MOSFET</b>

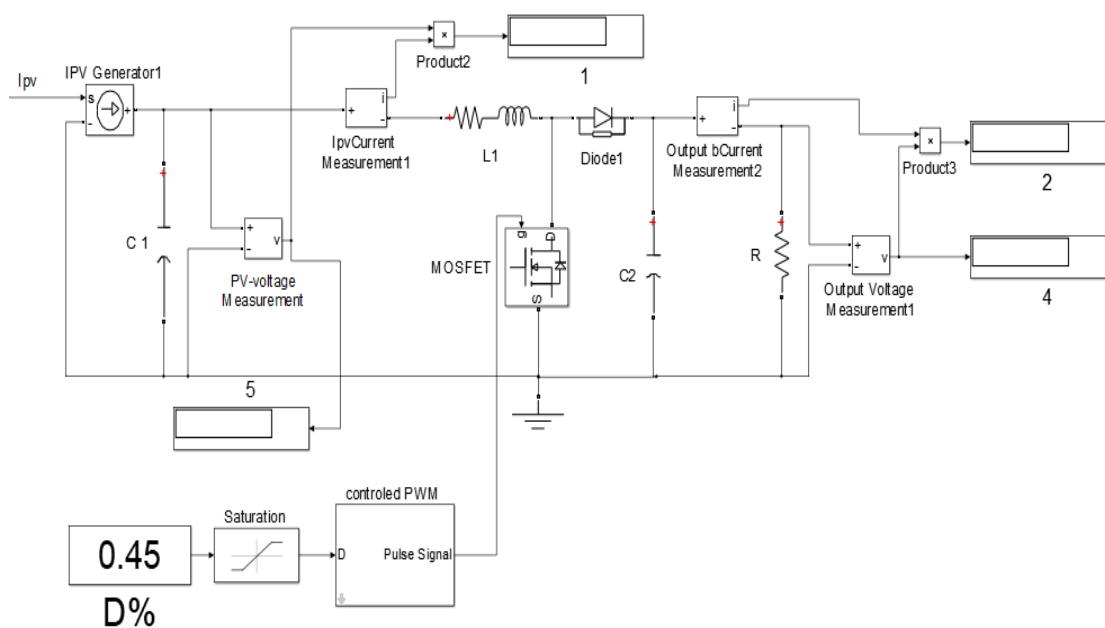


**Figure 4.10:** Boost convertor simulation circuit.

### 4.4 Perturb and Observe MPPT Controller

The first system is containing PV system and controlled based P&O MPPT method. P&O is made using MATLAB function and programed using MATLAB M-file based on flowchart in figure 3.4. The programed code is in appendix B.3.

The initial value of  $\Delta D$  is selected as 0.001 and the time sample of given decathlon is selected as 0.02 ms.

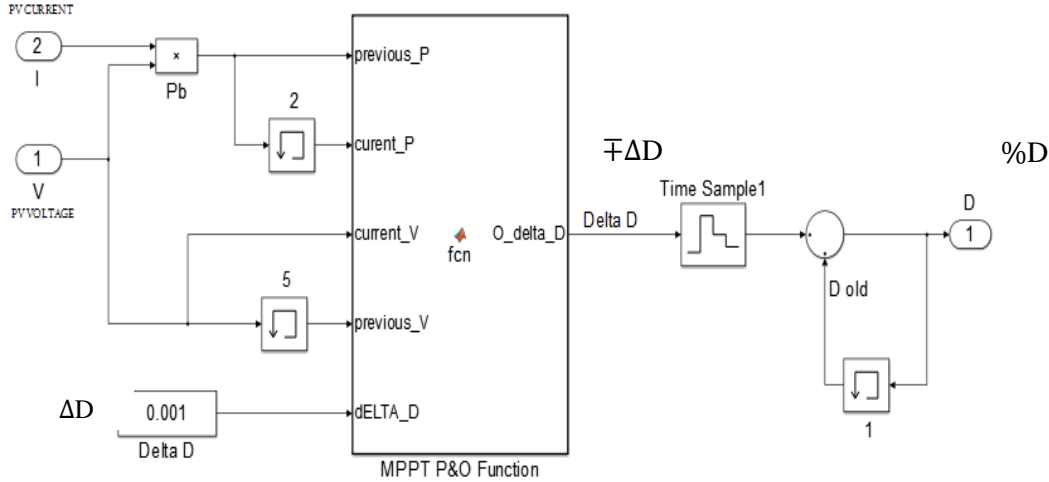


Figure 4.11: Simulation circuit of P&O MPPT controller.

4.5 Fuzzy Logic Controller Model

Fuzzy controller based MPPT is designed using MATLAB Fuzzy logic designer tool (figure 4.13). Based the concepts which is explained in chapter 3, the controller has two inputs. First one represents the calculated input error  $E(k)$  value and second input represents delay of error  $E(k)$ . One output represents the  $\Delta D$  decision and MFs for inputs and output is selected as shown figure 4.13.

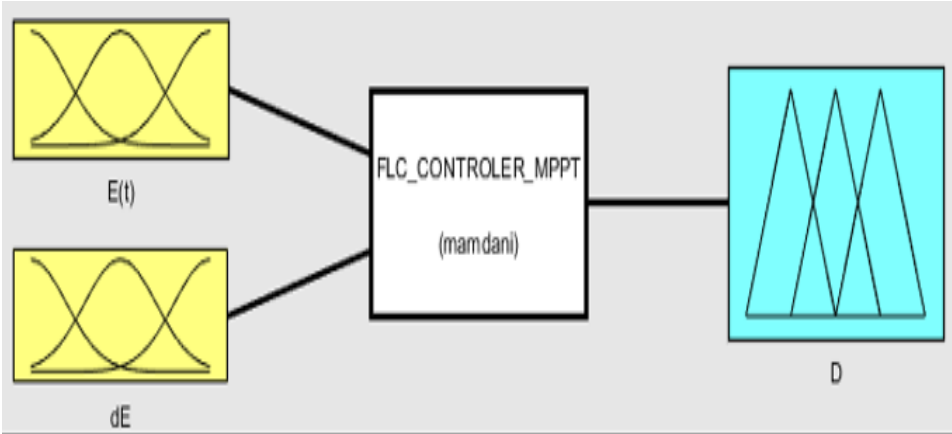
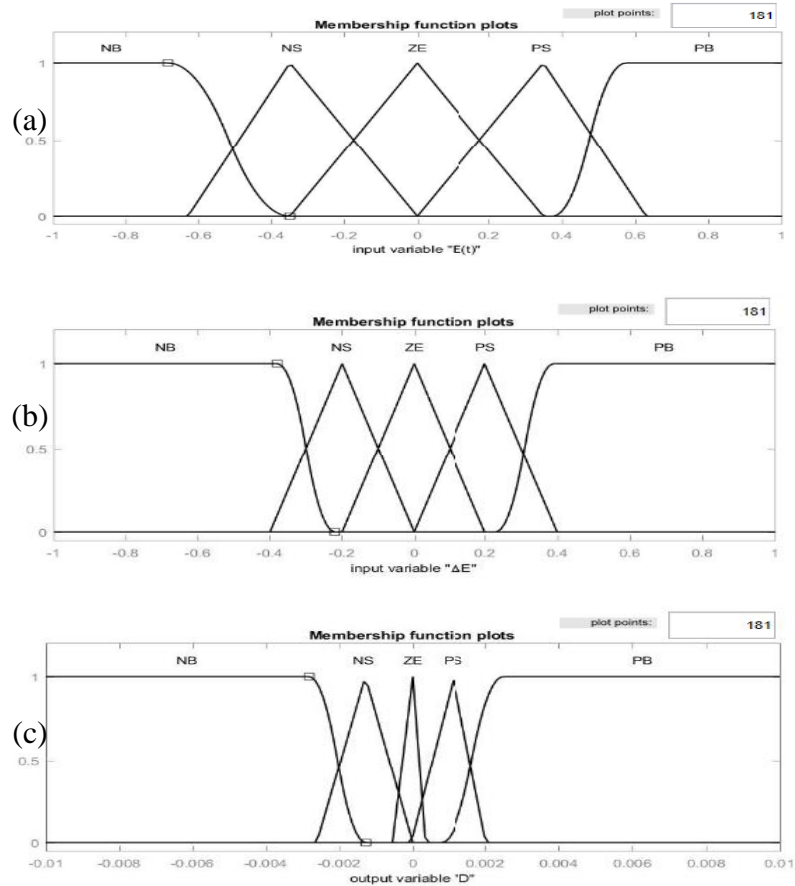
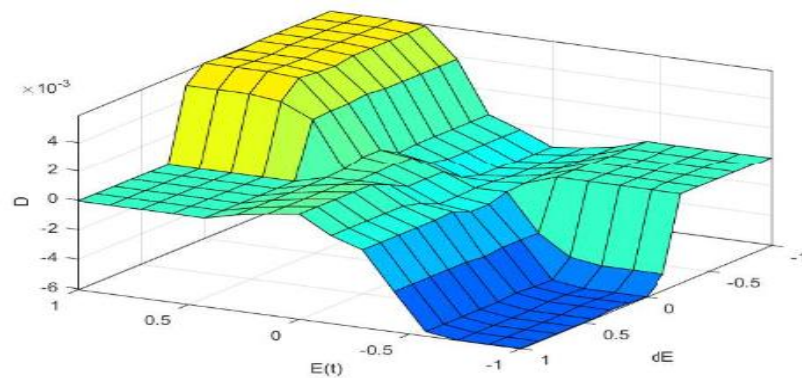


Figure 4.12: Properties of FLC based MPPT.



**Figure 4.13:** Memprship functions of FLC based MPPT. (a) MFs of input error  $E(k)$ . (b) MFs of input delta  $E(k)$ . (c) MFs of output decision delta  $D$  .

The rule base is designed based on Table 3.2 and the inference rule serfce is shown below .



**Figure 4.14:** Inference rule base surface of FLC based MPPT.

The designed fuzzy logic controller shoud be imported to work space to use it in simolink using fuzzy contrloller block . And the controller takes samples of calculated

$E(k)$  and  $E(k-1)$ . The time sample of given decision is selected as 0.08 ms to get efficient performance.

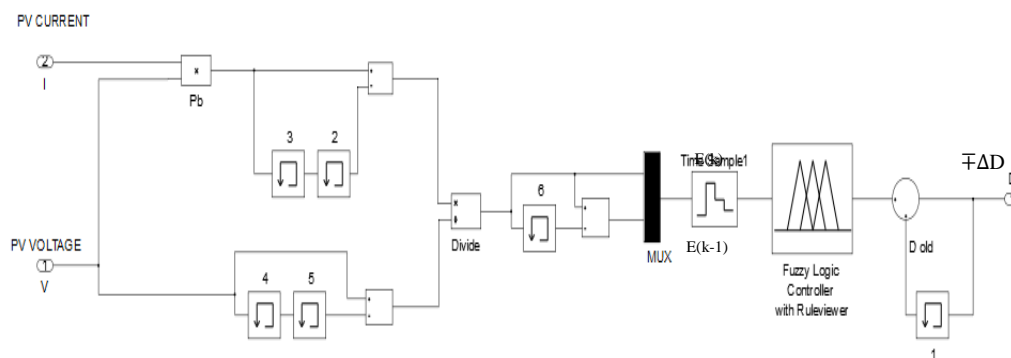


**Figure 4.15:** Simulation circuit of FLC controller based MPPT

#### 4.6 Neural Network Controller Model

The ANN controller based MPPT is designed using MATLAB M-file code. It has trained by backpropagation learning algorithm that uses training data which is in table C.1 in appendix C. The training points are obtained as it stated in appendix C1. the programmed code is in appendix C.2. The ANN which is shown in figure 4.16 is designed with ten hidden layers with two inputs and one output (figure 4.16).

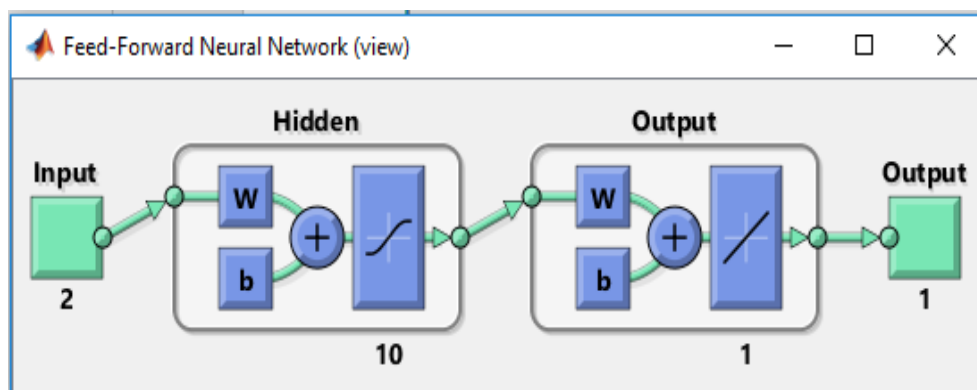


**Figure 4.16:** Neural network structure based MPPT.

The proposed ANN controller has two inputs: solar irradiance and temperature. one output that represents  $D$  that is operate at MPP. Between network and inputs there is MATLAB function used to arrange the value of the  $G$  and  $T$  as vector  $2 \times 1$  (figure 4.17).



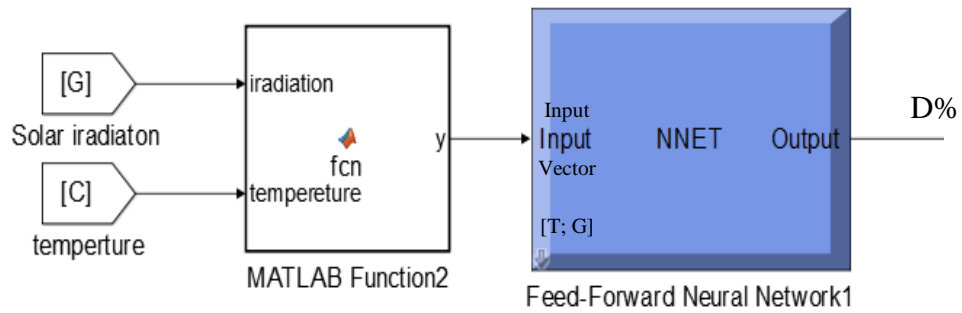


**Figure 4.17:** Simulation circuit of ANN controller based MPPT.

#### 4.7 Neuro-Fuzzy Controller Model

Seguno FLC is gotten from training the ANFIS, which is trained using training data that is used to train the ANN controller see appendix C. Backpropagation training algorithm is used to optimize the FLC parameters.

The structure of the FLC controller has two inputs representing T, G and one output represents the decision of the duty cycle D. MATLAB Neuro-Fuzzy designer tool is used to train the ANFIS and generate the system (figure 4.18), (appendix C).

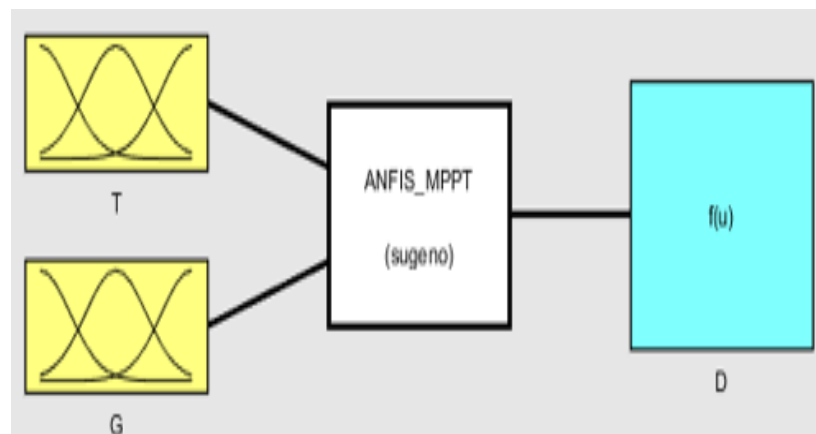


**Figure 4.18:** structure of generated Sugeno FLC system after training by ANFIS.

Four MFs is selected for each input and their parameters are selected during training process. The output MFs are is optimized as constant samples during the training process. Figure 4.19 shows the MFs membership functions of the input and outputs.

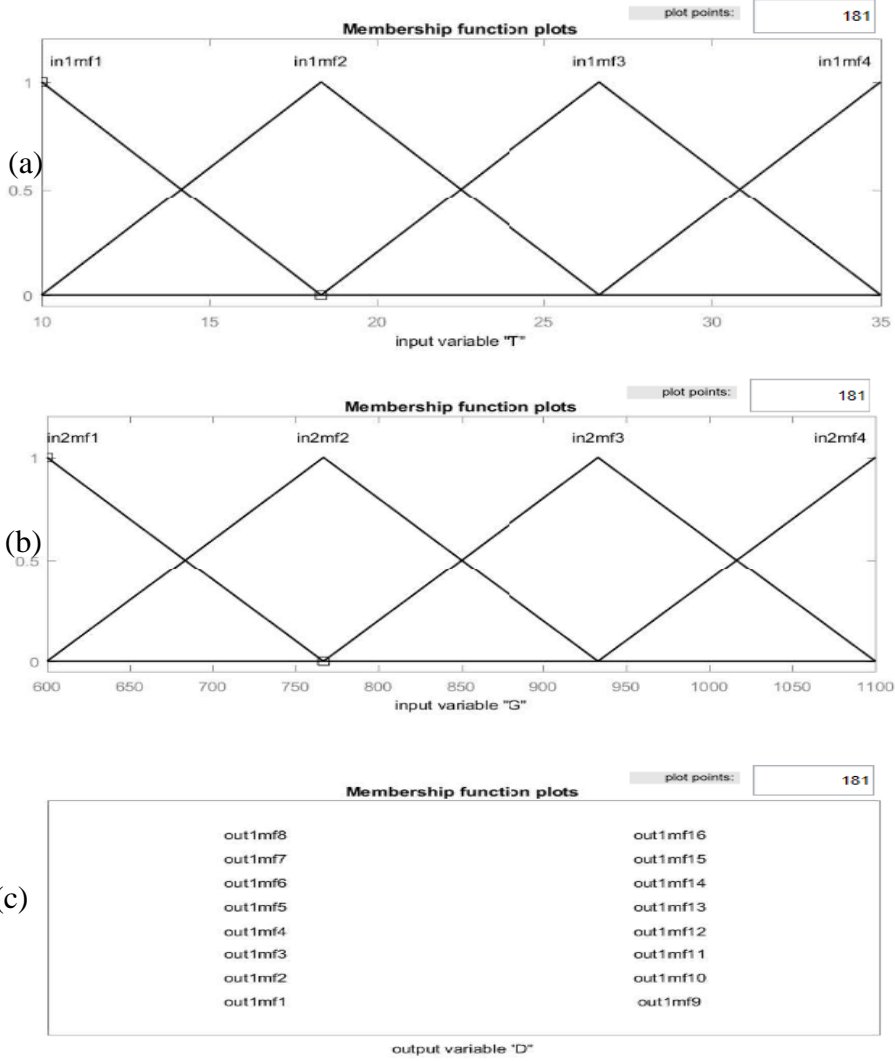


**Figure 4.19:** Generated membership functions (a)MFs of temperature. (b)MFs of solar irradiation. (c) Output samples of the Sugeno FLC system.

The inference rule bases are optimized during ANFIS training process (figure 4.20). and the inference rules surface is shown in figure 4.21.

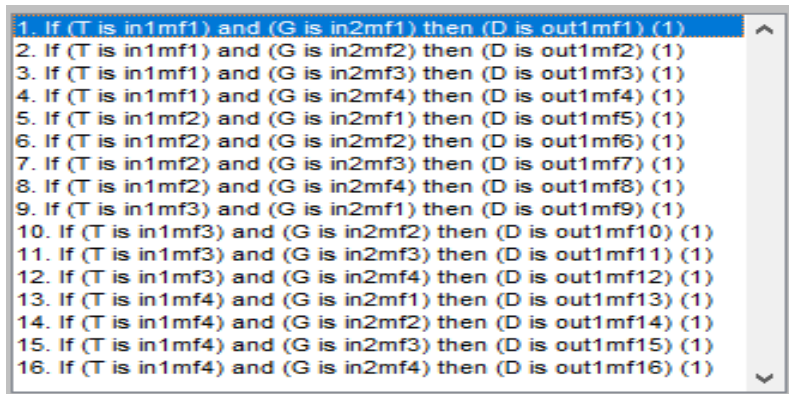


**Figure 4.20:** Generated rules base from ANFIS training.

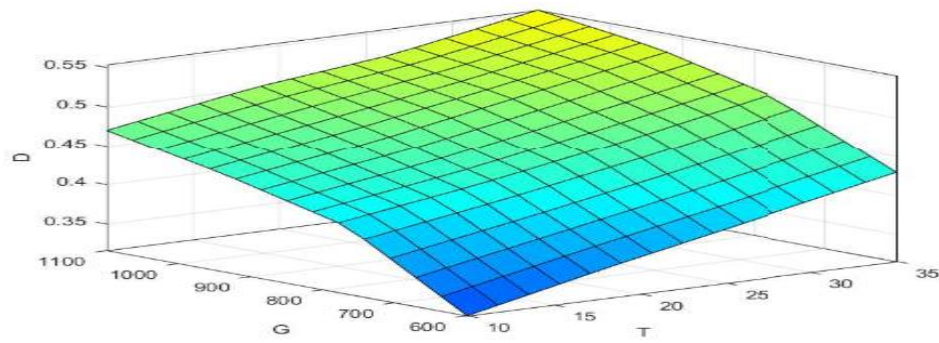


**Figure 4.21:** inference rule surface of FLC generated by ANFIS.

The previous generated FLC should be imported in MATLAB work space to use it as controller in Simulink environment. Simulated FLC controller is shown below. The Simulation circuit connections of PV system with FLC will be presented in next chapter.

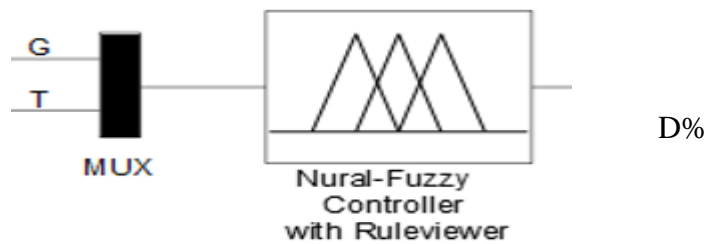


**Figure 4.22:** Purposed FLC controller based MPPT whose parameters generated by ANFIS training.

#### 4.8 Simulation Circuit of all Proposed PV Systems

The complete system is simulated using the MATLAB/SIMULINK (Figure 4.23). Each block in the simulation represents kind of PV system. The block1 represents PV system work without MPPT. The others represent in block 2, block 3, block 4 and block5. Each block has different MPPT from the other for compering the performance of each kind of MPPT, which are proposed in this chapter.

In next chapter, each internal system in the blocks (figure 4.23) will be presented. In addition, the all system will be run at same time with same signal value of temperature and solar irradiation.

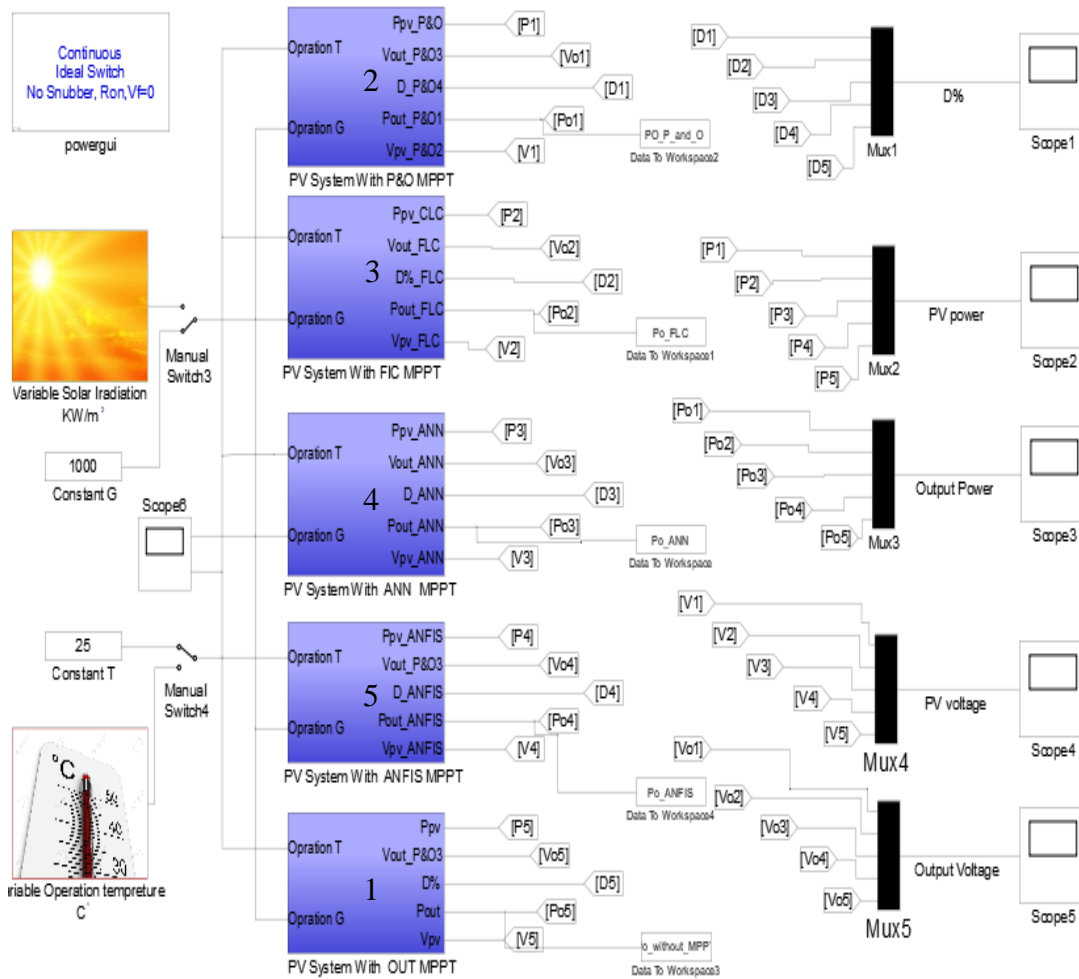


**Figure 4.23:** Simulation circuit of all PV systems for evaluating the performance of each MPPT.

Each system will be running with variation in T and G to see the affections on the output power of each system, to analyze the performance of each MPPT controller, and to see what happen to the output power of the PV system work without MPPT controlling algorithm. Figure 4.24 shown the variation signal value of G and T that is used evaluate the five PV systems figure 4.25.

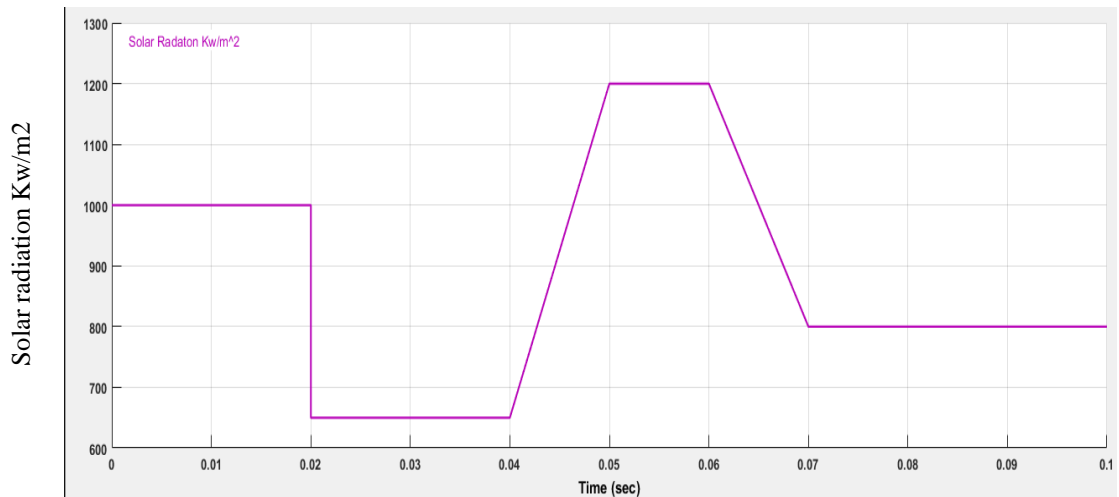


**Figure 4.24:** Variation value of slow and sudden changing on the operation Soler radiation.

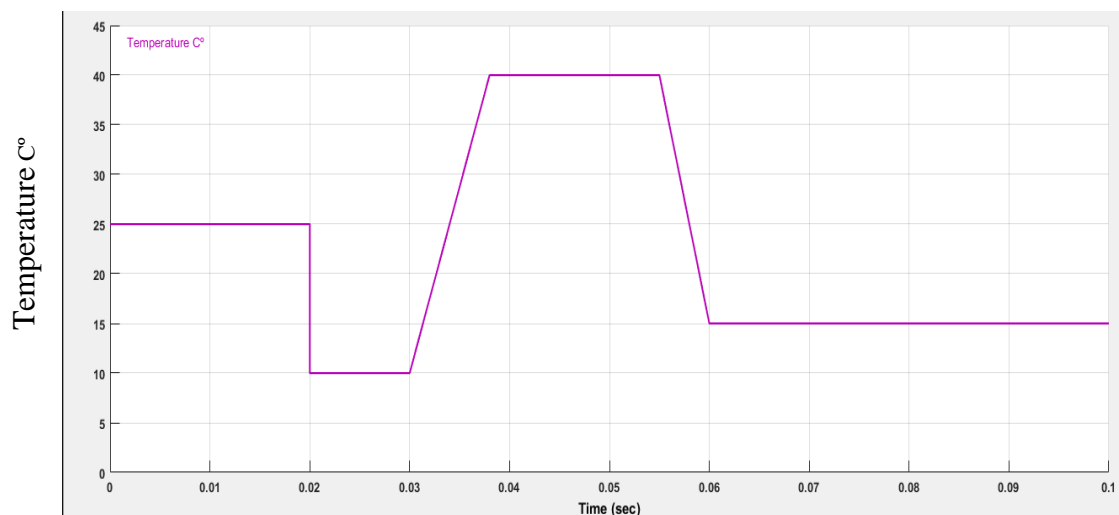


**Figure 4.25:** Variation value of slow and sudden changing on the operation temperature.

The simulation result of each system is presented in next section. The last section will be conclusion and compering the performance of results of all PV systems to see how the performance of each PV system is different from the other.



## 5 SIMULATION RESULTS AND CONCLUSION

### 5.1 Simulation Results

The simulation is done by operate the five PV systems, which are shown in previous section (figure 4.24). Each system has same PV model and boost converter parameters, but each one has different MPPT mechanism for controlling the duty cycle with each system:

- The first PV system operates without any controlling for tracking the MPP (block 1 in figure 4.24). The duty cycle is selected for operate at MPP with only case of solar irradiation equal  $1000 \text{ Kw/m}^2$  and with temperate of  $25 \text{ C}^\circ$ . Note that D is constant does not change with changing in value of G and T
- Second PV system works with MPPT of P&O algorithm to guide PV system to possible MPP operation (block 2 in the figure 4.24).
- Third PV system works with FLC controller based MPPT (block 3 in the figure4.24).
- Fourth PV system works with ANN controller based MPPT (block 4 in the figure 4.24).
- Fifth PV system works with FLC controller which is designed by ANFIS training based MPPT (block 5 in the figure 4.24).

The next sections present the subsystem simulation circuits of each purposed system with their results. They are presented as five cases.

#### 5.1.1 CASE 1: System without MPPT

In this case firstly, PV system is operated at T of  $25 \text{ C}^\circ$  and G of  $1000 \text{ Kw/m}^2$ . D is adjusted manually to get MPP operation. Then the performance of the PV system is studied with variation in temperature and solar irradiation and the affections on the output power with the PV system without any MPPT controlling algorithm are studied.

The duty is selected as 0.503 to operate PV system at its MPP in case of  $T=25\text{C}^\circ$  and  $G=1000\text{KW/m}^2$ . Figure 5.1 show the simulation circuit of PV system of case 1 which is internal subsystem of block 1 in figure 4.24.

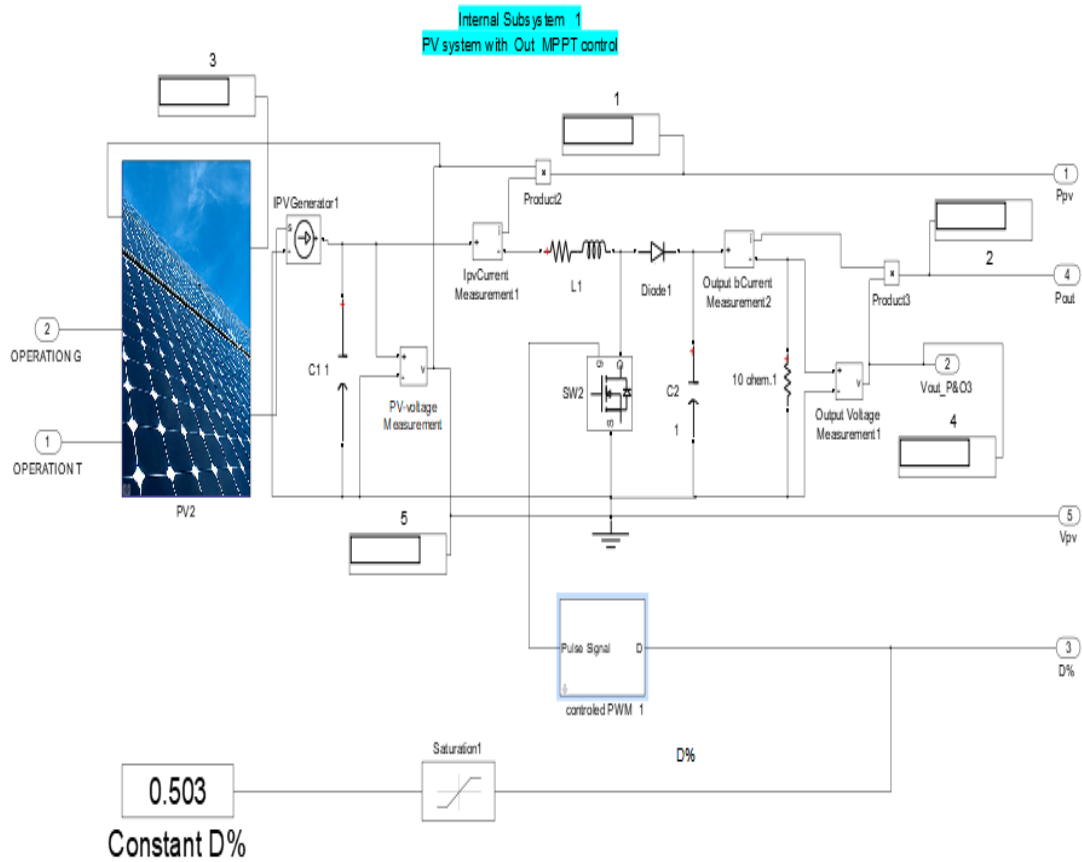


**Figure 5.1:** Connection simulation circuit of PV system without MPPT control.

Simulation results for this case are shown in figure 5.2 when operation solar radiation is varied and for varied operation temperature value results is shown in figure 5.3.



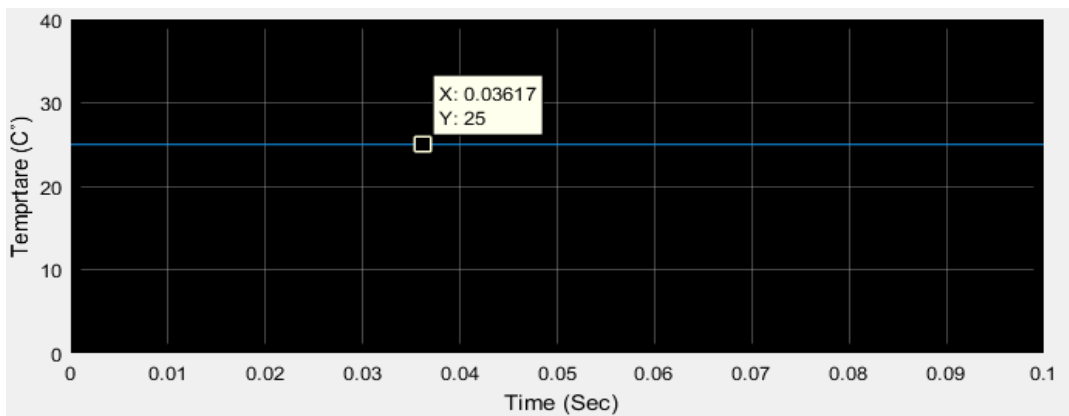
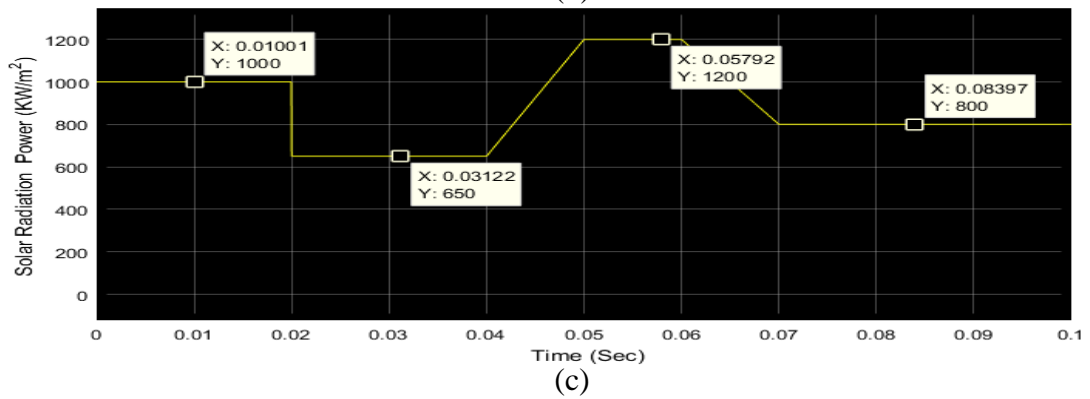
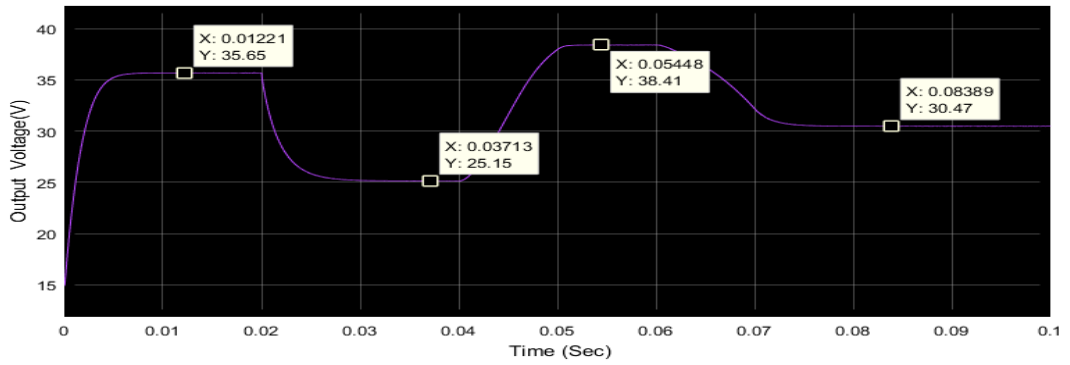
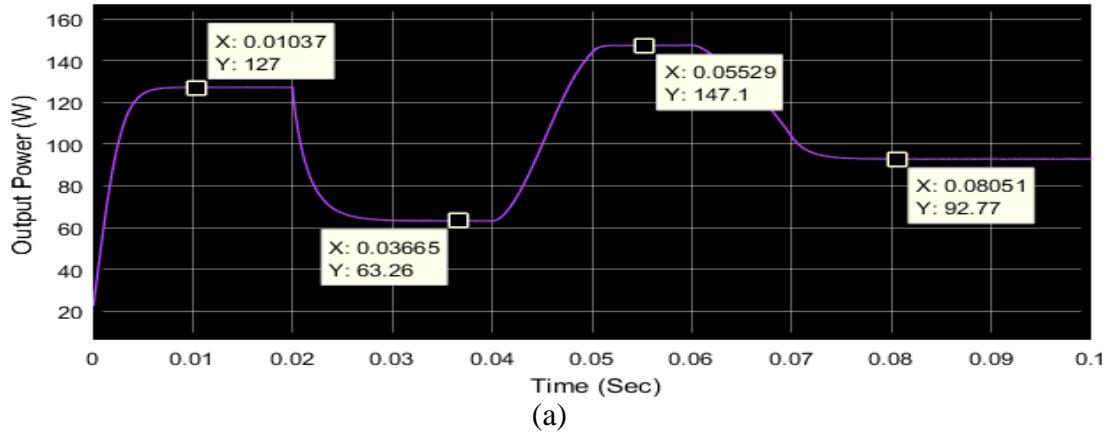


**Figure 5.2:** Case 1 simulation results with variation in G. (a) Output load power. (b) Output load voltage(c)Operation Solar Radiation Power. (d) Operation temperature.

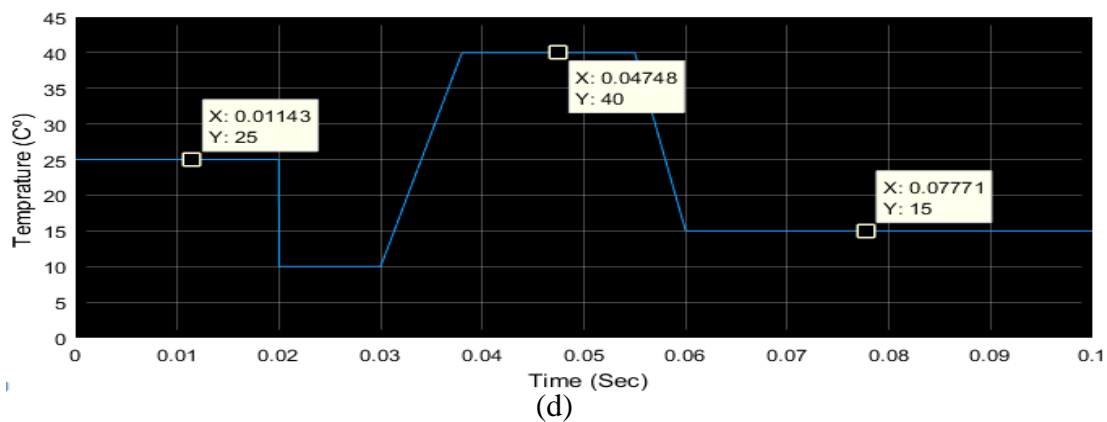
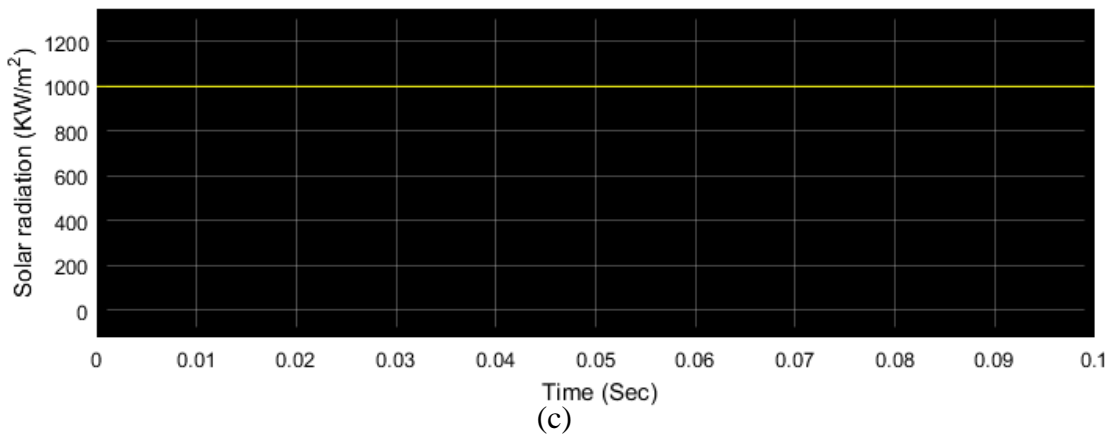
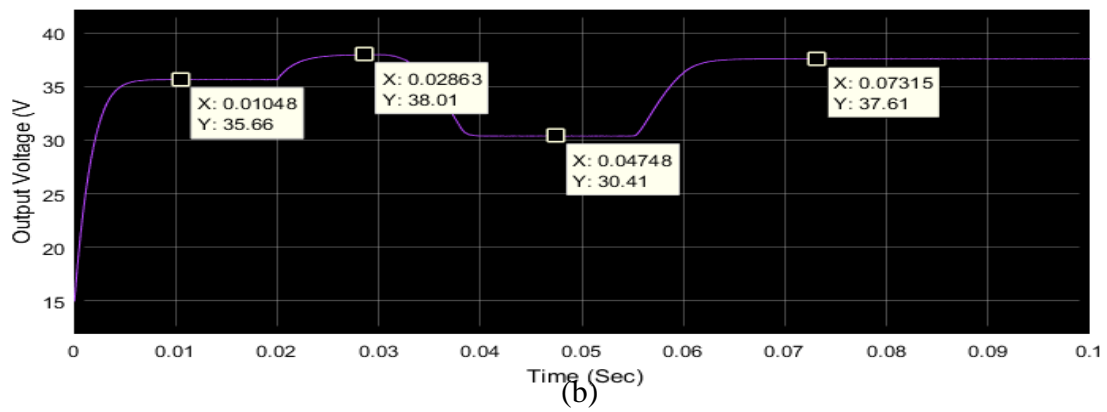
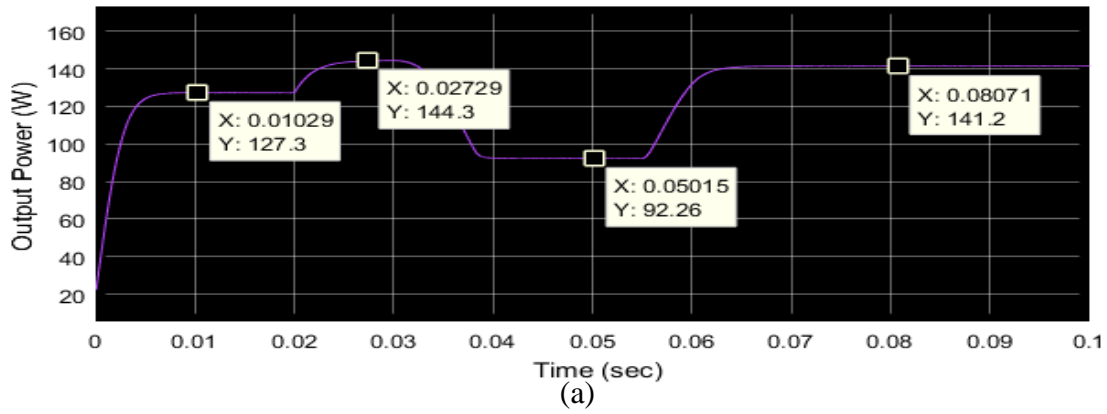


**Figure 5.3:** Case 1 simulation results with variation in T. (a) Output load power. (b) Output load voltage. (c) Operation Solar Radiation Power. (d) Operation temperature.

### 5.1.2 CASE 2: PV System with P&O MPPT algorithm

The simulation circuit in figure 5.4 represents the internal subsystem for block 2 (figure 4.24) that represents the case 2. The time sample of increasing and decreasing the duty cycle is selected as 0.02 m Sec.

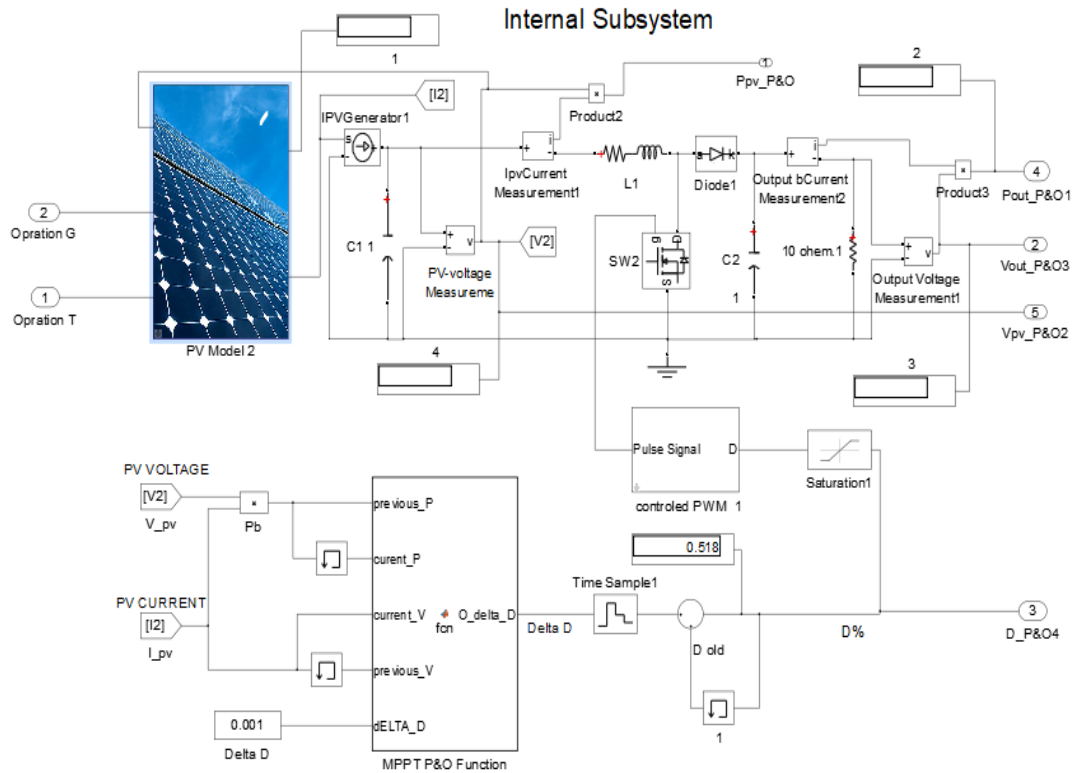
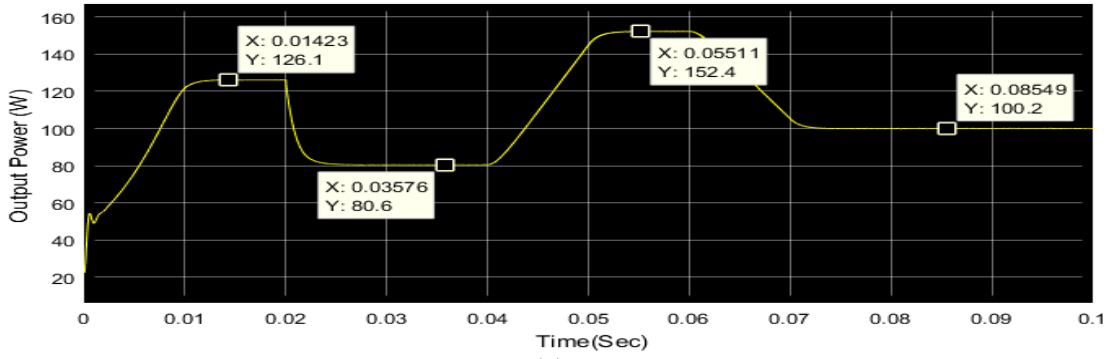
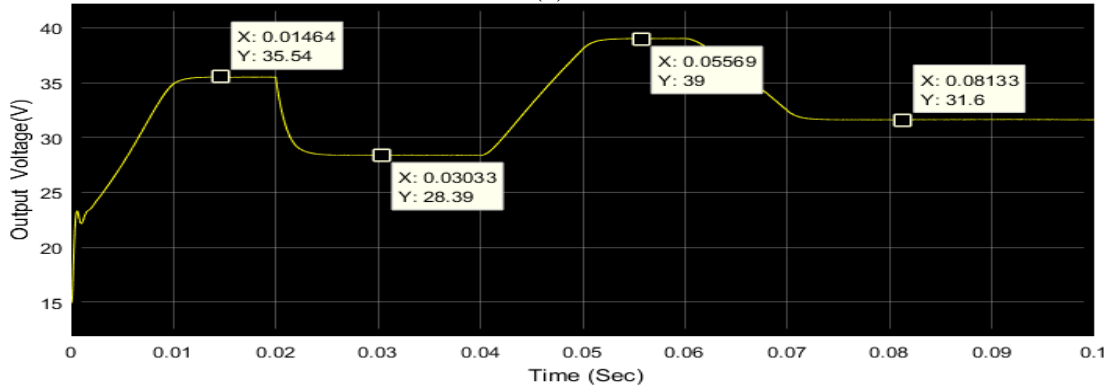


**Figure 5.4:** Connection simulation circuit of PV system with P&O MPPT controller.

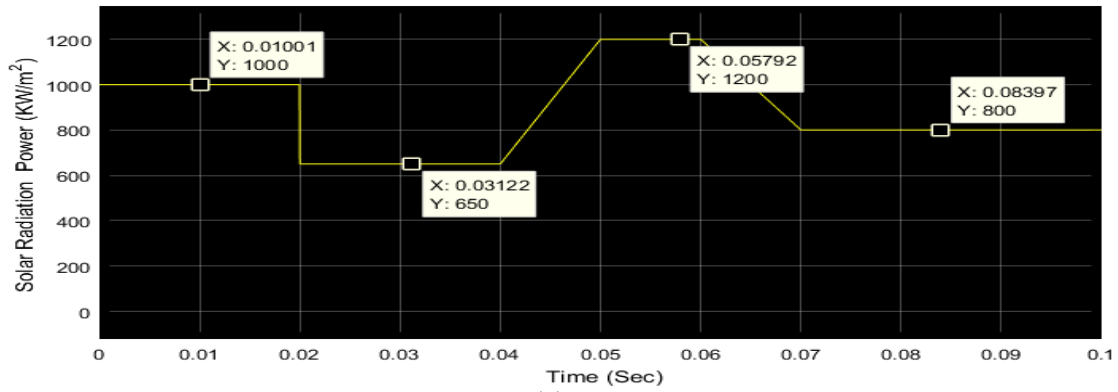
Simulation results for this case are shown in figure 5.5 for varying in operation solar radiation value, and for varying in operation temperature value results is shown in figure 5.6.



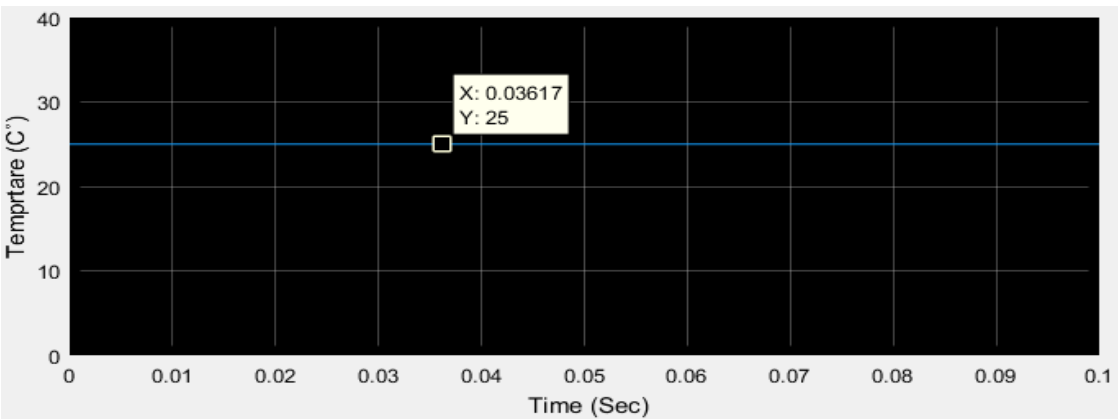
(a)



(b)



(c)



(d)

**Figure 5.5:** Case2 simulation results with variation in G. (a) Output load power. (b) Output load voltage. (c) Operation Solar Radiation Power. (d) Operation temperature.

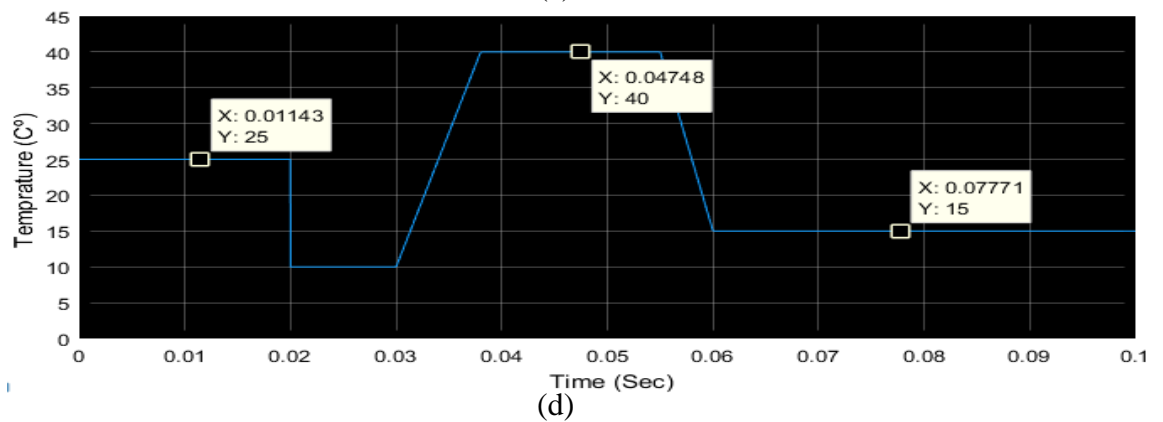
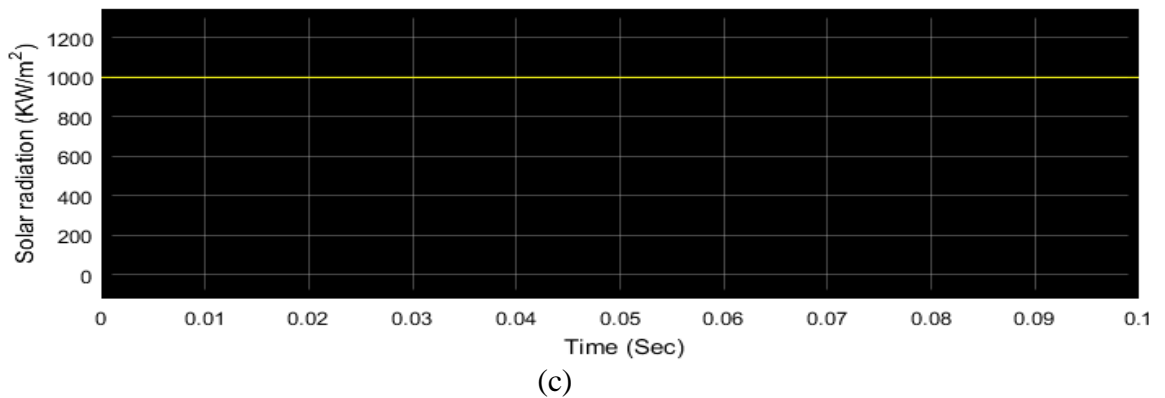
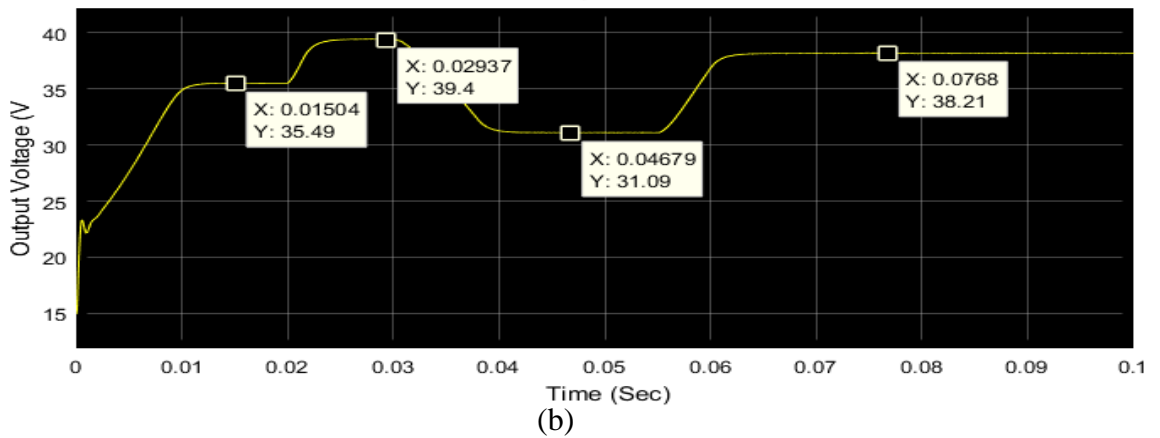
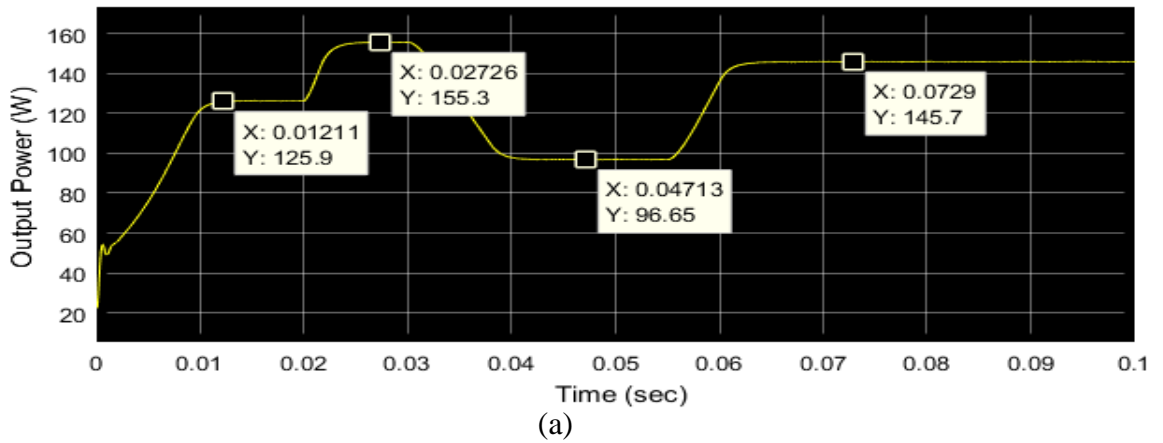


**Figure 5.6:** Case 2 simulation results with variation in T. (a) Output load power. (b) Output load voltage. (c) Operation Solar Radiation Power. (d) Operation temperature.

### 5.1.3 CASE 3: PV System with MPPT using the proposed FLC method

The simulation circuit in figure 5.7 represent the internal subsystem for block (figure 4.24) that represents the case 3. The time sample of increasing and decreasing the duty cycle is selected as 0.08 m Sec.

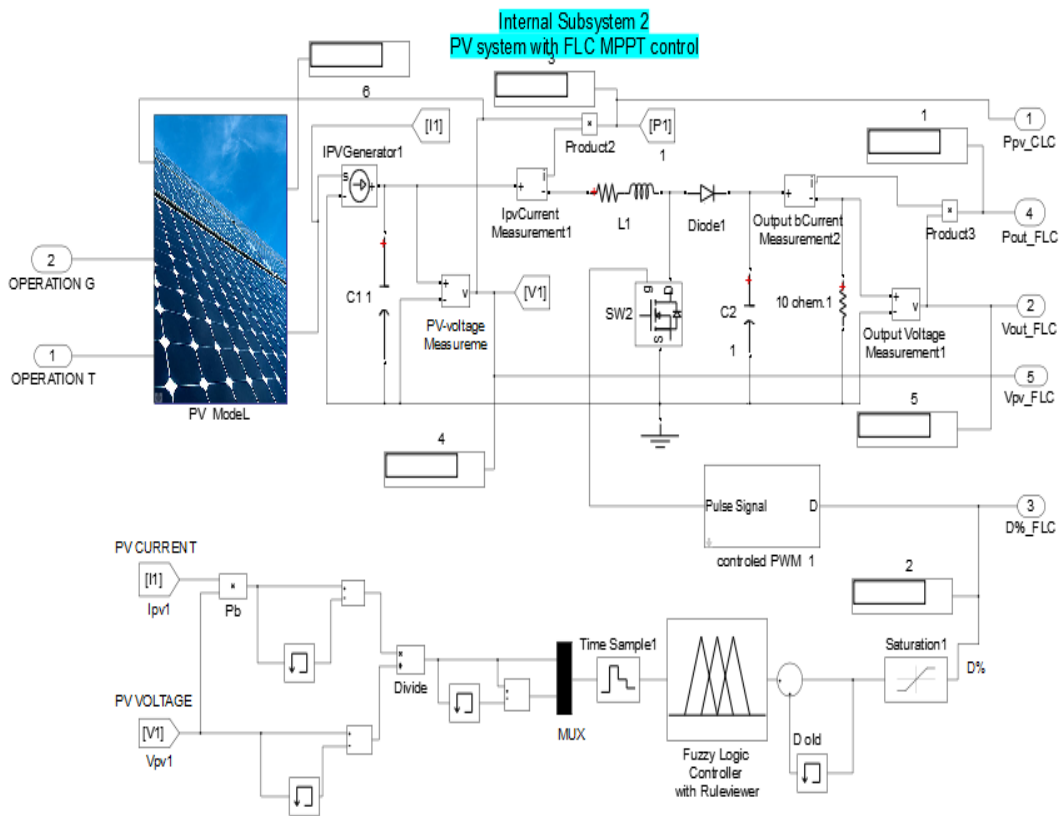
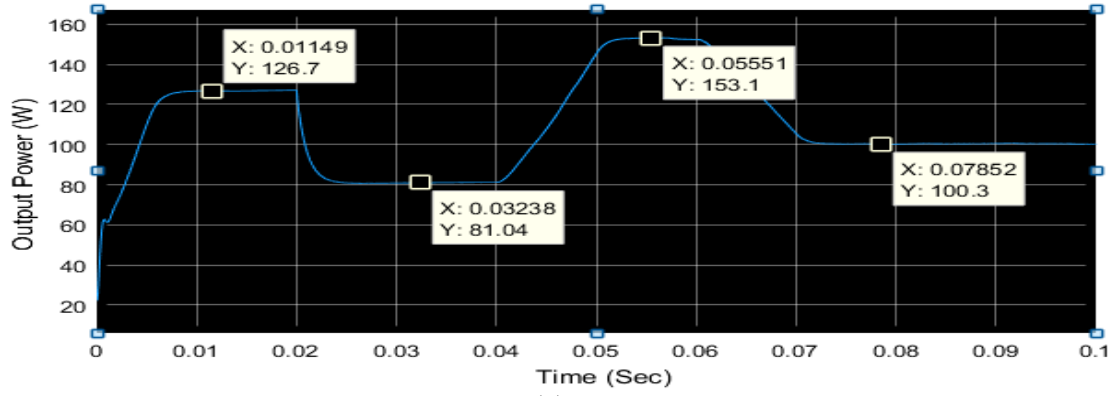
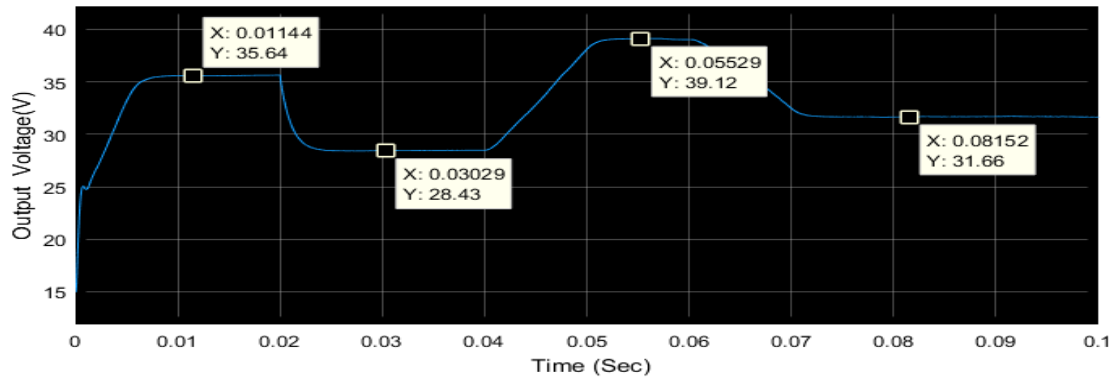


**Figure 5.7:** Connection simulation circuit of PV system with FLC based MPPT control.

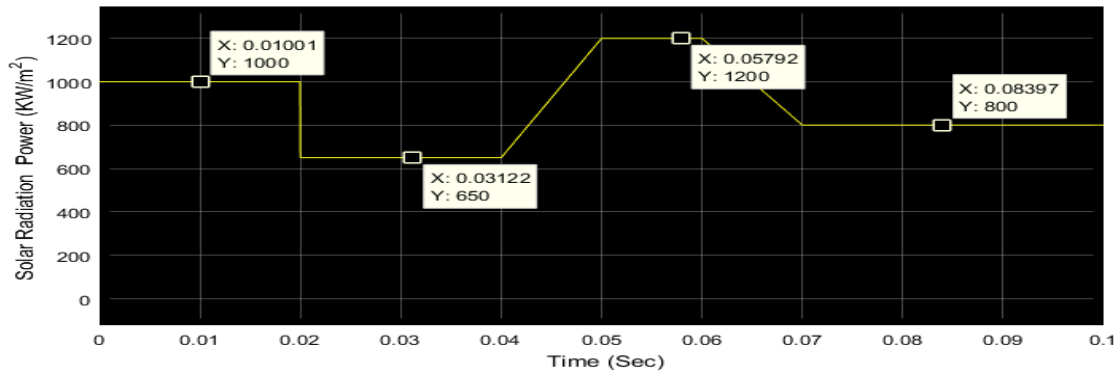
Simulation results for this case are shown in figure 5.8 for varying in operation solar radiation value, and for varying in operation temperature value results is shown in figure 5.9.



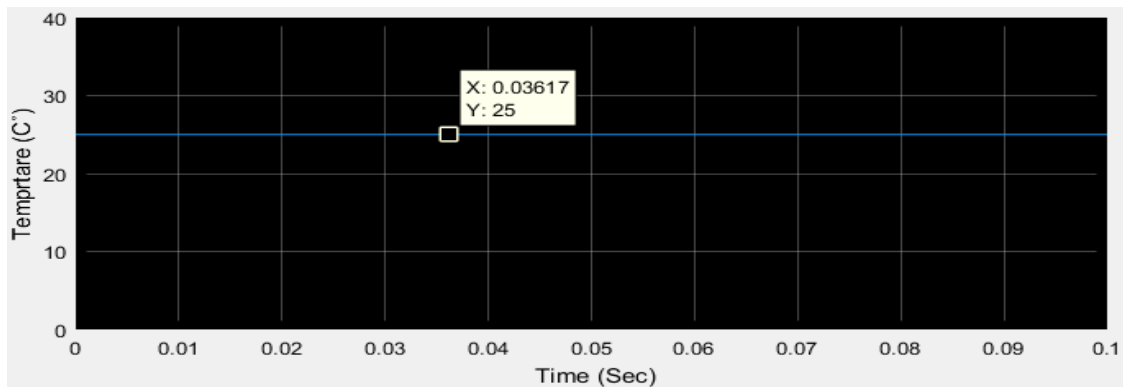
(a)



(b)

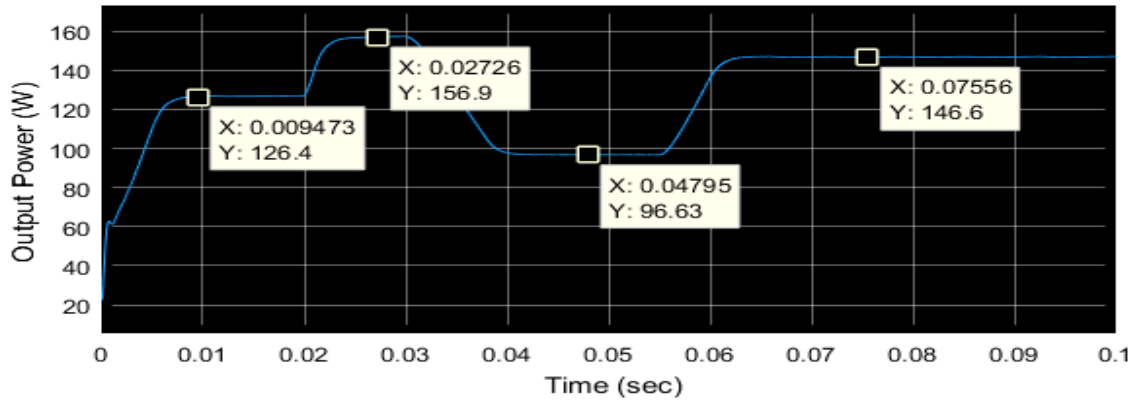


(c)

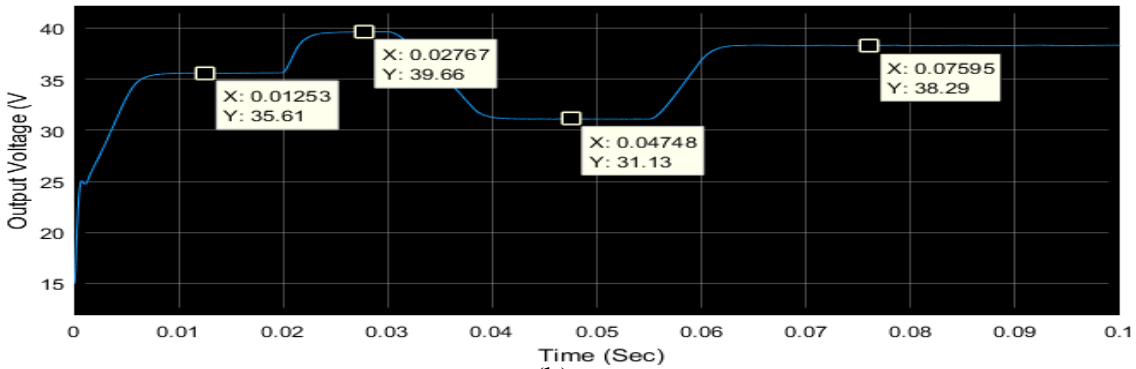


(d)

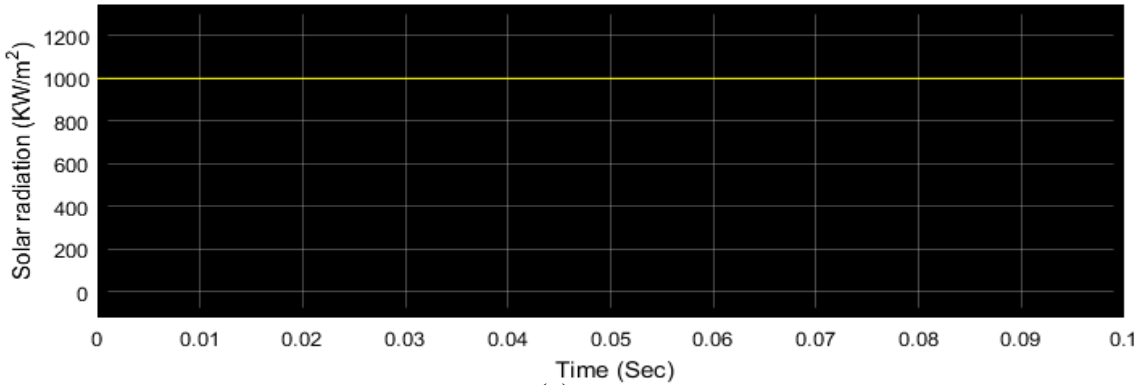
**Figure 5.8:** Case 3 simulation results with variation in G. (a) Output load power. (b) Output load voltage. (c) Operation Solar Radiation Power. (d) Operation temperature.



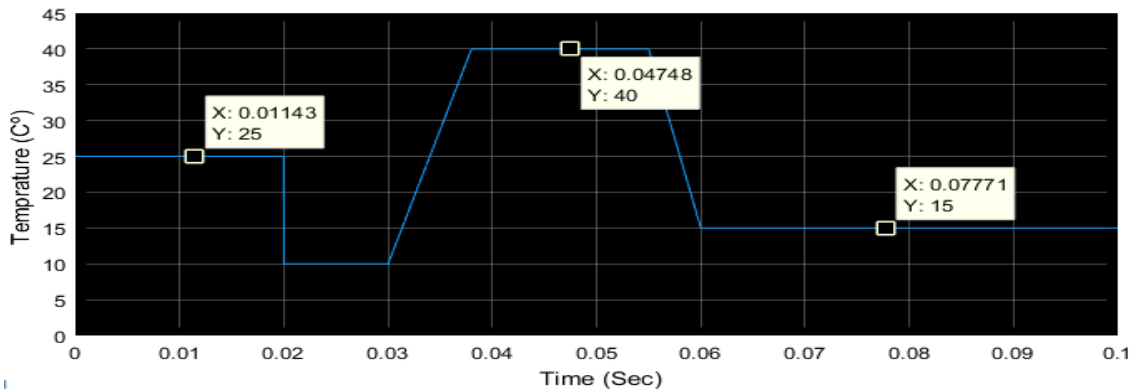
(a)



(b)



(c)



(d)

**Figure 5.9:** Case 3 simulation results with variation in T. (a) Output load power. (b) Output load voltage. (c) Operation Solar Radiation Power. (d) Operation temperature.



### 5.1.4 CASE 4: PV System with MPPT using the proposed ANN method

The simulation circuit in figure 5.10 represent the internal subsystem for block 4 (figure 4.24) that represents the case 4. No need for time sample for increasing and decreasing the duty cycle because ANN give right decision for value for any vale of T and G, as it learnt from the training process.

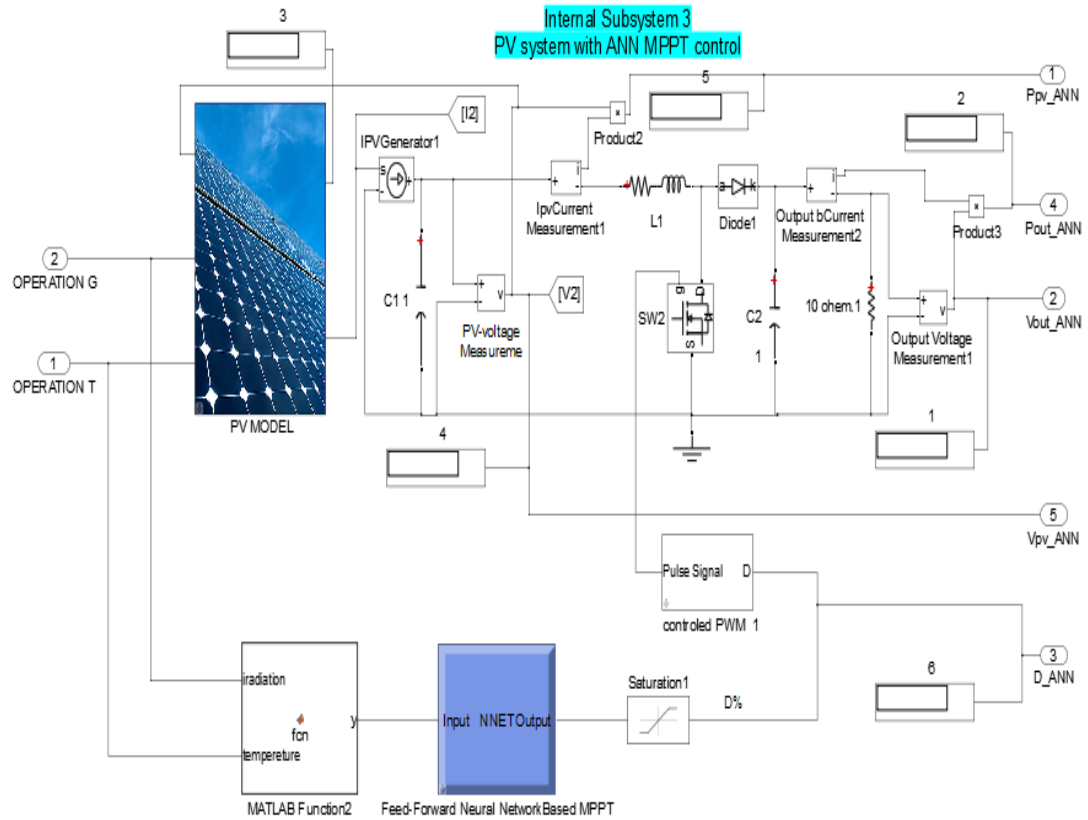


**Figure 5.10:** Simulation connection circuit of PV system with ANN based MPPT controller.

Simulation results for this case are shown in figure 5.11 for varying in operation solar radiation value, and for varying in operation temperature value results is shown in figure 5.12.

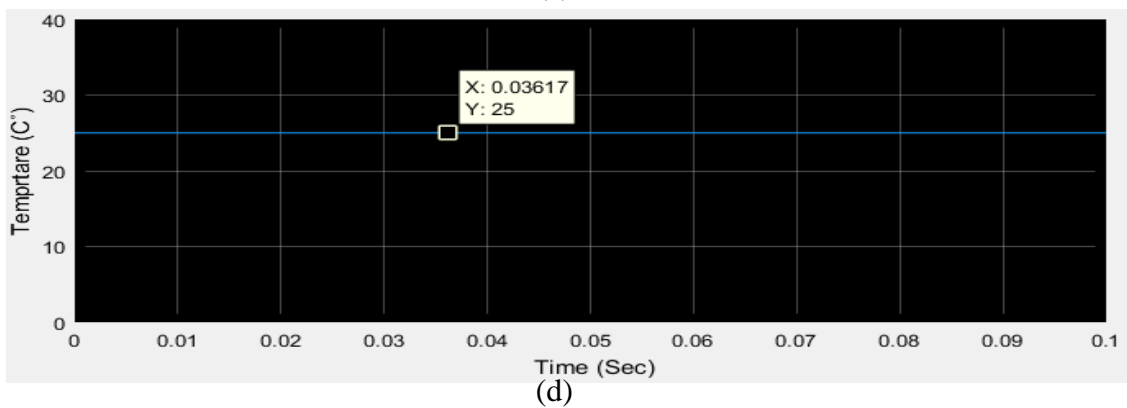
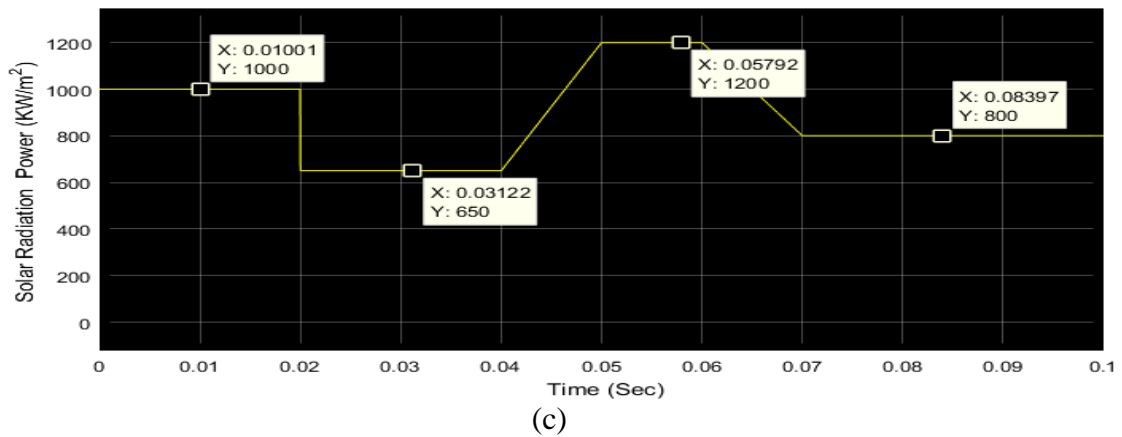
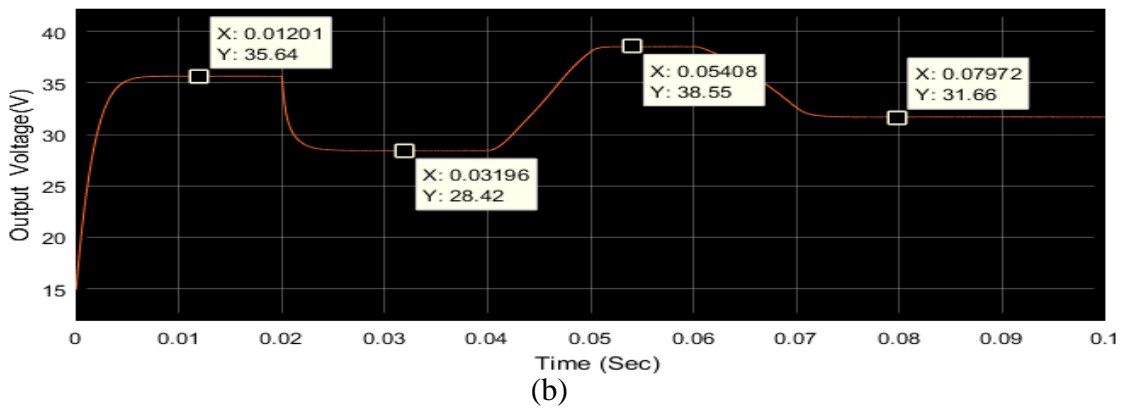
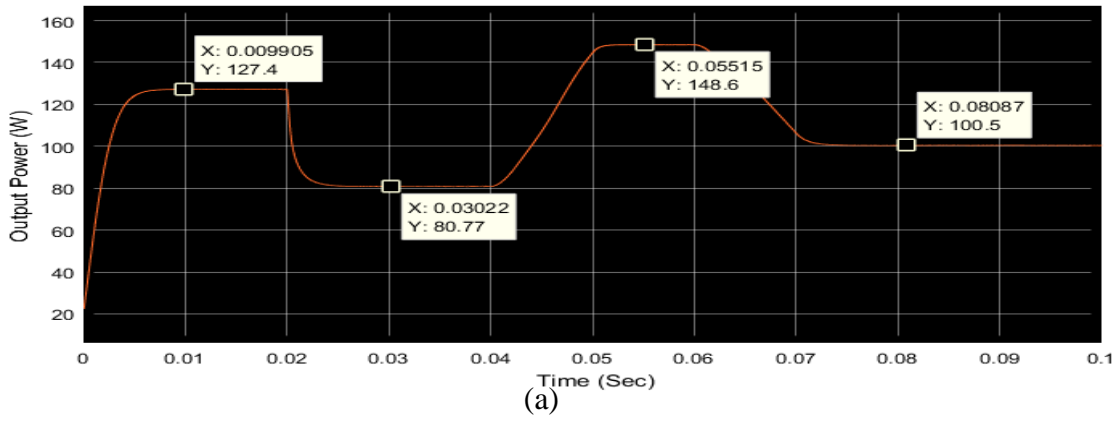


**Figure 5.11:** Case 4 simulation results with variation in G. (a) Output load power. (b) Output load voltage. (c) Operation Solar Radiation Power. (d) Operation temperature.

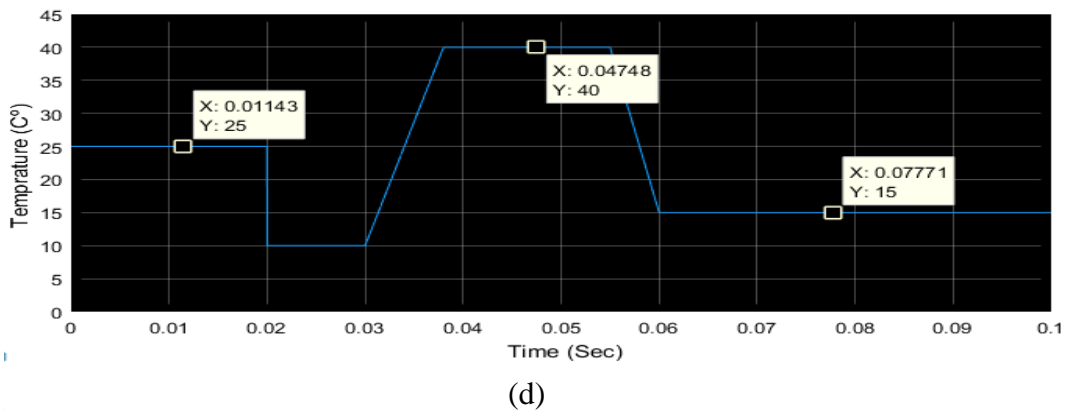
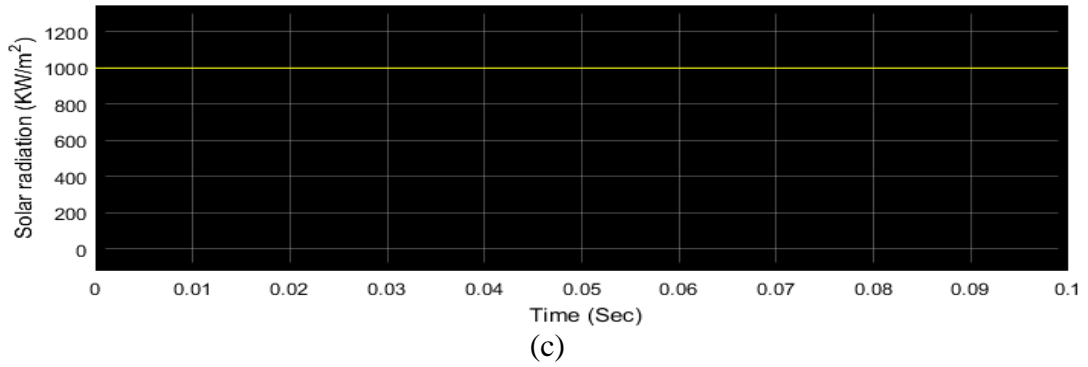
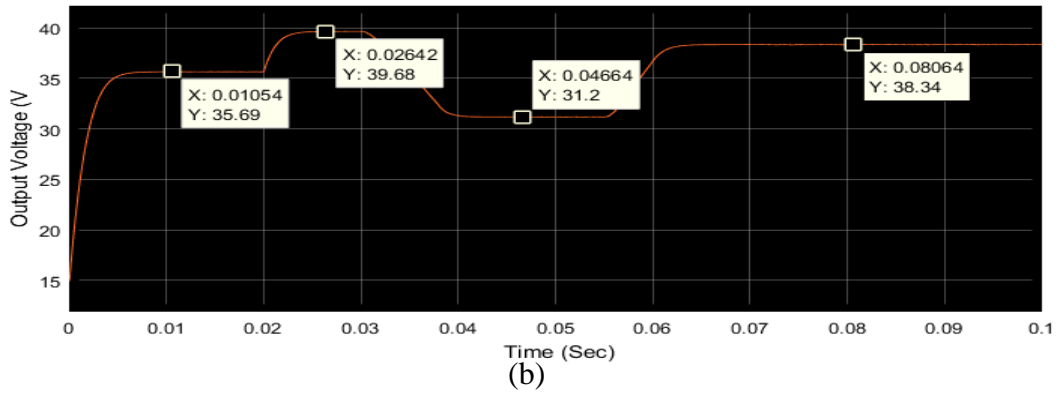
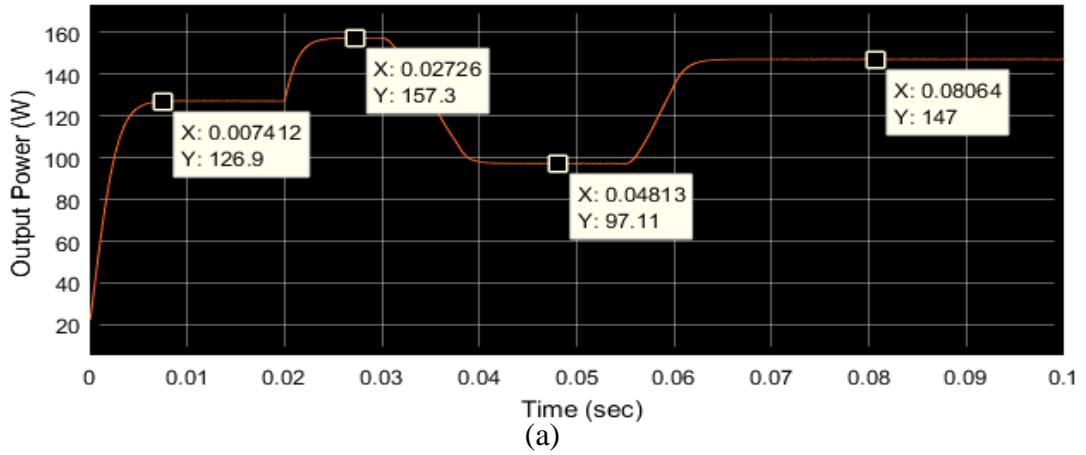


**Figure 5.12:** Case 4 simulation results with variation in T. (a) Output load power. (b) Output load voltage. (c) Operation Solar Radiation Power. (d) Operation Temperature

### 5.1.5 CASE 5: System with MPPT using the proposed ANFIS method

The simulation circuit in figure 5.13 represents the internal subsystem for block 5 (figure 4.24) that represents the case 5. The time sample is not important for increasing and decreasing the duty cycle, because FLC controller has optimized their parameters by ANFIS training process to give right decision for value for any vale of T and G, as it learnt from the training process.

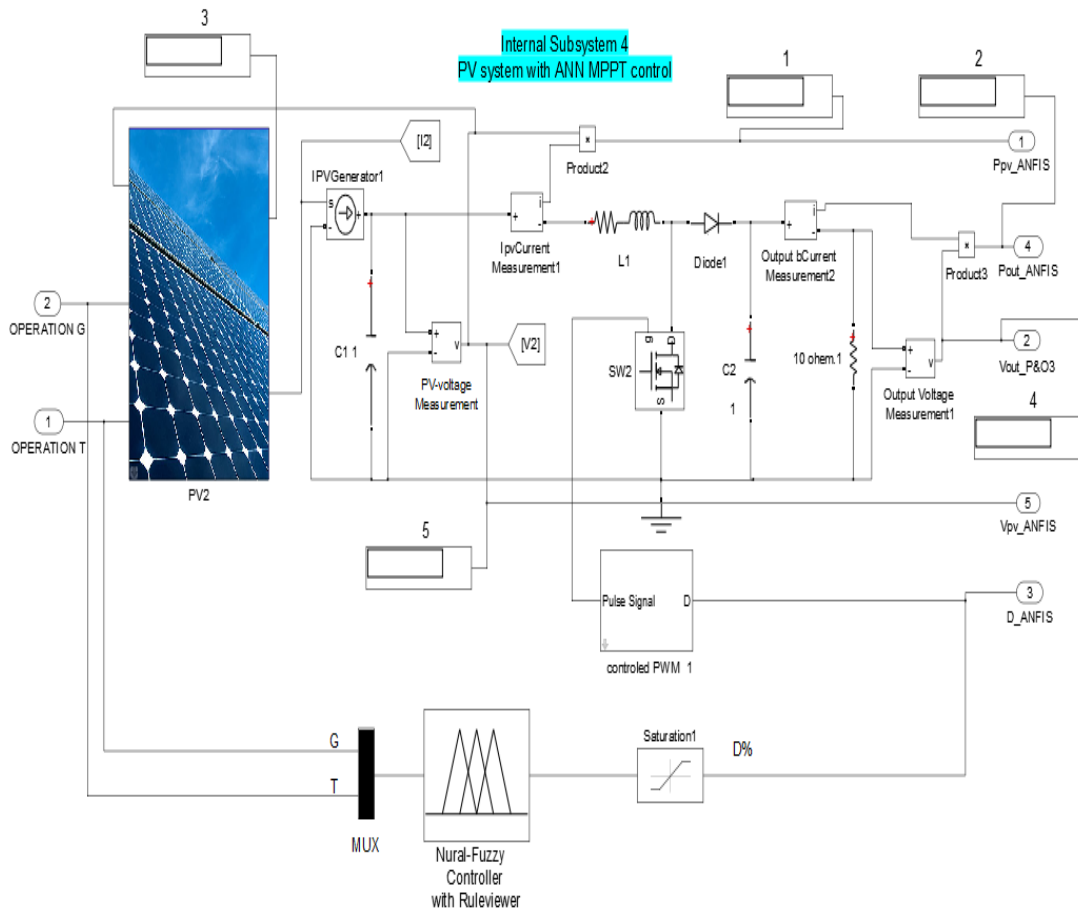
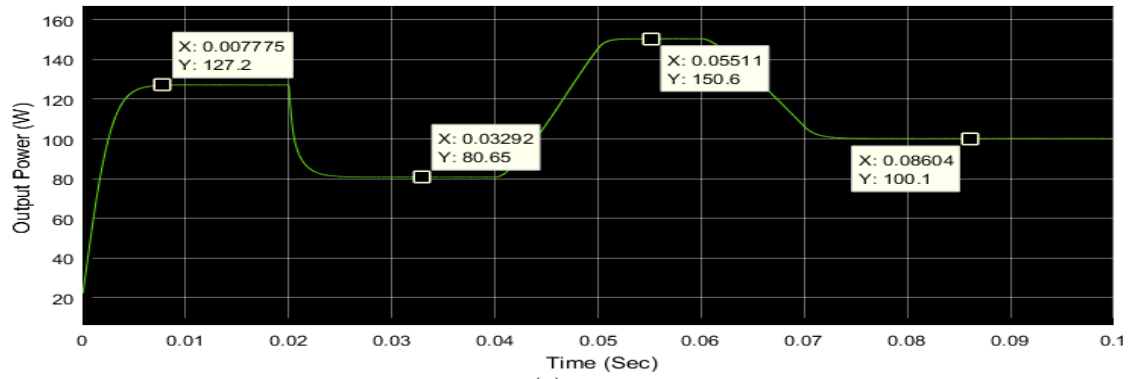
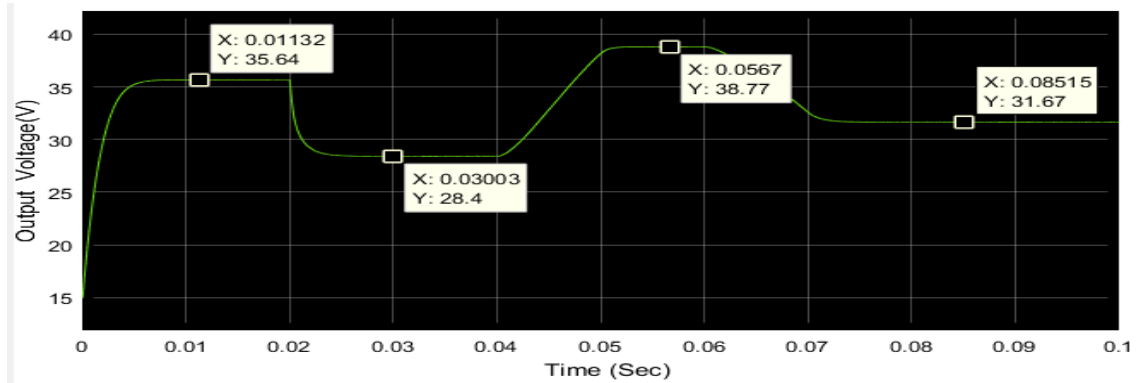


**Figure 5.13:** Simulation connection circuit of PV system with FLC based ANFIS training based MPPT.

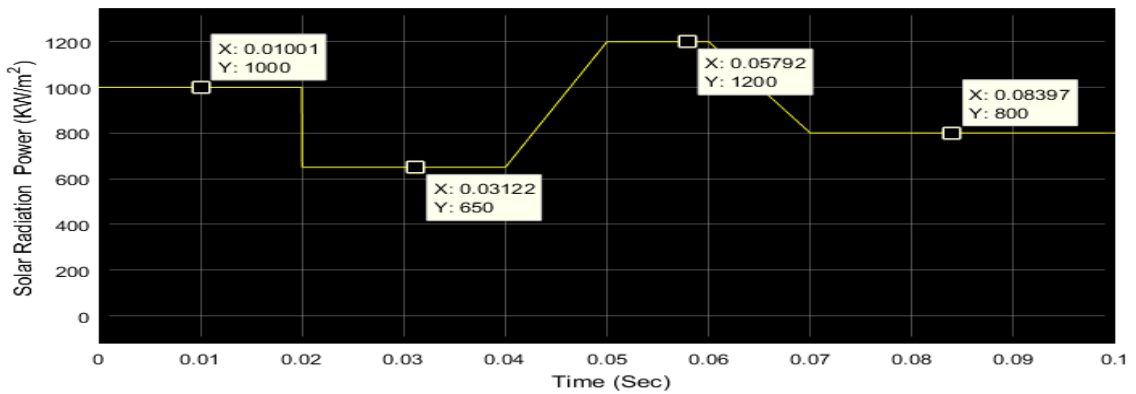
Simulation results for this case are shown in figure 5.14. For varying in operation solar radiation value, and for varying in operation temperature value results is shown in figure 5.15.



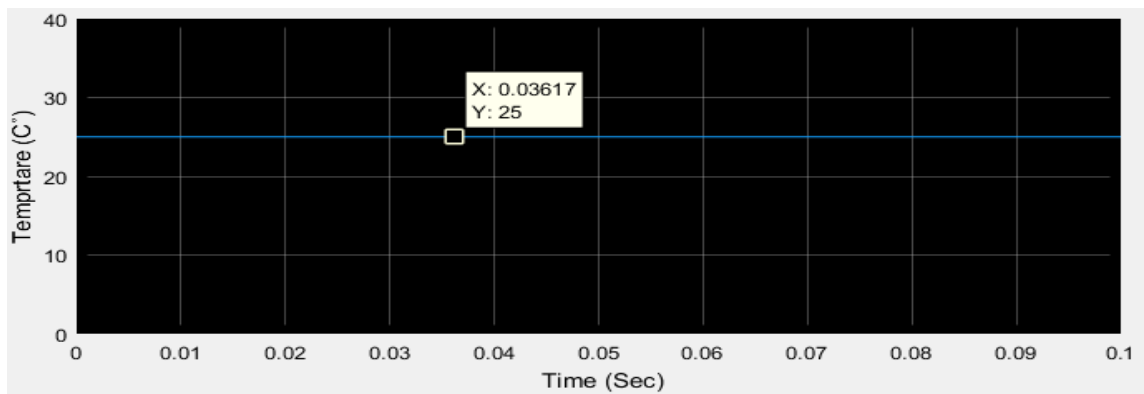
(a)



(b)

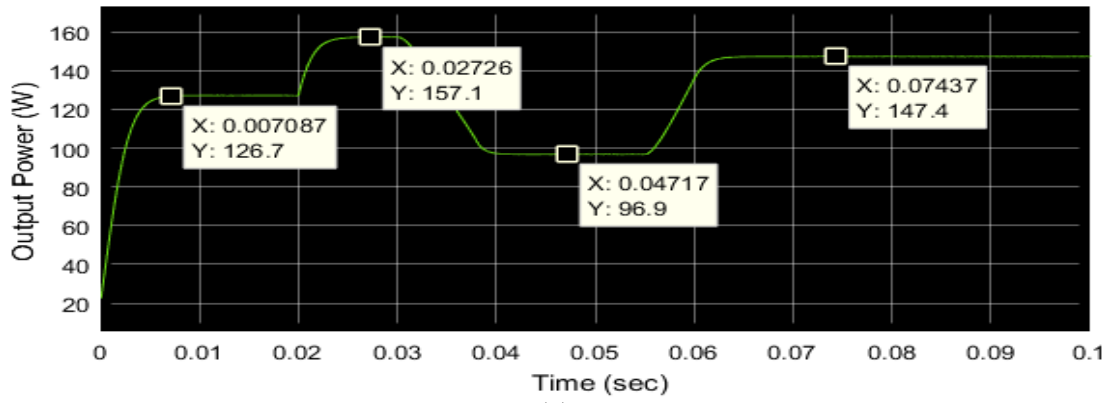


(c)

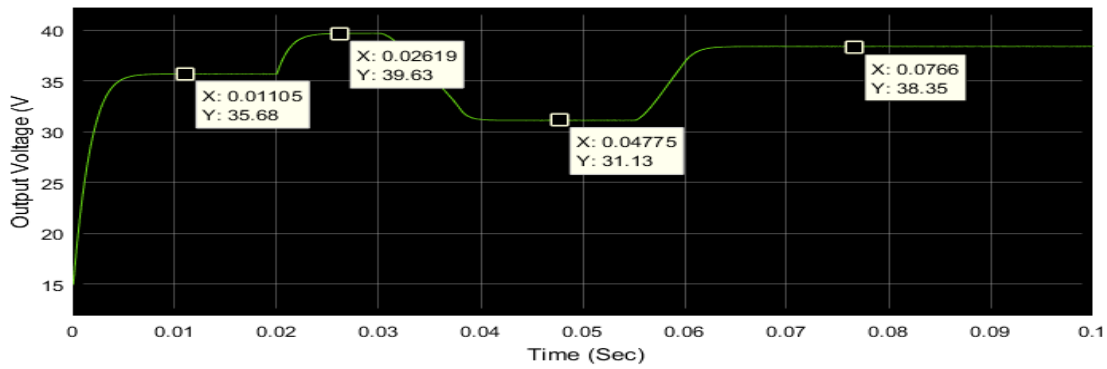


(d)

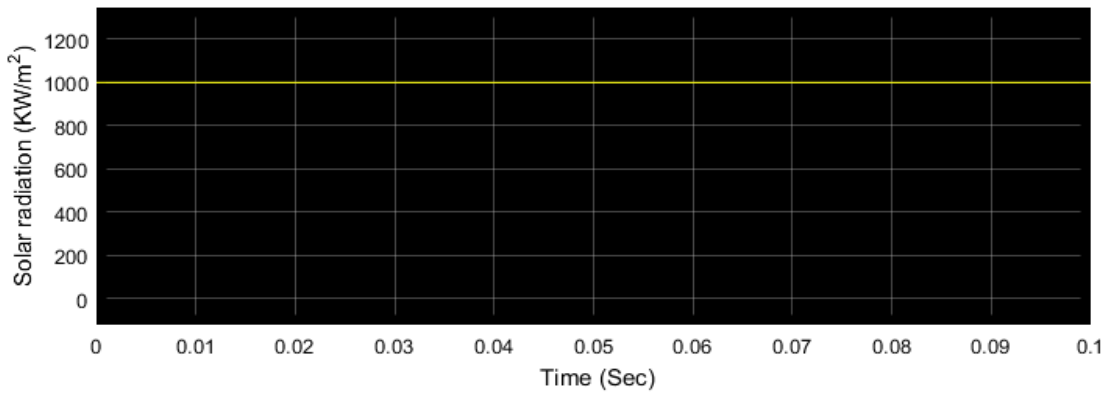
**Figure 5.14:** Case 5 simulation results with variation in G. (a) Output load power. (b) Output load voltage. (c) Operation Solar Radiation Power. (d) Operation Temperature.



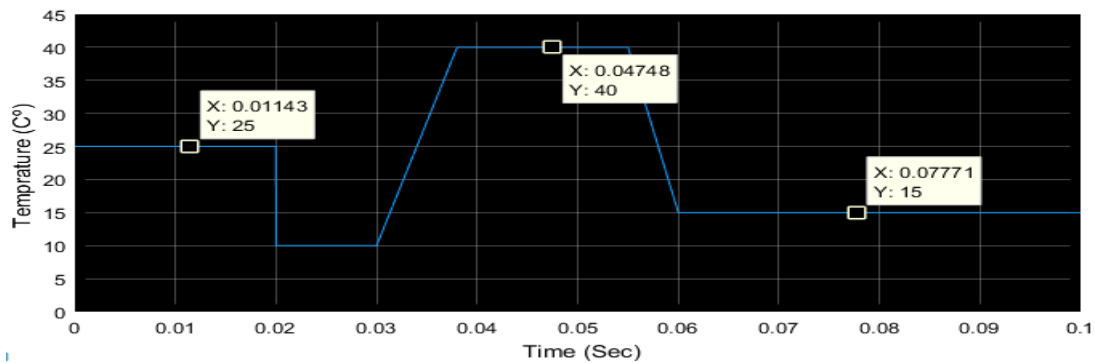
(a)



(b)



(c)



(d)

**Figure 5.15:** Case 5 simulation results with variation in T. (a) Output load power. (b) Output load voltage. (c) Operation Solar Radiation Power. (d) Operation temperature.

## 5.2 Conclusion

In this chapter, all simulations are done using MATLAB/SIMULINK software for evaluating the performance of the PV system work with four different MPPT. The purposed MPPT based ANFIS technique is hybrid of artificial neural network and fuzzy logic control system. The others are MPPT based FLC, MPPT based ANN, and the conventional P&O MPPT algorithm. To Compere the tracking of MPP when the operation solar radiation and temperature value is changing.

As it is seen in literatures and from the simulation results, we conclude that the output power of the PV system which does not work with MPPT is smaller than the other PV systems those work with MPPT technique. About 25% from the expected power lose (figure 5.16).

For system work with conventional P&O MPPT, we conclude that the time response for tracking MPP is slow and the MPP operation is has efficiency less than the other MPPT systems. For system work with MPPT based FLC, the time response for tracking the MPP is faster than P&O MPPT method and more efficient for tracing MPP.

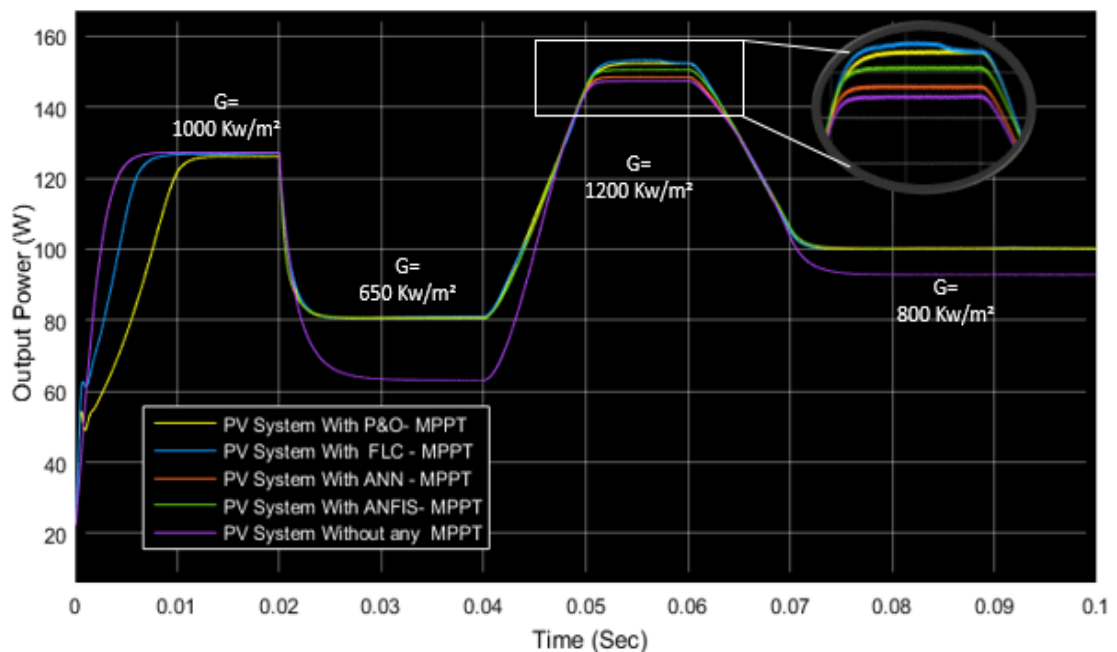


**Figure 5.16:** Output power of all simulations results for variation in G in one plot.

For the MPPT based ANN and ANFIS, these techniques have the fastest time response for tracking the MPP and have high efficiency for delivering the maximum power to the load. See table 5.1 summarizing the performance of five PV systems.

**Table 5.1:** Comparing results of purposed MPPT algorithms.

Type of PV System	Classification type	Control Sensors	Complexity	Time Response	Efficiency
<b>Without MPPT</b>	non	non	Simple	Normal	75.6%
<b>With P&amp;O MPPT</b>	Direct	I- PV AND	Simple	Slow 0.0142 Sec	97.43%
<b>With FLC MPPT</b>	Direct	V PV I-PV AND	Average	Fast 0.0094 Sec	98%
<b>With ANN MPPT</b>	Indirect	T and G	Complex	Fast 0.008 Sec	98.28%
<b>With ANFIS MPPT</b>	Indirect	T and G	Complex	Fast 0.007 Sec	98.88%

From the previous figure we noted that, the output power between time 0.05 Sec and 0.06 Sec where the solar radiation is equal to 1200 Kw/m<sup>2</sup>. The efficient MPPT is MPPT base FLC, then MPPT based P&O then MPPT based ANFIS than the less one is MPPT based ANN. The reasons which make the MPPT based ANN and MPPT based on ANFIS are not efficient in this position, those two methods are indirect MPPT algorithm which make decision of duty cycle based given values of G and T and because the ANN and ANFIS have been learning from data contains situation of system work from range of G between 600 Kw/m<sup>2</sup> to 1100 Kw/m<sup>2</sup>. so, the ANN and ANFS does not give right decision for a situation haven't learnt before. To overcome this problem the training process should be repeated with training data that contains the new situations of T and G.

### 5.3 Summary of the study

In section 2, the characteristic electrical equations of the Photovoltaic cell have reviewed. general PV model has built using MATLAB program for simulate any real electrical PV data. Also, it is used for showing the effect of changing the operation temperature and solar radiation on the electrical characteristic of the output power of PV model which it's data in appendix A and the results are shown in section 4. This



PV model is used for build PV system with resistive load and with boost converter to evaluate the performance of the system with the purposed MPPT algorithms.

Moreover, several MPPT techniques have been presented in this study and their Principe work have explained the Perturb and Observe (P&O), the Artificial Neural Network method based MPPT, the Fuzzy Logic method based on MPPT, and MPPT based Neuro Fuzzy inference technique. Also, the simulations of these methods with PV system have implemented in MATLAB Simulink for evaluation the performance of each MPPT method. The results are discussed in the previous section and showed the performance of MPPT based ANFIS that has fast response and high efficiency tracking the MPP compering with other MPPT methods.



## References

- [1]. Khaligh, A., and O. C. Onar. (2009) "Energy harvesting: solar, wind, and ocean energy conversion systems."
- [2]. Pelc, Robin, and Rod M. Fujita. (2002)."Renewable energy from the ocean." *Marine Policy* 26.6 [471-479].
- [3]. Faranda, Roberto, and Sonia Leva. (2008). "Energy comparison of MPPT techniques for PV Systems." *WSEAS transactions on power systems* 3.6 (2008): [446-455].
- [4]. David Sanz Morales, 2010. "*Maximum Power Point Tracking Algorithms for Photovoltaic Applications*", Faculty of Electronics, Communications and Automation. Espoo 14.12.2010.
- [5]. Saleh Elkelani Babaa, Matthew Armstrong, Volker Pickertm. (2014)."Overview of Maximum Power Point Tracking Control Methods for PV Systems" *Journal of Power and Energy Engineering*, [2014, 2, 59-72]
- [6]. Mukund R. Patel, (2006) *Design, Analysis, and Operation Wind and Solar Power Systems*, Published by CRC Press Taylor & Francis Group, Boca Raton, FL [33487-2742].
- [7]. ESRAM, Trishan, and Patrick L. Chapman. (2007). "Comparison of photovoltaic array maximum power point tracking techniques. 2005." *IEEE Transactions on energy conversion* 22.2 [439-449].
- [8]. Goetzberger, Adolf, and Volker Uwe Hoffmann. *Photovoltaic solar energy generation*. Vol. 112. Springer Science & Business Media.
- [9]. Rahim, Nasrudin Abd, Hew Wooi Ping, and Jeyraj Selvaraj. "Photovoltaic module modeling using Simulink/Matlab." *Procedia Environmental Sciences* 17 (2013): [537-546].
- [10]. Foster, Robert, Majid Ghassemi, and Alma Cota. *Solar energy: renewable energy and the environment*. CRC Press, 2009.
- [11]. Faranda, Roberto, and Sonia Leva. "Energy comparison of MPPT techniques for PV Systems." *WSEAS transactions on power systems* 3.6 (2008): [446-455].
- [12]. Sadek, Sahar M., et al. (2014). "Fuzzy P & O Maximum Power Point Tracking Algorithm for a Stand-Alone Photovoltaic System Feeding Hybrid Loads." *Smart Grid and Renewable Energy* 5.02.
- [13]. Luque, Antonio, and Steven Hegedus, (2011). eds. *Handbook of photovoltaic science and engineering*. John Wiley & Sons.
- [14]. Harjai, Arjav, Abhishek Bhardwaj, and Mrutyunjaya Sandhibigraha. (2011). *Study of maximum power point tracking (MPPT) techniques in a solar photovoltaic array*. Diss.
- [15]. Hasan Mahamudul, Mekhilef Saad, and Metselaar Ibrahim Henk. (2013). "Photovoltaic System Modeling with Fuzzy Logic Based Maximum Power Point Tracking Algorithm." *International Journal of Photo energy*.
- [16]. Gaurav, Amrit Kaur, and A. Kaur. (2012). "Comparison between conventional pid and fuzzy logic controller for liquid flow control: Performance evaluation of fuzzy logic and pid controller by using matlab/simulink." *International Journal of Innovative Technology and Exploring Engineering (IJITEE)* 1.1 [84-88].
- [17]. Femia, Nicola, et al. (2005) "Optimization of perturb and observe maximum power point tracking method." *IEEE transactions on Power Electronics* 20.4 [963-973].
- [18]. Zainuri, Muhammad Ammirul Atiqi Mohd, et al. (2013). "Development of adaptive perturb and observe-fuzzy control maximum power point tracking for photovoltaic boost dc-dc converter." *IET Renewable Power Generation* 8.2 [183-194].

- [19]. Pratik U. Mankar and R.M. Moharil , (2011) . "COMPARATIVE ANALYSIS OF THE PERTURB-AND-OBSERVE AND INCREMENTAL CONDUCTANCE MPPT METHOD", International Journal of Research in Engineering and Applied Sciences.
- [20]. Lynn, Paul A. (*Electricity from sunlight: an introduction to photovoltaics*. John Wiley & Sons,
- [21]. Aribisala, Henry A. (2013). "Improving the efficiency of solar photovoltaic power system." <http://digitalcommons.uri.edu/theses/161>.
- [22]. Daniel W. Hart ."Power Electronics", Book Published by McGraw- Companies, [TK7881.15.H373 2010 621.31'7—dc22], <http://www.mheducation.com>
- [23]. Sivagamasundari, M. S., P. Melba Mary, and V. K. Velvizhi. (2013). "Maximum power point tracking for photovoltaic system by perturb and observe method using buck boost converter." *International Journal of Advanced Research in Electrical, Electronics and Instrumentation Engineering* 2.6 [2433-2439].
- [24]. Zainudin, Hairul Nissah, and Saad Mekhilef. (2010). "Comparison study of maximum power point tracker techniques for PV systems." .
- [25]. Dolara, A., R. Faranda, and S. Leva. (2009). "Energy comparison of seven MPPT techniques for PV systems." *Journal of Electromagnetic Analysis and Applications*.
- [26]. Bendib, Boualem, Hocine Belmili, and Fateh Krim. (2015). "A survey of the most used MPPT methods: Conventional and advanced algorithms applied for photovoltaic systems." *Renewable and Sustainable Energy Reviews* 45 [637-648].
- [27]. Marian Raducu, Hoarcă Ioan Cristian, (2014)."Maximum power point tracking algorithms", ECAI 2014 - International Conference – 6th Edition Electronics, Computers and Artificial Intelligence 23, Bucharest, ROMÂNIA
- [28]. Ahmed, Jubaer, and Zainal Salam. (2016). "A Modified P&O Maximum Power Point Tracking Method with Reduced Steady-State Oscillation and Improved Tracking Efficiency." *IEEE Transactions on Sustainable Energy* 7.4 1506-1515.
- [29]. Demuth, Howard B., et al. *Neural network design*. Martin Hagan,2014.
- [30]. Prof. Laxmidhar Behera, "Electrical - Intelligent Systems and Control course" YouTube Lectures, Department of Electrical Engineering, Indian Institute of Technology, Kanpur. <https://www.youtube.com/playlist?list=PL080F1A848428C3FD>.
- [31]. Koivo, Heikki N. (2008). "Neural networks: Basics using matlab neural network toolbox." *Author Website*.
- [32]. Yang, Shih-Ming, Y. J. Tung, and Y. C. Liu. (1993). "A NEURO-FUZZY SYSTEM DESIGN METHODOLOGY FOR VIBRATION CONTROL." *Asian Journal of control* 7.4 (2005): [393-400].
- [33]. Jang, J-SR. "ANFIS: adaptive-network-based fuzzy inference system." *IEEE transactions on systems, man, and cybernetics* 23.3 [665-685].
- [34]. Iqbal, A., H. Abu-Rub, and Sk M. Ahmed. (2010)"Adaptive neuro-fuzzy inference system based maximum power point tracking of a solar PV module." *Energy Conference and Exhibition (EnergyCon), 2010 IEEE International*. IEEE.
- [35]. Bin-Halabi, Ahmed, Adel Abdenmour, and Hussein Mashaly. (2014), "An Accurate ANFIS-based MPPT for Solar PV System." *International Journal of Advanced Computer Research* 4.2 (2014): 588.
- [36]. Sarikaya, Nurcan, Kerim Guney, and Celal Yildiz. (2008). "Adaptive neuro-fuzzy inference system for the computation of the characteristic impedance and the effective permittivity of the micro-coplanar strip line." *Progress in Electromagnetics Research B* 6 225-237.
- [37]. Peter Vas, (1999) "ARTIFICIAL INTELLIGENT -BASED ELECTRICAL MACHIN AND DEVICES" , published in United States by Oxford university Press ,Inc, New York <https://books.google.com.tr/books?id=16Ai4r7qjuIC&printsec=frontcover&hl=ar#v=onepage&q&f=false>.
- [38]. M.Balaji Naik, Dr.P.Sujatha , "Adaptive fuzzy & Neuro-Fuzzy Inference controller based MPPT for photovoltaic systems", International Research Journal of Engineering and Technology (IRJET), Volume: 02 Issue: 08 | Nov-2015.

- [39]. Marańda, Witold, and Maciej Piotrowicz. (2014) "Efficiency of maximum power point tracking in photovoltaic system under variable solar irradiance." *Bulletin of the Polish Academy of Sciences Technical Sciences* 62.4. [713-721].
- [40]. Hansen, Anca D., et al. (2001). *Models for a stand-alone PV system*.



# 1. APPENDIX A

## A.1 DATA SHEET OF PPS130W AS8118 PV MODULE

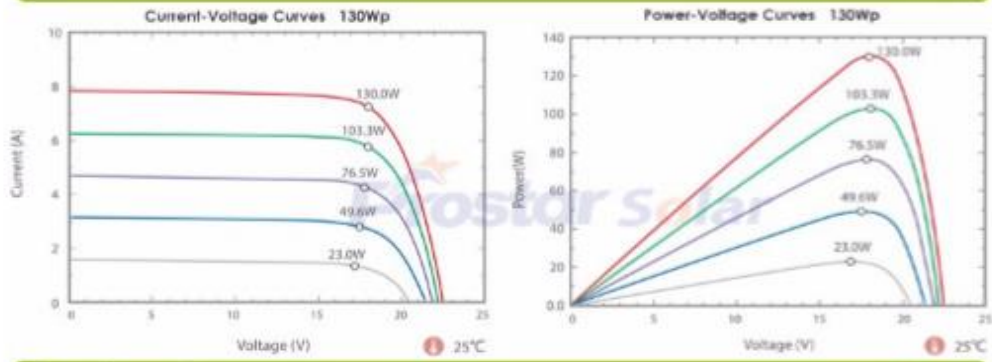
PV Solar Module is a Product available on Alibaba.com Home > Products > Electrical Equipment & Supplies > Batteries > Solar Cells, Solar Panel (250812)



Model		PPS130W	
<b>Warranty</b>			
Product Warranty	10 years limited product warranty		
Power Warranty	15 years at 90% of the minimal rated power output 25 years at 80% of the minimal rated power output		
<b>Electrical Data</b>			
	<b>STC</b>	<b>NOCT</b>	
Maximum Power (Pmax)	130Wp	95Wp	
Maximum Power Voltage (Vmpp)	18.0V	16.8V	
Maximum Power Current (Impp)	7.23A	5.66A	
Open Circuit Voltage (Voc)	22.5V	21.2V	
Short Circuit Current (Isc)	7.81A	6.28A	
Power Tolerance(Positive)	5%		
Module Efficiency STC	15.16%		
Operating Temperature Range	-40°C to +85°C		
Maximum System Voltage	1000VDC (IEC)		
Series Fuse Rating	15A		
Temperature Coefficient of Pmax	-0.44 %/°C		
Temperature Coefficient of Voc	-0.33 %/°C		
Temperature Coefficient of Isc	0.055 %/°C		
Nominal Operating Cell Temperature(NOCT)	45±2°C		
<b>Mechanical Characteristics</b>			
Cell Type	Polycrystalline 156x134 mm		
Cell Number	36(4x9)		
Dimensions (mm)	670x1280x35		
Weight(Kgs)	10.00		
Front Glass	3.2 mm, High Transmission, Low Iron, Tempered Glass		
Frame Type	Anodized Aluminium Alloy		
Junction Box Protection Class	IP 67 Rated		
Connector Type	MC4		
Output Cables	2.5 mm <sup>2</sup> , Length:900 mm		
<b>Standard Test Conditions (STC): Irradiance 1000W/m<sup>2</sup>, AM 1.5, Cell temperature 25°C</b>			
<b>Nominal Operating Cell Temperature (NOCT): Irradiance 800W/m<sup>2</sup>, AM 1.5, Wind Speed 1m/s, Ambient temperature 20°C</b>			

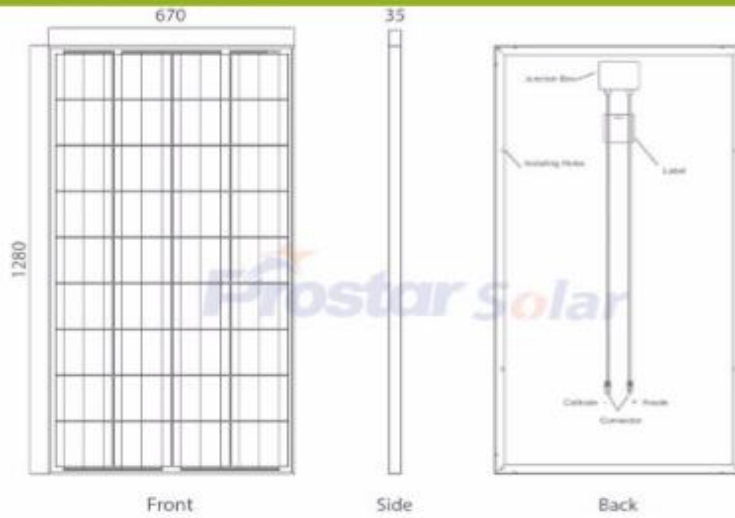
## I-V Curves

Frostar



## Product Dimension

Frostar





## A.2 SIMULATION A PV MODEL

Simulation PV model is done by **MATLAB Simulink** environment using math blocks that are available in Simulink tools to build equations 2.1, 2.2 ,2.3 and 2.4.

Photon current  $I_{ph}$ :

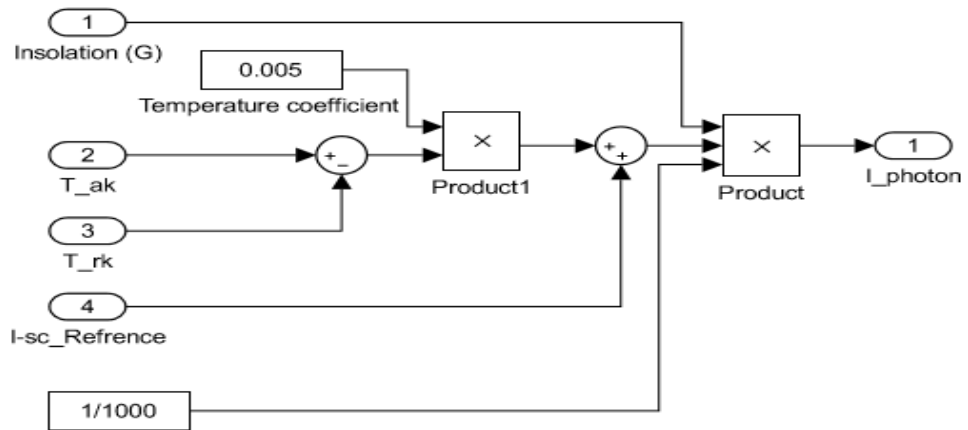


**Figure A.2.1:** Simulation circuit of Photon current ( $I_{ph}$ )

Saturation current  $I_o$ :

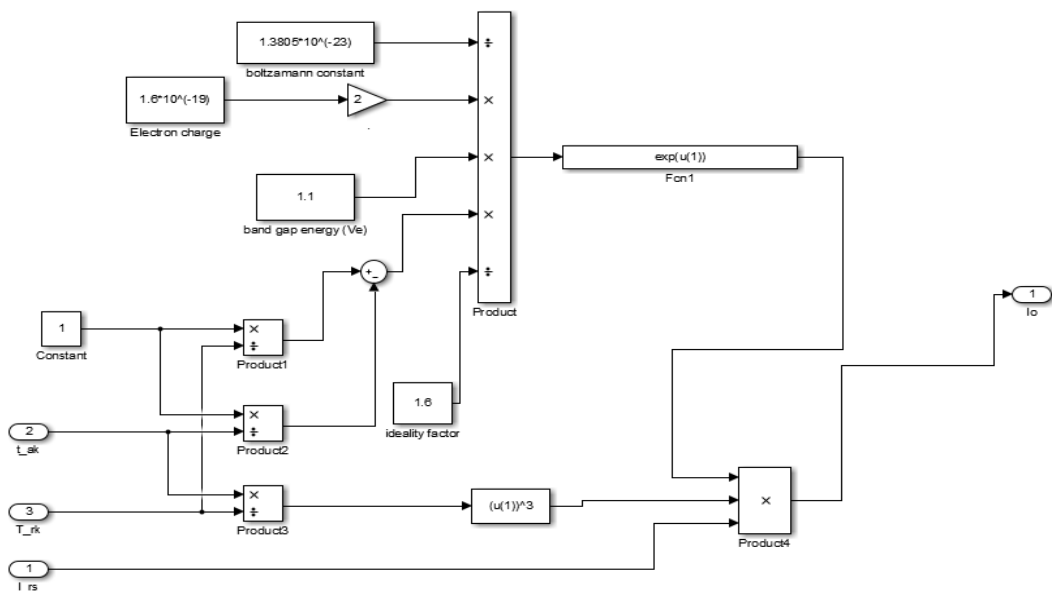


**Figure A.2.2:** Simulation circuit of saturation current ( $I_o$ )

Reverse saturation current  $I_{rs}$ :

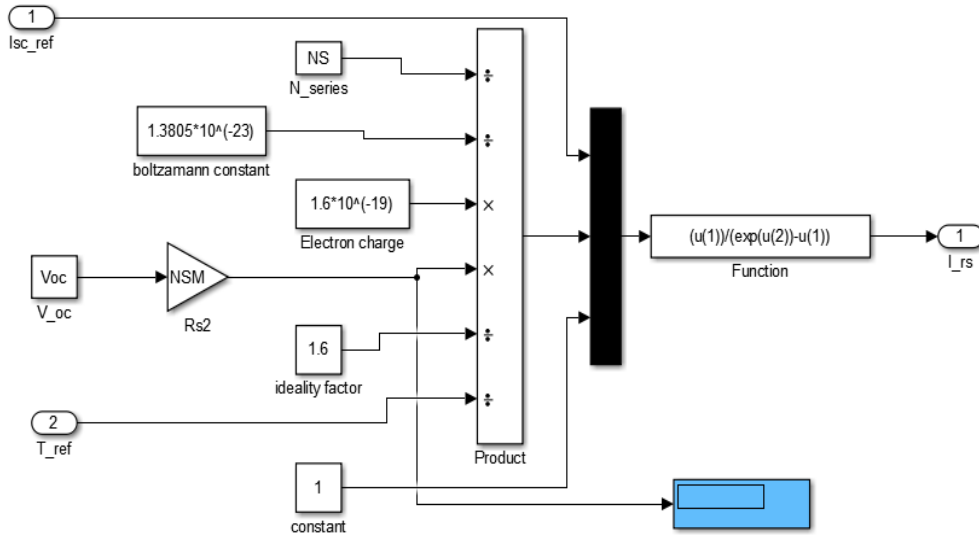


**Figure A.2.3:** Simulation circuit of the reverse saturation current ( $I_{rs}$ )

Output current  $I_{PV}$ :

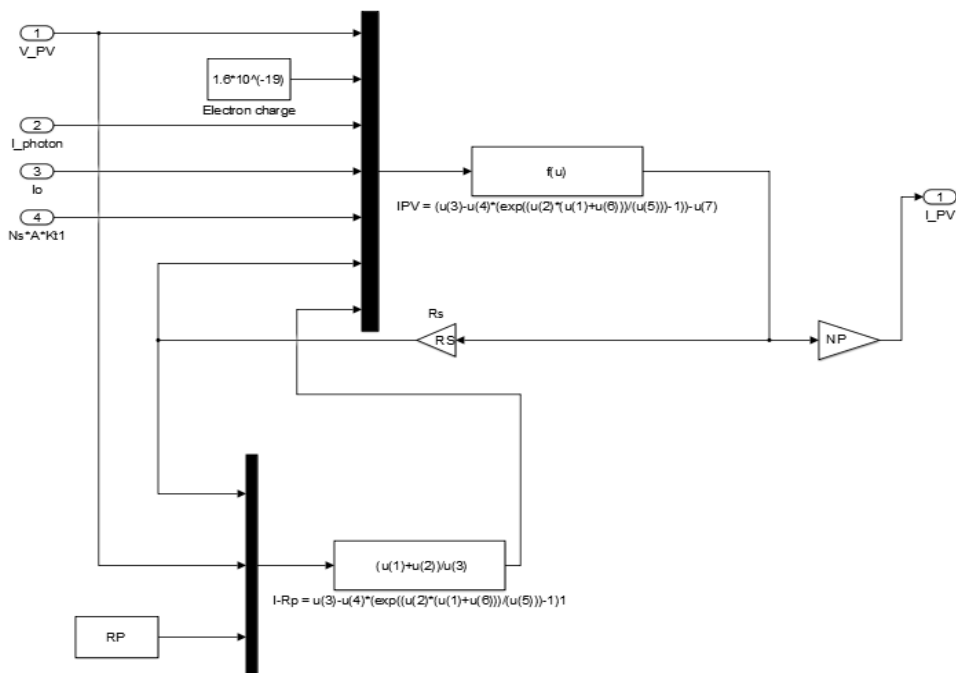


**Figure A.2.4:** Simulation circuit of the PV Output current ( $I_{PV}$ )

## 2. APPENDIX B

### MATLAB CODES

#### B.1 DATA GENERATING

Simulation circuit for collecting data and for analyze the effecting of changing operation temperature and solar irradiation on the PMPP and VMPP is shown in Figure B.1. Data results is imported to MATLAB work space to work on it to plot these affections on figures as it showed in the results.

Data sheet of PPS130W AS8118 PV model in appendix A are used to model the PV model in MATLAB Simulink

Eight PV model with same characteristic data is run at same time to generate the power and voltage data each PV model in figure B.1 has different constant operation temperature. And same operation solar radiation.

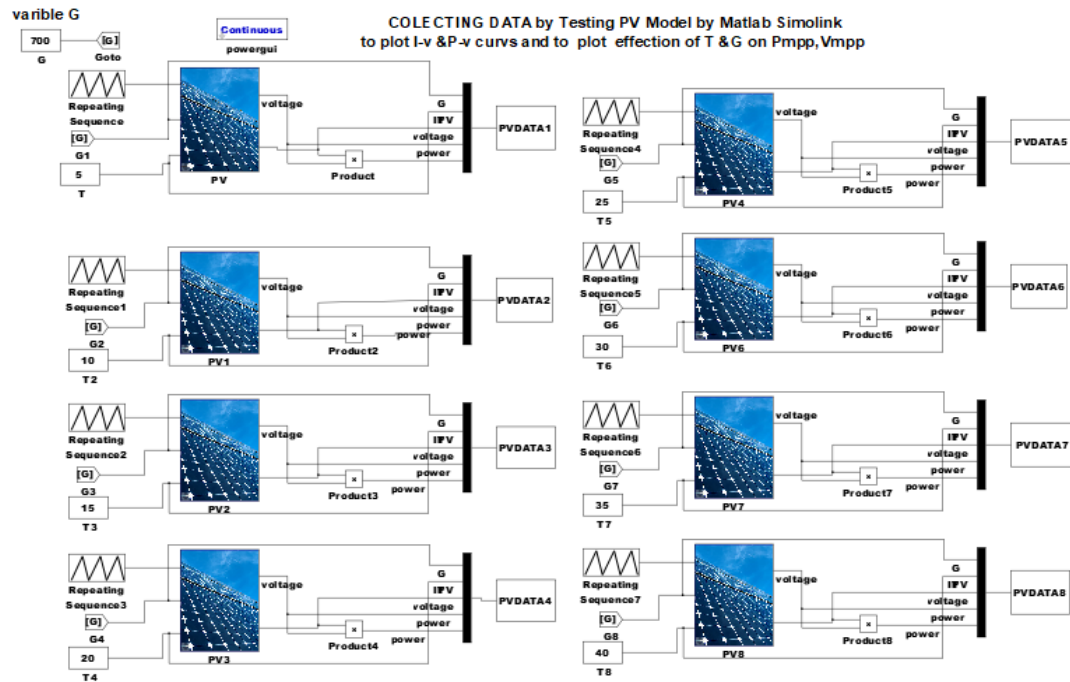


**Figure B.1:** Simulation circuits for analyzing the effect of varying  $G$  and  $T$  on the  $P_{mpp}$  and  $V_{mpp}$ .

## B.2 MATLAB CODES

```
%in these code shows how to find Impp, Vmpp, Pmpp from the simulation data result
% and plot the result in figures
%data is imported to work space to work on it
% for varying G from 600 kw/m2 to 1500kw/m2 and varying T from 2 to 40
%and we are going to arrange the results as matrix
```

```
k1= find(PVDATA1(:,5)==max(PVDATA1(:,5)));
Pmpp1=PVDATA1(k1,5);
Vmpp1=PVDATA1(k1,4);
Impp1=PVDATA1(k1,3);
```

```
k2= find(PVDATA2(:,5)==max(PVDATA2(:,5)));
Pmpp2=PVDATA2(k2,5);
Vmpp2=PVDATA2(k2,4);
Impp2=PVDATA2(k2,3);
```

```
k3= find(PVDATA3(:,5)==max(PVDATA3(:,5)));
Pmpp3=PVDATA3(k3,5);
Vmpp3=PVDATA3(k3,4);
Impp3=PVDATA3(k3,3);
```

```
k4= find(PVDATA4(:,5)==max(PVDATA4(:,5)));
Pmpp4=PVDATA4(k4,5);
Vmpp4=PVDATA4(k4,4);
Impp4=PVDATA4(k4,3);
```

```
k5= find(PVDATA5(:,5)==max(PVDATA5(:,5)));
Pmpp5=PVDATA5(k5,5);
Vmpp5=PVDATA5(k5,4);
Impp5=PVDATA5(k5,3);
```

```
k6= find(PVDATA6(:,5)==max(PVDATA6(:,5)));
Pmpp6=PVDATA6(k6,5);
Vmpp6=PVDATA6(k6,4);
Impp6=PVDATA6(k6,3);
```

```
k7= find(PVDATA7(:,5)==max(PVDATA7(:,5)));
Pmpp7=PVDATA7(k7,5);
Vmpp7=PVDATA7(k7,4);
Impp7=PVDATA7(k7,3);
```

```
k8= find(PVDATA8(:,5)==max(PVDATA8(:,5)));
Pmpp8=PVDATA8(k8,5);
Vmpp8=PVDATA8(k8,4);
Impp8=PVDATA8(k8,3);
```

```
figure (1) % plotting I-V curves in one figure
```

```
hold on
```

```
plot(PVDATA1(:,4),PVDATA1(:,5))% plot test result at T=5
```

```
hold on
```

```
plot(PVDATA2(:,4),PVDATA2(:,5))% plot test result at T=10
```

```
hold on
```

```
plot(PVDATA3(:,4),PVDATA3(:,5))% plot test result at T=15
```

```
hold on
```

```

plot(PVDATA4(:,4),PVDATA4(:,5))% plot test result at T=20
hold on
plot(PVDATA5(:,4),PVDATA5(:,5))% plot test result at T=25
hold on
plot(PVDATA6(:,4),PVDATA6(:,5))% plot test result at T=30
hold on
plot(PVDATA7(:,4),PVDATA7(:,5))% plot test result at T=35
hold on
plot(PVDATA8(:,4),PVDATA8(:,5))% plot test result at T=40
xlabel('Output Voltage (C?)','FontSize',12,...
'FontWeight','bold','Color','b')
ylabel('Output Power (W)','FontSize',12,...
'FontWeight','bold','Color','b')
figure(2)% plotting P-V curves in one figure
hold on
plot(PVDATA1(:,4),PVDATA1(:,3))% plot test result at G=600KW/M2
hold on
plot(PVDATA2(:,4),PVDATA2(:,3))% plot test result at G=600KW/M2
hold on
plot(PVDATA3(:,4),PVDATA3(:,3))% plot test result at G=600KW/M2
hold on
plot(PVDATA4(:,4),PVDATA4(:,3))% plot test result at G=600KW/M2
hold on
plot(PVDATA5(:,4),PVDATA5(:,3))% plot test result at G=600KW/M2
hold on
plot(PVDATA6(:,4),PVDATA6(:,3))% plot test result at G=600KW/M2
hold on
plot(PVDATA7(:,4),PVDATA7(:,3))% plot test result at G=600KW/M2
hold on
plot(PVDATA8(:,4),PVDATA8(:,3))% plot test result at G=600KW/M2
xlabel('Output Voltage (V)','FontSize',12,...
'FontWeight','bold','Color','b')
ylabel('Output Current (A)','FontSize',12,...
'FontWeight','bold','Color','b')

%now to arrange all mpp points in one matrix
%let b as matrix has 9 columns represent changing on the T
%and 14 ROWS FOR changing ON G
% first creat Pmpp_data =14x9 zero matrix ,Vmpp_data =14x9 zero matrix
%,Impp_data =14x9 zero matrix and in each matrix
%first column represent T from 2C to 40C step is 2c
% first row represent G from 600kw/m2 to 1500kw/m2 step is 5kw/m2
%now write power data at mpp in b matrix
j=15 % represents the ROW that no working to write data in
Pmpp_data(1,1)=0;
Pmpp_data(1,2)=PVDATA1(1,2);
Pmpp_data(1,3)=PVDATA2(1,2);
Pmpp_data(1,4)=PVDATA3(1,2);
Pmpp_data(1,5)=PVDATA4(1,2);
Pmpp_data(1,6)=PVDATA5(1,2);
Pmpp_data(1,7)=PVDATA6(1,2);
Pmpp_data(1,8)=PVDATA7(1,2);
Pmpp_data(1,9)=PVDATA8(1,2);

Pmpp_data(j,1)=PVDATA1(1,1); %as the value of G
Pmpp_data(j,2)=Pmpp1;
Pmpp_data(j,3)=Pmpp2;
Pmpp_data(j,4)=Pmpp3;
Pmpp_data(j,5)=Pmpp4;
Pmpp_data(j,6)=Pmpp5;

```

```
Pmpp_data(j,7)=Pmpp6;
Pmpp_data(j,8)=Pmpp7;
Pmpp_data(j,9)=Pmpp8;
```

```
%now write voltag data at mpp
```

```
Impp_data(1,:)=Pmpp_data(1,:); %represent the T culom
Vmpp_data(1,:)=Pmpp_data(1,:); %represent the T culom
```

```
%write voltag at mpp data
```

```
Vmpp_data(j,1)=PVDATA1(1,1); %as the value of G
Vmpp_data(j,2)=Vmpp1;
Vmpp_data(j,3)=Vmpp2;
Vmpp_data(j,4)=Vmpp3;
Vmpp_data(j,5)=Vmpp4;
Vmpp_data(j,6)=Vmpp5;
Vmpp_data(j,7)=Vmpp6;
Vmpp_data(j,8)=Vmpp7;
Vmpp_data(j,9)=Vmpp8;
```

```
%Writ current data at mpp
```

```
Impp_data(j,1)=PVDATA1(1,1); %as the value of G
Impp_data(j,2)=Impp1;
Impp_data(j,3)=Impp2;
Impp_data(j,4)=Impp3;
Impp_data(j,5)=Impp4;
Impp_data(j,6)=Impp5;
Impp_data(j,7)=Impp6;
Impp_data(j,8)=Impp7;
Impp_data(j,9)=Impp8;
```

```
% after finishing writing the Pmpp data and Vmpp data matrixes now print it
% to see the affection of changing in G and T on the Pmpp AND Vmpp
figure(3) % Represents Affection of temperature on Pmpp
```

```
hold on
plot(Pmpp_data(1,2:9),Pmpp_data(10,2:9),'LineWidth',1);
hold on
plot(Pmpp_data(1,2:9),Pmpp_data(14,2:9),'LineWidth',1);
```

```
ylabel('Power at Mpp (w)','FontSize',12,...
'FontWeight','bold','Color','b')
xlabel('Operation Tempreture (C) (A)','FontSize',12,...
'FontWeight','bold','Color','b')
```

```
figure(4) % Represents Affection of temperature on Vmpp
plot(Vmpp_data(1,2:9),Vmpp_data(6,2:9),'LineWidth',1);
hold on
plot(Vmpp_data(1,2:9),Vmpp_data(10,2:9),'LineWidth',1);
hold on
plot(Vmpp_data(1,2:9),Vmpp_data(14,2:9),'LineWidth',1);
```

```
ylabel('Power at Mpp (w)','FontSize',12,...
'FontWeight','bold','Color','b')
xlabel('Operation Tempreture (C) (A)','FontSize',12,...
'FontWeight','bold','Color','b')
```

figure(5) %Represents Affection of solar radiation on Pmpp

```
plot(Pmpp_data(2:9,1),Pmpp_data(2:9,9),'LineWidth',1);
hold on
plot(Pmpp_data(2:9,1),Pmpp_data(2:9,6),'LineWidth',1);
hold on
plot(Pmpp_data(2:9,1),Pmpp_data(2:9,3),'LineWidth',1);

ylabel('Power at Mpp (w)','FontSize',12,...
'FontWeight','bold','Color','b')
xlabel('Solar Irradiation(G) (A)','FontSize',12,...
'FontWeight','bold','Color','b')
```

figure(6)% Represents Affection of solar radiation on Vmpp

```
plot(Vmpp_data(2:9,1),Vmpp_data(2:9,9),'LineWidth',1);
hold on
plot(Vmpp_data(2:9,1),Vmpp_data(2:9,6),'LineWidth',1);
hold on
plot(Vmpp_data(2:9,1),Vmpp_data(2:9,3),'LineWidth',1);

ylabel('Voltage at MPP(w)','FontSize',12,...
'FontWeight','bold','Color','b')
xlabel('Solar Irradiation(G) (A)','FontSize',12,...
'FontWeight','bold','Color','b')
```

The voltage data and power data at MPP which is generated by previous code below:

**Table B.2.1:** PV Power at MPP as function of varing G AND T.

T \ G	5	10	15	20	25	30	35	40
<b>1200</b>	205.68	193.58	181.48	169.37	157.26	145.16	133.12	121.13
<b>1150</b>	196.89	185.28	173.68	162.06	150.46	138.86	127.31	115.81
<b>1100</b>	188.10	177.00	165.89	154.75	143.64	132.56	121.50	110.48
<b>1150</b>	196.89	185.28	173.68	162.06	150.46	138.86	127.31	115.81
<b>1000</b>	170.52	160.41	150.27	140.17	130.05	119.94	109.86	99.83
<b>950</b>	161.73	152.11	142.49	132.87	123.24	113.64	104.06	94.53
<b>900</b>	152.94	143.82	134.7	125.56	116.4	107.34	98.267	89.228
<b>850</b>	144.16	135.54	126.92	118.28	109.6	101.05	92.464	83.92
<b>800</b>	135.38	127.26	119.13	111.01	102.88	94.764	86.688	78.638
<b>750</b>	126.61	118.99	111.36	103.73	96.109	88.502	80.913	73.359
<b>700</b>	117.84	110.73	103.59	96.478	89.354	82.243	75.145	68.093
<b>650</b>	109.10	102.47	95.85	89.23	82.603	75.998	69.409	62.851
<b>600</b>	100.3	94.25	88.12	82.0	75.88	69.76	63.68	57.62

**Table B.2.2:** PV Voltage at MPP as function of varying G AND T.

T G	5	10	15	20	25	30	35	40
1200	23.58	22.29	20.91	19.54	18.21	16.96	15.51	14.31
1150	23.58	22.13	20.83	19.54	18.21	16.80	15.51	14.21
1100	23.58	22.13	20.83	19.54	18.09	16.80	15.50	14.21
1050	23.42	22.13	20.83	19.41	18.09	16.80	15.50	14.21
1000	23.42	22.11	20.67	19.41	18.09	16.71	15.50	14.05
950	23.42	22.11	20.67	19.38	18.09	16.71	15.34	14.05
900	23.42	21.96	20.67	19.38	17.93	16.63	15.34	14.01
850	23.31	21.96	20.61	19.22	17.93	16.63	15.34	14.01
800	23.31	21.96	20.61	19.22	17.91	16.47	15.21	13.89
750	23.26	21.81	20.51	19.11	17.76	16.47	15.18	13.89
700	23.10	21.80	20.51	19.11	17.76	16.41	15.02	13.73
650	23.10	21.80	20.35	19.06	17.61	16.31	15.02	13.71
600	23.01	21.64	20.31	18.90	17.60	16.3	14.91	13.56

### B.3 MATLAB FUNCTION CODE BASED P&O MPPT ALGORITHM

The algorithm is implemented using MATLAB function block and programmed using MATLAB M-file see the block function below

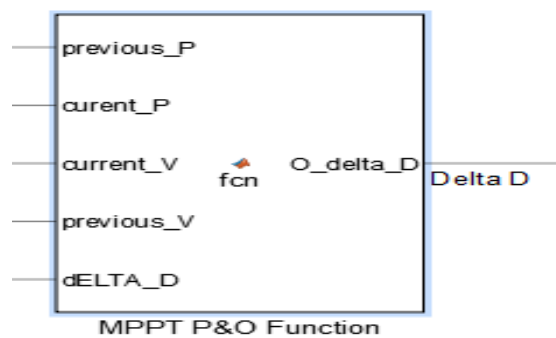


Figure B3: MATLAB function block based P&O MPPT algorithm

The MATLAB function is programmed as code below:

```

%%%%%%%%%%%%%%%%%%%%%%%%%%%%%%%%%%%%%%%%%%%%%%%%%%%%%%%%%%%%%%%%%%%%%%%% MATLAB FUNCTION BASED P&O MPPT ALGORETHM
%%%%%%%%%%%%%%%%%%%%%%%%%%%%%%%%%%%%%%%%%%%%%%%%%%%%%%%%%%%%%%%%%%%%%%%%

% previous_P : calculated previous power
% curent_P   : current POWER AT TIOM t
% current_V  : current PV Voltage at time t
% previous_V : previous pv voltage at time (t-1)
% dELTA_D   : inital value of delta D
% O_delta_D : output of the Function give decision

```



```

function O_delta_D = fcn (previous_P,current_P,current_V,previous_V, dDELTA_D)

    for i= 1:2
    if (curent_P>previous_P) && (current_V>previous_V)
        x=dELTA_D;
    elseif(curent_P>previous_P) && (current_V<previous_V)
        x=-dELTA_D;
    elseif(curent_P<previous_P) && (current_V>previous_V)
        x=-dELTA_D;
    elseif(curent_P<previous_P) && (current_V<previous_V)
        x=dELTA_D;
        elseif(curent_P==previous_P) && (current_V>previous_V)
            x=0;
    end
    i=i+1;
    end ,O_delta_D = x

```

### 3. APPENDIX C

#### BAILDING ANN & ANFIS AND TRAINING DATA

##### C.1 TRAINING DATA ARRAY

The training data is used to train ANN & ANFIS controlers and it is generated by operate the two PV systems. The first one work with P&O MPPT with smaller constant value just to knew the rang of the duty cycle. than copy it to the second system that running the with adjustable duty cycle for increasing and decreasing the duty cycle to get the accurate and reliable result. See Table C.1

**Table C.1:** ANN & ANFIS Training Data.

Temperature C°	Solar Irradiation KW/m <sup>2</sup>	Duty cycle at MPP Operation	Temperature C°	Solar Irradiation KW/m <sup>2</sup>	Duty cycle at MPP Operation
10	600	0.312000000000000;	10	925	0.440100000000000;
15	600	0.340700000000000;	15	925	0.465100000000000;
20	600	0.361900000000000;	20	925	0.482410000000000;
25	600	0.384900000000000;	25	925	0.499400000000000;
30	600	0.407400000000000;	30	925	0.517200000000000;
35	600	0.430300000000000;	35	925	0.534700000000000;
10	625	0.332700000000000;	10	950	0.437000000000000;
15	625	0.353500000000000;	15	950	0.449500000000000;
20	625	0.375000000000000;	20	950	0.465100000000000;
25	625	0.396600000000000;	25	950	0.479900000000000;
30	625	0.418500000000000;	30	950	0.507100000000000;
35	625	0.440700000000000;	35	950	0.525100000000000;
10	650	0.345500000000000;	10	975	0.439500000000000;
15	650	0.366000000000000;	15	975	0.459500000000000;
20	650	0.386700000000000;	20	975	0.481000000000000;
25	650	0.407800000000000;	25	975	0.492000000000000;
30	650	0.429200000000000;	30	975	0.511100000000000;
35	650	0.451000000000000;	35	975	0.531100000000000;
10	675	0.357200000000000;	10	1000	0.449100000000000;
15	675	0.377600000000000;	15	1000	0.469100000000000;
20	675	0.397900000000000;	20	1000	0.485110000000000;
25	675	0.418500000000000;	25	1000	0.501100000000000;
30	675	0.439600000000000;	30	1000	0.521100000000000;
35	675	0.460700000000000;	35	1000	0.537900000000000;
10	700	0.368700000000000;	10	1025	0.455100000000000;
15	700	0.388800000000000;	15	1025	0.469100000000000;
20	700	0.408300000000000;	20	1025	0.489100000000000;
25	700	0.428600000000000;	25	1025	0.501100000000000;
30	700	0.449200000000000;	30	1025	0.521100000000000;
35	700	0.469800000000000;	35	1025	0.541100000000000;
10	725	0.379800000000000;	10	1050	0.459500000000000;
15	725	0.398800000000000;	15	1050	0.479800000000000;
20	725	0.417600000000000;	20	1050	0.492900000000000;
25	725	0.437800000000000;	25	1050	0.511900000000000;
30	725	0.457600000000000;	30	1050	0.529900000000000;
35	725	0.478300000000000;	35	1050	0.549900000000000;

Temperature C°	Solar Irradiation KW/m <sup>2</sup>	Duty cycle at MPP Operation	Temperature C°	Solar Irradiation KW/m <sup>2</sup>	Duty cycle at MPP Operation
10	750	0.3904000000000000;	10	1075	0.4711000000000000;
15	750	0.4086000000000000;	15	1075	0.4921000000000000;
20	750	0.4279000000000000;	20	1075	0.5061000000000000;
25	750	0.4473000000000000;	25	1075	0.5161000000000000;
30	750	0.4668000000000000;	30	1075	0.5361000000000000;
35	750	0.4868000000000000;	35	1075	0.5552000000000000;
10	775	0.3998000000000000;	10	1100	0.4759000000000000;
15	775	0.4178000000000000;	15	1100	0.4859000000000000;
20	775	0.4367000000000000;	20	1100	0.5111000000000000;
25	775	0.4552000000000000;	25	1100	0.5222000000000000;
30	775	0.4747000000000000;	30	1100	0.5398000000000000;
35	775	0.4944000000000000;	35	1100	0.5550000000000000]
10	800	0.4088000000000000;	10	925	0.4401000000000000;
15	800	0.4268000000000000;	15	925	0.4651000000000000;
20	800	0.4452000000000000;	20	925	0.4824100000000000;
25	800	0.4638000000000000;	25	925	0.4994500000000000;
30	800	0.4828000000000000;	30	925	0.5172000000000000;
35	800	0.5022000000000000;	35	925	0.5347000000000000;
10	825	0.4178000000000000;	10	950	0.4370000000000000;
15	825	0.4354000000000000;	15	950	0.4495000000000000;
20	825	0.4532000000000000;	20	950	0.4651000000000000;
25	825	0.4713000000000000;	25	950	0.4799000000000000;
30	825	0.4972;	30	950	0.5071000000000000;
35	825	0.5292000000000000;	35	950	0.5251000000000000;
10	825	0.4262000000000000;	10	975	0.4395000000000000;
15	850	0.4434000000000000;	15	975	0.4595000000000000;
20	850	0.4611000000000000;	20	975	0.4810000000000000;
25	850	0.4791000000000000;	25	975	0.4920000000000000;
30	850	0.4972000000000000;	30	975	0.5111000000000000;
35	850	0.5161000000000000;	35	975	0.5311000000000000;
10	875	0.4342000000000000;	10	1000	0.4491000000000000;
15	875	0.4511000000000000;	15	1000	0.4691000000000000;
20	875	0.4683000000000000;	20	1000	0.4851100000000000;
25	875	0.4862000000000000;	25	1000	0.5011000000000000;
30	875	0.5038000000000000;	30	1000	0.5211000000000000;
35	875	0.5224000000000000;	35	1000	0.5379000000000000;
10	900	0.4418000000000000;	10	1025	0.4551000000000000;
15	900	0.4586000000000000;	15	1025	0.4691000000000000;
20	900	0.4753000000000000;	20	1025	0.4891000000000000;
25	900	0.4931000000000000;	25	1025	0.5011000000000000;
30	900	0.5508000000000000;	30	1025	0.5211000000000000;
35	900	0.5287000000000000;	35	1025	0.5411000000000000;

## C.2 CODE OF BUILDING AND TRAINING ANN BASED MPPT TRAINING DATA

The ANN based MPPT is generated and trained by this code:

```
%load training data set matrix 126x3
trainingData =[10,600,0.3120000000000000;
15,600,0.3407000000000000;
20,600,0.3619000000000000;
```

25,600,0.3849000000000000;  
30,600,0.4074000000000000;  
35,600,0.4303000000000000;  
10,625,0.3327000000000000;  
15,625,0.3535000000000000;  
20,625,0.3750000000000000;  
25,625,0.3966000000000000;  
30,625,0.4185000000000000;  
35,625,0.4407000000000000;  
10,650,0.3455000000000000;  
15,650,0.3660000000000000;  
20,650,0.3867000000000000;  
25,650,0.4078000000000000;  
30,650,0.4292000000000000;  
35,650,0.4510000000000000;  
10,675,0.3572000000000000;  
15,675,0.3776000000000000;  
20,675,0.3979000000000000;  
25,675,0.4185000000000000;  
30,675,0.4396000000000000;  
35,675,0.4607000000000000;  
10,700,0.3687000000000000;  
15,700,0.3888000000000000;  
20,700,0.4083000000000000;  
25,700,0.4286000000000000;  
30,700,0.4492000000000000;  
35,700,0.4698000000000000;  
10,725,0.3798000000000000;  
15,725,0.3988000000000000;  
20,725,0.4176000000000000;  
25,725,0.4378000000000000;  
30,725,0.4576000000000000;  
35,725,0.4783000000000000;  
10,750,0.3904000000000000;  
15,750,0.4086000000000000;  
20,750,0.4279000000000000;  
25,750,0.4473000000000000;  
30,750,0.4668000000000000;  
35,750,0.4868000000000000;  
10,775,0.3998000000000000;  
15,775,0.4178000000000000;  
20,775,0.4367000000000000;  
25,775,0.4552000000000000;  
30,775,0.4747000000000000;  
35,775,0.4944000000000000;  
10,800,0.4088000000000000;  
15,800,0.4268000000000000;  
20,800,0.4452000000000000;  
25,800,0.4638000000000000;  
30,800,0.4828000000000000;  
35,800,0.5022000000000000;  
10,825,0.4178000000000000;  
15,825,0.4354000000000000;  
20,825,0.4532000000000000;  
25,825,0.4713000000000000;  
30,825,0.4972;  
35,825,0.5292000000000000;  
10,850,0.4262000000000000;  
15,850,0.4434000000000000;  
20,850,0.4611000000000000;

25,850,0.4791000000000000;  
30,850,0.4972000000000000;  
35,850,0.5161000000000000;  
10,875,0.4342000000000000;  
15,875,0.4511000000000000;  
20,875,0.4683000000000000;  
25,875,0.4862000000000000;  
30,875,0.5038000000000000;  
35,875,0.5224000000000000;  
10,900,0.4418000000000000;  
15,900,0.4586000000000000;  
20,900,0.4753000000000000;  
25,900,0.4931000000000000;  
30,900,0.5508000000000000;  
35,900,0.5287000000000000;  
10,925,0.4401000000000000;  
15,925,0.4651000000000000;  
20,925,0.4824100000000000;  
25,925,0.4994500000000000;  
30,925,0.5172000000000000;  
35,925,0.5347000000000000;  
10,950,0.4370000000000000;  
15,950,0.4495000000000000;  
20,950,0.4651000000000000;  
25,950,0.4799000000000000;  
30,950,0.5071000000000000;  
35,950,0.5251000000000000;  
10,975,0.4395000000000000;  
15,975,0.4595000000000000;  
20,975,0.4810000000000000;  
25,975,0.4920000000000000;  
30,975,0.5111000000000000;  
35,975,0.5311000000000000;  
10,1000,0.4491000000000000;  
15,1000,0.4691000000000000;  
20,1000,0.4851100000000000;  
25,1000,0.5011000000000000;  
30,1000,0.5211000000000000;  
35,1000,0.5379000000000000;  
10,1025,0.4551000000000000;  
15,1025,0.4691000000000000;  
20,1025,0.4891000000000000;  
25,1025,0.5011000000000000;  
30,1025,0.5211000000000000;  
35,1025,0.5411000000000000;  
10,1050,0.4595000000000000;  
15,1050,0.4798000000000000;  
20,1050,0.4929000000000000;  
25,1050,0.5119000000000000;  
30,1050,0.5299000000000000;  
35,1050,0.5499000000000000;  
10,1075,0.4711000000000000;  
15,1075,0.4921000000000000;  
20,1075,0.5061000000000000;  
25,1075,0.5161000000000000;  
30,1075,0.5361000000000000;  
35,1075,0.5552000000000000;  
10,1100,0.4759000000000000;  
15,1100,0.4859000000000000;  
20,1100,0.5111000000000000;

```

25,1100,0.5222000000000000;
30,1100,0.5398000000000000;
35,1100,0.5550000000000000]

% first before training take the transport of the training data
%to be the matrix as three rows and 126 columns
%selecting input vectors
P=trainingData1(1:2,:); %defining the input vector
T=trainingData1(3,:);% defining target vector
% Built Neural Network Structure of 10 hidden layers with Pack propagation training algorithm
'trainrp'
net2=feedforwardnet(10,'trainrp');
selecting the minimum error to stop the training
net2.trainParam.goal=0.00001;
[net2,tr]=train(net2,P,T);% train the network net2
view(net2)
y = net2(trainingData1(1:2,:));
% command below to build generated net1 as black function in Simulink library
gensim(net2);

```

### C.3 BUILDING AND TRAINING ANFIS BASED MPPT TRAINING DATA

ANFIS controller is built using MATLAB Neuro-Fuzzy Designer tool first load training data to MATLAB work space and open Neuro-Fuzzy Designer tool as seen in figure C.3.1 below and load training data using button and the FIS membership function for inputs is selected as triangular MFs and the training algorithm is selected as backpropagation the trainee the ANFIS network. Loaded data is shown in circus samples in the figure below:

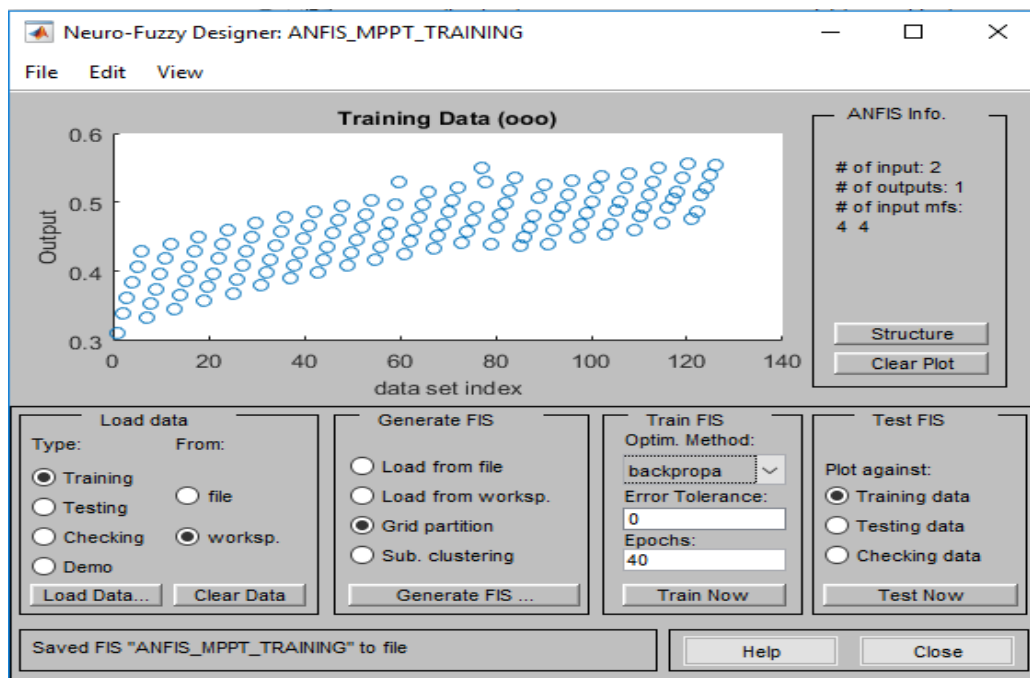
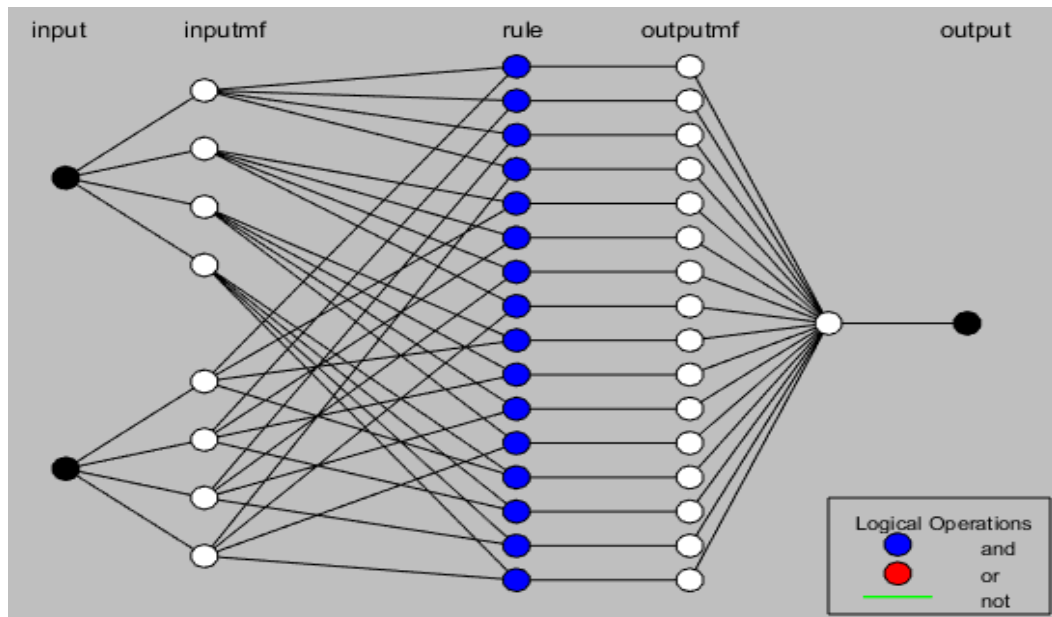


Figure C.3.1: Loading training data using neuro fuzzy designer.

ANFIS structure:



**Figure C.3.2:** ANFIS structure with 16 rule bases.

Training process reaches minimum error of 0.0065 in Epoch 68. see figure below:

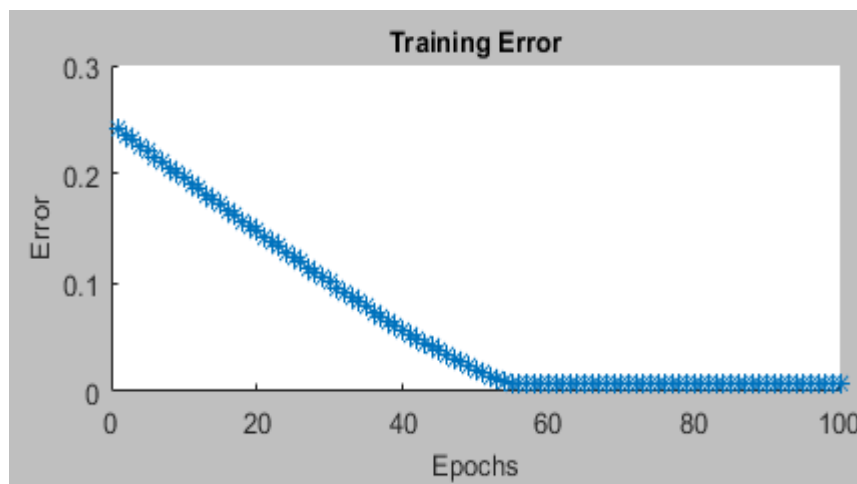


**Figure C.3.4:** Mean square error of the output during the ANFIS training process.

ANFIS designed information :

Number of training data pairs: 126

Number of fuzzy rules: 16

Testing training data seen in figure below get average error of 0.0065155 .

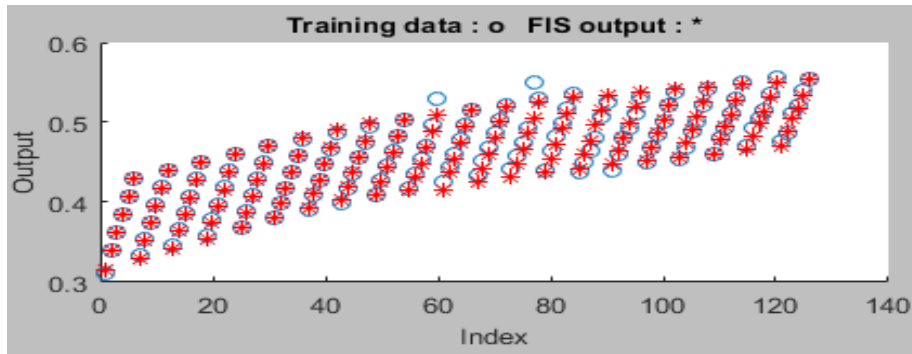


Figure C.3.5: Comparing output of trained ANFIS with training data.

#### C.4 Testing ANN and FLC Controllers based MPPT with the training data

Testing is done in MATLAB Simulink by giving samples of G and T to the two controllers. That for comparing the decision of duty cycle with the actual duty cycle of the training data to see the accuracy of two controller. See Table C.4 result of the testing.

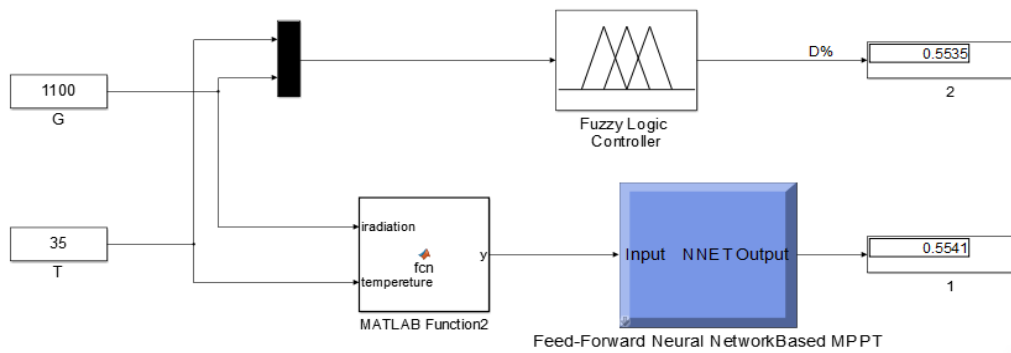


Figure C.4: Simulation circuit for testing ANN and FLC based ANFIS

Table C.4: Testing result of ANN and FLC based ANFIS duye cycle decition.

Temperature C°	Solar Irradiation KW/m <sup>2</sup>	Actual Duty cycle at MPP Operation	ANN D Decision	FLC- ANFIS D Decision
10	600	0.3220	0.3242	0.3161
35	700	0.4698	0.44340	0.4696
25	825	0.4713	0.46980	0.4684
25	900	0.4753	0.4916	0.4861
15	975	0.4395	0.4483	0.4641
25	1100	0.5222	0.5055	0.5167
35	775	0.4944	0.4928	0.4983
15	625	0.3535	0.3541	0.3516
20	1025	0.4891	0.04942	0.4906
10	975	0.4395	0.4484	0.4471



## RESUME

**Name Surname:** A bd El Hakim Ali Bobakir Elagori

**Place and Date of Birth:** 14/4/1989 , Benghazi - Libya



**E-Mail:** [abdelhakimabobakirel@stu.aydin.edu.tr](mailto:abdelhakimabobakirel@stu.aydin.edu.tr) , [alagorei89@gmail.com](mailto:alagorei89@gmail.com)

### Education :

- **Bachelor** : 2013, Benghazi University, Faculty of Engineer, Department of Electrical & Electronic Engineering, Benghazi, Libya.
- **The title of the Bachelor project was “Fuzzy Logic Control Theritical and Applications “. A hardware application was designing “ Sun Traking system for photovoltaic PV panel”.**

### Given Presentation:

- Give presentation about the mechanisim of image compressing by using JPEG algorithim at **IAU**.
- Give presentation about coding and in coding image using JPEG algorithim at **IAU**

### Experiences And Searcheres

- Designing Fuzzy Logic Controller (FLC) based Incremental Conductance Method for Maximum Power Point Tracking for PV panel using MATLAB.
- Designing a general PV system for modling any PV cell, model and array using MATLAB simulink.
- Impelminting the **K MEANS** Algorithem for image classification using MATLAB.